ANALYSIS OF OLIGOMERIC AND SUBUNIT SIZES OF MEMBRANE RECEPTORS

BY

FRANCIS ANTHONY CHI CHOI LAI

Department of Biochemistry,

Imperial College,

London SW7 2AZ.

A thesis submitted for the degree of Doctor of Philosophy of the University of London and for the Diploma of Membership of the Imperial College.

March 1986

ABSTRACT

The first part of the thesis (Section I) describes the oligomeric and subunit characterisation of a putative neuronal nicotinic acetylcholine receptor (pnAChR) from chick optic lobe.

By performing gel filtration chromatography, and sucrose density gradient centrifugation in H_2O and D_2O, a molecular weight of 354,000 was calculated for the pnAChR oligomer solubilised in Triton X-100. In addition, the solubilised pnAChR exhibited a sedimentation coefficient of 11.76, partial specific volume of 0.766 ml/g, Stokes radius of 7.6nm and a frictional ratio of 1.49.

Purification of the pnAChR to a specific activity of 2600nmol/g protein was achieved by α BuTX affinity chromatography followed by specific elution with nicotine. Analysis of the purified pnAChR by SDS-polyacrylamide gel electrophoresis, revealed four subunits of molecular weight 47,000, 57,000, 72,000 and ~98,000, suggesting the existence of a heterooligomeric structure, as has been found for muscle nicotinic acetylcholine receptors (nAChR). The purified subunits from larger scale pnAChR preparations, were individually isolated and submitted to amino- terminal amino acid sequence analysis in a gas-phase sequencer. The amino-terminal sequence obtained for the 47,000 molecular weight subunit, showed definite homology to corresponding sequences from the α subunit of various muscle nAChRs, suggesting that the neuronal and muscle nAChR diverged very early during vertebrate evolution. No amino-terminal sequence was obtained for the other subunits, which were found to have been chemically blocked prior to subunit isolation, hence subunit stoichiometry could not be deduced.

Poly(A)$^+$-mRNA isolated from chick optic lobe and

microinjected into Xenopus laevis oocytes, was shown to direct the synthesis of pnAChR, by its immunoprecipitation with a monoclonal antibody. Radiolabelling of oocyte-synthesized pnAChR was achieved by coinjection of poly(A)$^+$-mRNA with ^{35}S-methionine. The ^{35}S-methionine-pnAChR purified by α BuTX affinity chromatography and nicotine elution, was subjected to SDS-polyacrylamide gel electrophoresis/autoradiography and revealed an identical subunit pattern to the unlabelled pnAChR. This suggests that the four subunits identified, are part of the pnAChR oligomer.

The latter part of the thesis (Section II), describes the application of target size analysis by radiation inactivation. Following a study of the factors affecting radiation inactivation, a molecular weight calibration curve of a series of soluble enzymes was constructed from their relative rates of inactivation by high energy electrons. Several mitochondrial membrane-associated enzymes were then used, to demonstrate the validity of using enzyme markers for molecular weight calibration of relative radiation sensitivity.

Radiation inactivation studies of the asymmetric molecules IgG and acetylcholinesterase, resulted in target sizes significantly less than their molecular size, and which corresponded to the inactivation of domains and subunits, respectively. Finally, target sizes obtained from radiation inactivation studies of the integral membrane proteins, Ca^{2+}-ATPase, opioid receptor, GABA/benzodiazepine receptor and pnAChR, are discussed in relation to their molecular sizes determined otherwise.

Dedicated to

MY WIFE AND MY PARENTS

Acknowledgements

I would like to thank my supervisor, Professor E.A. Barnard, FRS, for the unique opportunity and experience of working in his laboratory, and for the continual support and guidance he has given me during difficult times and throughout this study.

Many of these studies were conducted with the expert assistance of colleagues and collaborators. I am grateful to all who have helped, especially Drs. G. Bilbe, O. Dolly, S. Dunn, J. Lai, L. Newman, R. Shipolini, M. Smith, A. Stephenson, Mr. V. Cockroft, Mr. K. Tsim and Mr. J. Skinner and many others too numerous to list.

The studies on Ca^{2+}-ATPase were conducted in the laboratory of Dr. N.M. Green, FRS, at the National Institute for Medical Research, Mill Hill, London NW7, to whom I am extremely grateful for the use of laboratory facilities, his friendly advice and the many helpful discussions.

Amino-terminal amino acid microsequencing was kindly performed by Dr. B. Conti-Tronconi at the California Institute of Technology, Pasadena, California, USA.

Finally, special thanks are due to Dr. R. Shipolini for helpful suggestions during the writing of the thesis, and to Miss A. Bartlett for her help and patience in the preparation of the thesis.

TABLE OF CONTENTS PAGE NO.

SECTION II

LIST OF TABLES

LIST OF FIGURES

SECTION I

CHAPTER 1 INTRODUCTION

In the nervous system, specialised nerve cells, or neurons, form a network of pathways through which direct and rapid communication between different regions of the body is effected. The signals of communication are electrical impulses, or action potentials, which arise from a transient change in the neuron cell membrane's permeability to Na^+ then K^+ ions sequentially, along the neuron (Hodgkin, 1951). When the action potential reaches a synapse, the site at which two neurons make functional contact, the signal is transmitted from one neuron to the other by either electrical or chemical transmission.

At electrical synapses (Furshpan and Potter, 1959), the current from an action potential in the presynaptic nerve terminal spreads directly into the next neuron via a pathway of low electrical resistance or gap junction, where the intercellular space is about 2nm (Sotelo et al, 1974).

At chemical synapses (Dale et al, 1936), depolarisation of the presynaptic nerve terminal by the arrival of an action potential, evokes the Ca^{2+}-dependent quantal release of a neurotransmitter into the synaptic cleft (Eccles, 1964). The neurotransmitter then diffuses approximately 50nm across the synapse to interact with specific receptors embedded in the post-synaptic membrane (Heuser et al, 1974; Porter and Barnard, 1975). This specific interaction results in changed membrane permeability to either Na^+ ions, which produces depolarization of the membrane (Takeuchi and Takeuchi, 1960), or Cl^- and/or K^+ ions which causes hyperpolarisation (Kehoe, 1972).

1.1 Cholinergic neurotransmission

Of the approximately 40 chemical transmitters so far identified, acetylcholine (ACh) has been the most widely studied, both in peripheral and central nervous systems (review Krnjevic, 1974).

Convincing evidence for the transmitter role of ACh has been shown by the presence of choline acetyltransferase (CAT) in presynaptic terminals, and acetylcholinesterase (AChE) in the synaptic cleft. These two enzymes have been found to catalyse the synthesis and degradation of ACh respectively (Phillis, 1974). Release of ACh from presynaptic terminals was demonstrated when, after injection of radiolabelled choline into Aplysia neurons, the presence of radiolabelled ACh was detected in the synapse (Koike et al, 1974). Also, direct measurements of an excitatory postsynaptic action produced by iontophoretic application of ACh to both muscle endplates and neuronal synapses have been made using intracellular microelectrode recordings (Nastuk, 1953; Dennis et al, 1971).

ACh produces two pharmacologically distinct depolarising responses at the postsynaptic membrane; a rapid response of short duration (30-100 msec) mimicked by application of nicotine, and a delayed reponse of long duration (0.5-3 sec) mimicked by muscarine. This has led to the terms nicotinic acetylcholine receptor (nAChR) and muscarinic acetylcholine receptor (mAChR), for the postsynaptic membrane proteins to which ACh binds specifically.

mAChRs are present in the cholinergic pathways of the autonomic nervous system (ANS). This system innervates most tissues and organs of the body, and modulate, often by opposing the β-adrenergic receptor system, heart rate, smooth muscle

contraction and glandular secretions. nAChRs are found at the neuromuscular junctions (nmj) of vertebrate skeletal muscle, fish electroplax, the adrenal gland and the central nervous system (CNS) (Field, 1960).

1.2 Function of the nAChR

At nicotinic synapses, ACh is released from active zones in the presynaptic nerve membrane, adjacent to folds in the postsynaptic membrane where nAChRs are concentrated (Porter and Barnard, 1975; Heuser and Salpeter, 1979). The $\sim 10^4$ ACh molecules released in each quantum, takes 2 msec to diffuse across the synaptic gap. Binding of ACh to the nAChR triggers a conformational change which opens its cation channel (Katz and Miledi, 1965; Kuffler and Yoshikami, 1975a,b). The open channel has a functional diameter of ~ 7Å and translocates mainly Na^+ and K^+ ions (Dwyer et al, 1980). Although the channel does not conduct anions, neutral or cationic organic molecules as large as glucosamine have been shown to pass through its pore (Huang et al, 1978). Channel opening, which occurs in <100 µsec, is believed to require the cooperative binding of two ACh molecules (Dreyer et al, 1978; Dionne et al, 1978). In activated nAChRs, the elementary ACh-induced conductance (γ) is ~ 34 picoSiemens (pS) and the channel open time (τ) is ~ 1msec, corresponding to transport of $\sim 10^4$ monovalent cations (Sakmann, 1978). After activation, spontaneous channel closure is caused by the rapid dissociation of either of the two ACh molecules bound, which diffuse away and are immediately hydrolyzed by AChE present in the synapse (Leibowitz and Dionne, 1984).

In the continued presence of ACh or other agonists, the nAChR undergoes a transition into a desensitized state (Katz and

Thesleff, 1957). This transition involves a conformational change in the nAChR, which has been examined by various techniques such as, change in the protein's intrinsic fluorescence (Barrantes, 1978), initial rate of toxin binding (Sine and Taylor, 1979), stop-flow (Boyd and Cohen, 1980) and electron spin resonance (Weiland et al, 1976). The rate of desensitization depends on the agonist concentration and is enhanced by the presence of divalent cations or increased temperature (Rang and Ritter, 1970; Scubon-Mulieri and Parsons, 1977).

The desensitized conformation of the nAChR is characterised by a closed channel and increased binding affinity for agonists (~300 fold). Although activation is a very rapid process, complete in milliseconds, recovery from desensitization is slow, occurring over minutes. The two processes of activation and desensitization are believed to be effected through agonist binding to the same pair of ACh binding sites (Changeux et al, 1984; Hess et al, 1982), however, other authors have suggested the presence of additional distinct sites on the nAChR, through which desensitization takes place (Dunn et al, 1983; Raftery et al, 1984).

Compounds such as carbamylcholine (CCh), decamethonium and suberyldicholine, as well as ACh, are classical agonists of the nAChR and activate ion channel opening. Classical competitive antagonists of the nAChR are (+)-tubocurarine, hexamethonium, gallamine and α-bungarotoxin, which block agonist action and inhibit channel opening. The two ACh binding sites appear to differ significantly in their affinity for competitive antagonists, with occupation of one site sufficient to block nAChR activation (Neubig and Cohen,1979; Sine and Taylor, 1979).

Non-competitive antagonists are a heterogeneous group of compounds including local anaesthetics, histrionicotoxin, chlorpromazine and phencyclidine. These are thought to block ion translocation by entering and sterically blocking the ion channel and also by facilitating desensitization (Adams, 1981; Heidmann et al, 1983).

1.3 Use of snake venom α-neurotoxins

The discovery that snake venom α-neurotoxins (α toxins) specifically labelled nAChRs, has greatly facilitated the rapid advances made in their purification and characterization from vertebrate muscle and electroplax (Changeux et al, 1970). The α-toxins are small basic proteins with molecular weights of 6000-8000, and bind with high affinity and specificity to the ACh binding site in nAChRs, thereby blocking function (Lee, 1970). Two common examples are cobratoxin, purified from Naja naja siamensis venom (Karlsson et al, 1971) and α-bungarotoxin (α BuTX) from Bungarus multicinctus (Chang and Lee, 1963).

α-Toxins can be classified into two groups, based on polypeptide length. The "short" toxins have 60-62 amino acids and 4 disulphide bridges e.g. erabutoxin a, whereas the "long" toxins have 71-74 amino acids and 5 disulphide bridges e.g. α BuTX. The primary structures of many neurotoxins have been determined (review Dufton and Hider, 1983). The α-toxin molecules have been shown to possess multiple groups that can each interact with the nAChR, with disulphide bridges also playing an important role in maintaining the active configuration. Recent observations using chemical modifications of the toxins, have indicated that no single amino acid of the molecule was essential for toxin activity (Martin et al, 1983).

Three dimensional structure determination of many α-toxins have shown that they comprise 3 major polypeptide loops around a globular head, with the central, longest loop containing residues 21-40. The α BuTX molecule has been suggested to sit on top of the nAChR, about 55 Å above the plane of the membrane (Kistler et al, 1982), implying that its antagonist action is accompanied by conformational changes from the top of the receptor to the gating site of the channel. Localisation of the α BuTX binding site has shown it to be present on the α-subunit (see 1.4) of the nAChR (Tzartos and Changeux, 1983; Gershoni et al, 1983), although some studies found evidence of minor binding to other subunits (Oswald and Changeux, 1981; Mishina et al, 1984).

Initial attempts to tritiate α BuTX with ^{3}H-acetic anhydride gave low specific activities of ∿ 5Ci/mmol (Barnard et al, 1971), however, higher values of ∿60 Ci/mmol have been obtained since, using N-succinimidyl (2,3-^{3}H) propionate (Dolly et al, 1981). Radiolabelling with ^{125}I is more often used, as very high specific activities up to 1000 Ci/mmol can be obtained (Vogel et al, 1972; Lukasiewicz et al, 1978). Labelling of α-toxins with peroxidase, rhodamine, ^{3}H and ^{125}I has enabled the localisation and quantitation of nAChRs (Barnard et al, 1971; Berg et al, 1972; Schmidt and Raftery, 1973). Covalent coupling of α-toxins to an inert gel matrix by CNBr activation, has enabled purification of nAChRs by affinity chromatography (Karlsson et al, 1972; Schmidt and Raftery, 1972).

1.4 The muscle nAChR

The majority of studies have been on the nAChR from vertebrate skeletal muscle or muscle-derived tissues, such as the electroplax (electric organs) of freshwater teleosts (electric

eel) and marine elasmobranchs (electric ray). Electroplax cells have lost their contractile properties and become specialised in producing electric discharges (Krenz et al, 1980). Each cell receives dense cholinergic innervations resulting in 100mg of nAChR/kg of tissue(in electric rays).

Many reviews on the nAChR from muscle and electroplax are available (Karlin, 1980; Changeux, 1981; Conti-Tronconi and Raftery, 1982; Barrantes, 1983; Barnard and Dolly, 1984), therefore only a brief summary will be made.

1.4.1 Purification

Electroplax membranes in which 50% of the protein is nAChR, can be obtained by differential centrifugation (Sobel et al, 1977). Subsequent extraction of extrinsic proteins by a pH 7, low ionic strength treatment produces membranes containing nearly pure nAChR (Neubig et al, 1979).

Purification of detergent solubilized nAChR by affinity chromatography, can be achieved using various ligands immobilised on a gel matrix. Many ligands have been used, including toxins (Lindstrom et al, 1980a), monoclonal antibodies (mAbs, Momoi and Lennon, 1982), bromoacetylcholine (BAC, Reynolds and Karlin, 1978) and other cholinergic ligands (Michaelson et al, 1974). Most commonly used are toxin affinity columns, which are more stable and highly specific, whereas columns using ACh analogues are susceptible to the action of AChE. Biospecific elution of nAChR is achieved with high concentrations of competing cholinergic ligands. The nAChR's property as a glycoprotein has also been utilised by the use of lectin columns followed by elution with glycosides (Sumikawa et al, 1982a).

A substantial reduction in activity (and yield) during

purification is due to proteolysis of the nAChR (Lindstrom et al, 1980b; Shorr et al, 1981). The cytoplasmic surface of the nAChR is more susceptible to proteolysis than its extracellular surface (Klymkowsky et al, 1980). Inadequate control of proteolysis in early studies led to ambiguities about its subunit structure. Most procedures now use a range of protease inhibitors including ethylene diamine tetraacetate, Na salt (EDTA) to inhibit divalent cation-activated proteases and phenylmethyl sulphonyl fluoride (PMSF) to inactivate serine proteases.

^{125}I-radiolabelled α-toxin binding is routinely used for quantitation of nAChR content throughout purification. Membrane nAChR is assayed by filtration through glass fibre filters, whilst soluble nAChR can be assayed by retention of toxin-nAChR complex on DEAE cellulose filter discs (Schmidt and Raftery, 1973).

Purification by affinity chromatography has yielded preparations with specific activities ranging from 5-10 μmoles of toxin binding sites/g of protein. The expected value for an nAChR monomer of molecular weight 280,000 containing 2 toxin binding sites is ∿7 μmoles/g protein.

1.4.2 Properties and structure

Solubilised nAChRs from Torpedo (electric ray) species are present in monomeric and dimeric forms with sedimentation coefficients of 9S and 13S, respectively. Reduction with dithiothreitol (DTT) converts the 13S dimers into 9S monomers without loss of function (Anholt et al, 1980). Vertebrate muscle nAChRs are found to display only the 9S monomeric forms on sedimentation analysis (Shorr et al, 1981; Gotti et al, 1982).

The isoelectric point (pI) of nAChRs from all sources are similar, with values ranging from 4.9-5.3 (Sobel et al, 1977; Barnard et al, 1978) Molecular weight estimates by chemical cross-linking of the nAChR, followed by gel electrophoresis, have yielded values of ~270,000 (Lo et al, 1982; Hucho, et al, 1978), whereas estimates of 300,000 - 400,000 were obtained from gel filtration (Colquhoun and Rang, 1976; Dolly and Barnard, 1977). The Stokes radius (S_r) of the nAChR in detergent, has been shown to be ~73Å (Meunier et al, 1973; Reynolds and Karlin, 1978). The subunit structure of the electroplax nAChR, appears as four polypeptide bands on SDS-polyacrylamide gels, with apparent molecular weights of 40,000 (40K), 50,000 (50K), 57,000 (57K) and 64,000 (64K) designated α,β, γ and δ, respectively (Karlin et al, 1976; Lindstrom et al, 1978). Amino-terminal amino acid analysis of the subunits, after extraction from SDS gels, have shown that the subunit stoichiometry for α:β:γ:δ is 2:1:1:1 (Raftery et al, 1980; Conti-Tronconi et al, 1982b).

Although early studies reported that mammalian muscle nAChR subunit patterns consisted of less than four polypeptides, it is now generally agreed this was due to partial degradation of the higher molecular weight subunits and that these nAChRs also comprise 4 subunits in the α_2 β γ δ stoichiometry (Merlie and Sebbane, 1981; Einarson et al, 1982).

Electron microscopy of negatively stained electroplax membranes show the nAChRs as 80-90Å diameter, doughnut shaped particles each containing a 20Å wide central pit, and at a surface density of ~10,000 nAChRs/μm^2 (Heuser and Salpeter, 1979; St. John et al, 1982). X-ray diffraction and low angle neutron scattering data suggest that nAChRs traverse the membrane, with an overall length of ~110Å, protruding 55Å

extracellularly and 15Å towards the cytoplasmic side (Klymkowsky and Stroud, 1979; Wise et al, 1979). Kistler et al (1982) have proposed that all 5 subunits line up across the membrane like the staves of a barrel (Fig 1.1). The precise topographic distribution of subunits around the central pit is not clear (Zingsheim et al, 1982a,b), although Karlin et al (1983), recently found evidence for an $\alpha\ \gamma\ \alpha\ \beta\ \delta$ arrangement based on crosslinking evidence.

1.4.3 Recent advances

Application of molecular genetics techniques has had a major impact on nAChR studies. When messenger RNA (mRNA) extracted from Torpedo electroplax was translated in a conventional cell free system, no nAChR activity was produced (Mendez et al, 1980). However, when the same mRNA was microinjected into Xenopus oocytes (Gurdon et al, 1971), incorporation of newly synthesized nAChRs into the oocyte membrane was observed (Sumikawa et al, 1981a). This nAChR possessed all the physical properties characteristic of native nAChRs, and was further shown to have a functional cation channel (Barnard et al, 1982). Similar studies with mammalian muscle mRNA have been made, which also found synthesis of functional nAChRs (Miledi et al, 1982).

From the N-terminal sequencing studies of nAChR subunits (Raftery et al, 1980), DNA hybridisation probes were constructed and used to screen cDNA libraries derived from nAChR mRNA. In this way, the cDNA coding for the α subunit precursor of Torpedo marmorata nAChR was identified and sequenced (Sumikawa et al, 1982b; Devillers-Thiery et al, 1983). cDNA encoding the α,β,γ and δ subunit precursors of Torpedo californica nAChR have similarly been isolated (Claudio et al, 1983; Noda et al, 1982,

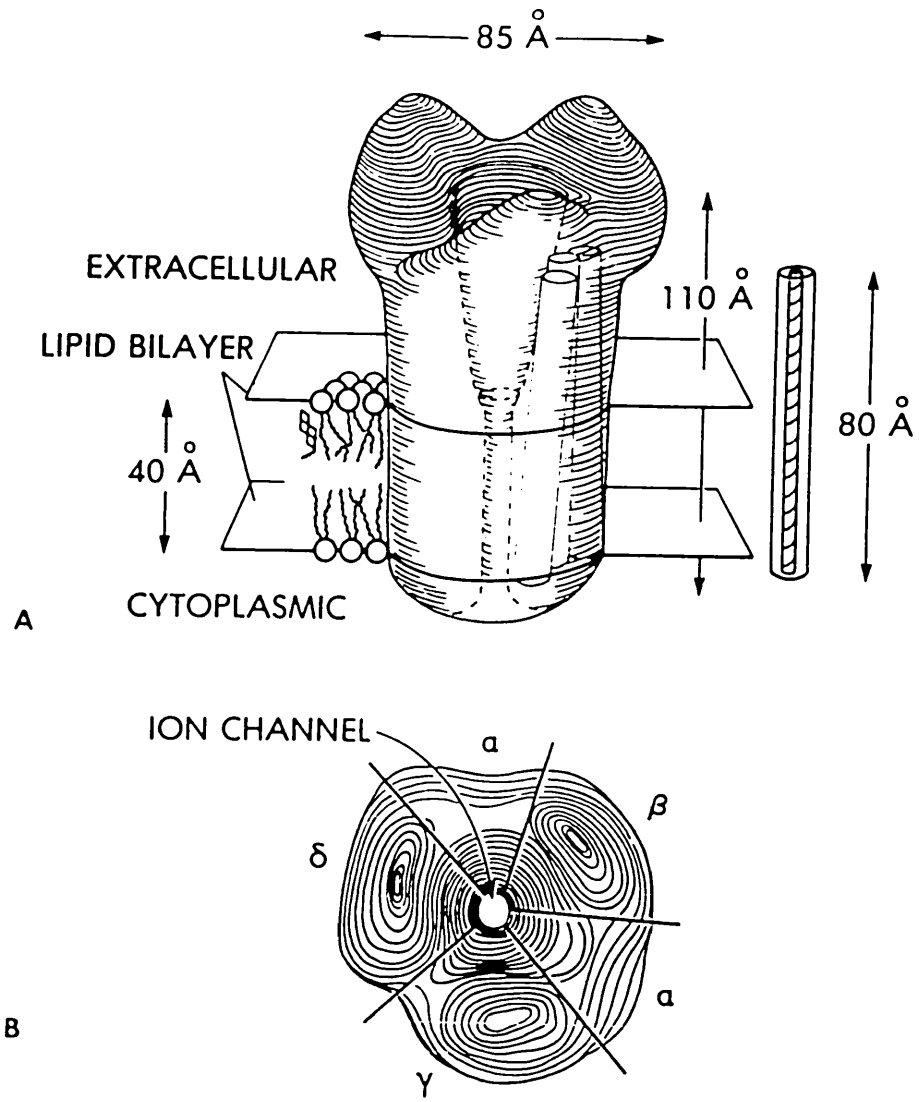

Fig 1.1 A three dimensional model for the nAChR molecule in the lipid bilayer

(A) Side view showing elongated shape of subunits arranged perpendicular to the membrane channel.

(B) View from synaptic side with borders arbitrarily drawn between subunits and tentative assignment of subunit positions (from Kistler et al, (1982).

1983a,b). From the cloned cDNA for the T. californica nAChR subunits, Numa and colleagues made probes to screen mammalian muscle cDNA libraries. They thus isolated the cDNA encoding the α, β and γ subunit precursors of calf muscle nAChR (Noda et al, 1983c; Tanabe et al, 1984; Takai et al, 1984), as well as the cDNA for the α subunit of human muscle (Noda et al, 1983c).

Alignment of the cDNA deduced amino acid sequences of all four subunit precursors of T. californica nAChR, shows extensive homology between them, with 19% of the positions having identical residues and 54% of positions having conservative substitutions (Noda et al, 1983b). Homology between similar subunits is even greater. An α subunit sequence comparison shows identical homology of 80%, 81% and 97% between the Torpedo / human, Torpedo / calf and human/calf pairs, respectively.

1.5 The putative neuronal nAChR

In contrast to the nAChR of muscle and electroplax, advances in the study of neuronal nAChRs have been much slower. Although neuronal nAChRs have been demonstrated electrophysiologically in many parts of the brain (Bland et al, 1974; Miledi and Szczepaniak, 1975; Bradley and Dray, 1976; Schmidt and Freeman, 1980), progress in its research has been hindered by the absence of an antagonist that both binds to neuronal nAChRs and blocks its physiological activity.

1.5.1 The controversial nature of neuronal αBuTX binding sites

The snake toxin α BuTX is known to bind with high affinity and specificity to muscle nAChRs, thereby blocking ion channel function (1.2 and 1.3). Similarly, high affinity binding sites for α BuTX have been displayed in brain membranes from

vertebrates and invertebrates, as well as neuronal cell cultures (reviews Oswald and Freeman, 1981a; Morley and Kemp, 1981). However, the identification of these sites as nAChRs is still controversial since α BuTX fails to block synaptic transmission at most known nicotinic cholinergic sites in the CNS and ANS. For this reason many authors have suggested that nAChRs are distinct molecules from the α BuTX binding sites, which are not directly involved in nAChR function. Conclusions of other authors have opposed this view on the basis of the striking similarity, in binding and molecular properties, of neuronal α BuTX sites and muscle nAChRs. Although various lines of evidence have been used for, and against, calling the neuronal α BuTX binding site a nAChR, reference to this entity in the text will be as the putative nAChR (pnAChR) or α BuTX binding protein.

1.5.2 Localisation

Localisation of the pnAChR has been approached using a variety of techniques including subcellular fractionation, histological dissection followed by biochemical assay, autoradiographic localisation and electron microscopic localisation.

Subcellular fractionation of rat brain homogenates by Salvaterra *et al* (1975), Eterovic and Bennett (1974) and Tindall *et al* (1978), has indicated that toxin binding occurs mainly to the isolated synaptosomal fraction described by Gray and Whittaker (1962). The high levels of binding found in microsomal fractions in most reports were further analysed by sedimentation in sucrose gradients, and found also to be derived from Grays Type II synaptic structures (De Blas and Mahler, 1978).

These results are in accord with the observation by Yoshida and Imura (1979), that the majority of nicotine binding in rat brain also occurred in the synaptosomal fraction.

Histological dissection of rat brain regions followed by α BuTX binding assays, have shown that the highest levels of binding occur in the hippocampus and colliculi, with moderate levels in the cerebral cortex and very low levels in the cerebellum (Schechter et al, 1978; Morley et al, 1977; Segal et al, 1978). Similar patterns were reported for dissections of mouse brain regions (Salvaterra and Foders, 1979). Studies in the chick, toad and goldfish brain have found highest levels of binding occurring in the optic lobes, with lowest levels again in the cerebellum (Kouvelas and Greene, 1976; Oswald and Freeman, 1981b; Salvaterra and Foders, 1979).

Autoradiographic localisation using ^{125}I-α BuTX, has allowed a comprehensive analysis of the binding patterns in rat brain (Hunt and Schmidt, 1978,1979). These show that the major regions of binding correspond to the sensory (e.g. superior colliculus - homologue of the optic tectum in lower vertebrates) and limbic (e.g. hippocampus) areas. In similar studies on chick, toad and goldfish brain, toxin binding within the optic lobes was found to occur in discrete layers of the tectal neuropil (Freeman and Lutin, 1975; Oswald et al, 1980). Polz-Tejera et al (1975) suggested that these sites were localised on the radial dendrites of tectal cells.

Ultrastructural localisation showed that ^{125}I-α BuTX labelling occurred predominantly at synaptic regions in rat and mouse brain (Arimatsu et al, 1978; Hunt and Schmidt, 1978). In several studies with peroxidase-conjugated α BuTX, labelling was further localised to the postsynaptic membrane in chick optic

tectum (Barnard et al, 1979), rat brain (Lentz and Chester, 1977) and frog sympathetic neurons (Marshall, 1981). However, two recent reports have presented evidence for an extrasynaptic localisation of α BuTX sites. Using peroxidase-conjugated α BuTX (Jacob and Berg, 1983) and ^{125}I-α BuTX (Fumagalli and DeRenzis, 1984) on chick ciliary ganglion neurons and rat superior cervical ganglion neurons respectively, specific labelling confined only on neuronal cell bodies was found, with no significant labelling occurring at synapses.

Although there are considerable regional variations, the overall concentration of pnAChRs in brain tissues is generally low. Values for tissue homogenates range between 1 and 5 pmoles of toxin binding/g of tissue wet weight (Table 1.1), significantly less than in electroplax. This is in close agreement with the value of 3pmoles/g estimated for nicotine binding sites in mouse brain by Schleifer and Eldefrawi (1974). The optic lobes of lower vertebrates (chick, toad and goldfish) appear to be an exception, with significantly higher levels of toxin binding present (Table 1.1). The ontogeny of these sites has been studied in chick brain and shown to vary enormously, with peak concentrations, (in terms of toxin binding/g of tissue wet weight), occurring just before hatching (Wang et al, 1978).

1.5.3 Electrophysiology

Intracellular recording techniques have shown that addition of α BuTX sufficient to saturate nAChR sites on Renshaw cells (Curtis and Crawford, 1969; Duggan et al, 1976), sympathetic neurons (Carbonetto et al, 1978; Kouvelas et al, 1978, parasympathetic neurons (Ascher et al, 1979; Chiappinelli et al, 1981) and the pheochromocytoma cell line, PC 12 (Patrick and Stallcup, 1977a) has no detectable effect on the excitatory

Table 1.1 Levels of αBuTX binding in brain

Source	pmols/g tissue wet weight	Reference
Rat		
Superior colliculus	3.7	Morley et al (1977)
Hypothalamus	3.5	" "
Hippocampus	2.5	" "
Reticular formation	2.0	" "
Caudate	0.7	" "
Superior olivary complex	0.6	" "
Septum	0.4	" "
Cerebellum	0.04	" "
Whole brain	0.75	Lowy et al (1976)
" "	2.0	Moore + Brady (1976)
" "	2.2	Schmidt (1977)
Mouse		
Whole brain	1.7	Seto et al (1977)
Chick		
Whole brain	4.6	Norman et al (1982)
Optic lobe	26.0	" "
Toad		
Whole brain	1.0	Oswald + Freeman (1981b)
Optic lobe	10.0	Salvaterra + Foders (1979)
Goldfish		
Whole brain	1.1	Oswald + Freeman (1979)
Optic lobe	80.0	Salvaterra + Foders (1979)

nicotinic ACh response. Similar results were found for retinal neurons in culture (Betz, 1981).

Reports of electrophysiological studies on rat superior cervical ganglion neurons have been more equivocal. Brown and Fumagalli (1977) found α BuTX was ineffective on this ganglion, when tested in vitro, but when tested in vivo by intracarotid injection, Toldi et al (1983) reported observing toxin inhibition of nicotinic transmission.

Two proposals have been made to account for the lack of electrophysiological effect of α BuTX. Carbonetto et al, (1978) have suggested that α BuTX does not bind to neuronal nAChRs but to an "α BuTX receptor", whilst Betz (1981) proposed that α BuTX does bind to neuronal nAChRs but without affecting their physiological function.

Although the majority of studies show no effect of α BuTX on neuronal nAChR function, there have been several important exceptions. The ACh response in the frog sympathetic ganglion (Marshall, 1981) and human medulloblastoma cell line, TE671 (Syapin et al, 1982) were both shown to be blocked by application of α BuTX. Also, using current source density measurements (Freeman and Nicholson, 1975), retinotectal synaptic transmission in the optic lobes of toad, goldfish and pigeon was shown to be blocked by application of 10^{-6}M α BuTX (Freeman et al, 1980; Schmidt and Freeman, 1979). This observation, combined with the increased levels of α BuTX binding found in lower vertebrate optic lobes and rat brain superior colliculus, were suggested to indicate that these regions do contain functional neuronal nAChRs.

1.5.4 Properties of α BuTX binding

1.5.4.1 Pharmacology

Interactions of various drugs with the pnAChR have been investigated by measuring the inhibition of α BuTX binding produced by addition of each drug. Studies on rat brain have shown that the α BuTX binding site displays a pharmacology very similar to the classical nicotinic pharmacology of muscle nAChRs. The nicotinic agonist and antagonist, nicotine and (+)-tubocurarine, respectively, were the two most potent inhibitors of α BuTX binding, whilst muscarinic ligands and other putative neurotransmitters diplayed only very weak inhibition (Table 1.2). One exception, was the potent muscle nAChR agonist, decamethonium, which displayed a relatively weak effect on the neuronal pnAChR.

1.5.4.2 Kinetics

The binding of α BuTX to brain pnAChR displays many kinetic similarities to binding to muscle nAChR. Apparent equilibrium dissociation constants (K_D) of 10^{-9}-10^{-10} M have been found for the high affinity α BuTX binding sites in most studies on CNS membranes (Table 1.3). This is similar to the 10^{-11}-10^{-12} M value observed for muscle nAChRs.

The slightly lower K_D values for the neuronal pnAChR are due to a difference in the dissociation, rather than association kinetics of binding. α BuTX binding to muscle nAChR is only very slowly reversible, with $t_{1/2}$>100 hours (Brockes and Hall, 1975), whereas dissociation of α BuTX from neuronal binding sites is much more rapid, with $t_{1/2}$ of 2-5 hours found in most studies (Table 1.3). The study of α BuTX binding to rat brain by Lukasiewicz and Bennet (1978) is an exception however, with a

Table 1.2 K_I of various ligands for neuronal α BuTX binding sites (μM)

Ligand	1	2	3	4	5	6
Nicotine	0.33	0.25	1.9	0.01	0.93	
(+) tubocurarine	4.0	0.19	3.1	0.04	0.2	0.22
Gallamine	3.82	3.5				
Tetramethylammonium		19.0	20.0			
Acetylcholine		37.5	30.0			0.47
Decamethonium	339	26.6	500		0.18	2.1
Carbamylcholine		63.5	90	1.26	0.12	3.5
Hexamethonium	708	251	900	11.2	120	118
Atropine			1600	104		
Scopolamine		376				

K_I = concentration of ligand at which α BuTX binding is reduced to 50%, determined either by equilibrium binding or initial binding rate.

1 Chick optic lobe, M - Norman, (1981).

2 Chick optic lobe, D - Wang et al, (1978).

3 Rat brain, M - Schmidt, (1977).

4 Goldfish brain, M - Oswald and Freeman, (1979).

5 T. californica electroplax, M - Blanchard et al, (1979).

6 Rat diaphragm muscle, M - Colquhoun and Rang, (1976).

M = membranes

D = detergent solubilised membranes

Table 1.3 Binding properties of neuronal α BuTX binding sites

	K_D(nM)	$t_{1/2}$(hrs)	$k_1 x10^5$ ($M^{-1}S^{-1}$)	$k_{-1} x10^5$ (S^{-1})	T(°C)
Rat Brain					
1	0.04	3.5	13.5	5.8	23
2	0.32	15.6	0.38	1.23	23
3	0.056	5.1	6.8	3.8	23
Chick					
4	0.13	2	7.4	9.6	23
5	1.1	4.2	40	4.6	23
6	0.57	1.5	1.76	3.78	21
7	0.18	3.1	3.67	6.49	25

1 M - Schmidt, (1977).

2 D - Salvaterra and Mahler, (1976).

3 D - Lowry *et al*, (1976).

4 Brain, D - Kouvelas and Greene, (1976).

5 Sympathetic ganglion, M - Betz, (1981).

6 Embryo retina, M - Betz, (1981).

7 Optic lobe, D - Norman, (1981).

M = membranes

D = detergent solubilized membranes

reported $t_{1/2}$ of 62.3 hours.

The important observation of Schmidt (1977) and Lukas et al (1979), that rat brain α BuTX binding sites display a time-dependent increase in affinity for nAChR agonists, suggests that this phenomenon could be related to the process of receptor desensitization, characteristically observed in muscle nAChRs (Heidmann and Changeux, 1978).

1.5.5 Biochemical characterisation

Many striking similarities have been found between muscle nAChRs and the neuronal pnAChR in several biochemical studies. These have included determination of Stokes radius, hydrodynamic properties, pI and lectin binding ability (Table 1.4). Isoelectric focussing determinations of the neuronal pnAChR have all observed a pI in the region of 5, identical to the pI of the muscle nAChR (Barnard and Dolly, 1982). In most hydrodynamic studies however, the neuronal pnAChR displays a greater sedimentation velocity in sucrose gradients, than muscle nAChRs, with reported molecular weight (MW) estimates of 340,000 and 357,000 for rat and goldfish brain pnAChR, respectively, after correction for bound detergent (Salvaterra and Mahler, 1976; Oswald and Freeman, 1979).

The presence of sugar residues on neuronal pnAChRs has been confirmed by their binding to the plant lectins, Concanavalin A (Con A), lentil lectin (LCH), wheat germ agglutinin (WGA) and castor bean lectin (CBL), indicating the presence of mannosyl, glucosyl and galactosyl sugar groups (Table 1.4). This is consistent with similar analyses of muscle nAChRs, which has shown the presence of all these sugars, as well as N-acetyl neuraminic acid (Vandlen et al, 1979). Similarly, the Stokes

Table 1.4 Biochemical properties of neuronal α-BuTX binding proteins

		pI	Sedimentation coefficent	Lectin binding	Stokes radius (Å)
1.	Guinea pig	4.8	N/D	N/D	N/D
2.	Rat	4.9	11.4	N/D	70-80
3.	Mouse	4.9	N/D	LCH/Con A	70-80
4.	Goldfish	5.0	11.4	N/D	74
5.	Chick	5.4	11.8/9.1*	LCH/Con A	N/D

1 Cerebral cortex - Bosmann, (1972).

2 Whole brain - Lowy et al, (1976).

3 Whole brain - Seto et al, (1977,1981).

4 Whole brain - Oswald and Freeman, (1979).

5 Optic lobe (apparent sedimentation coefficients given) - Norman, (1981).

All values determined in Triton X-100

N/D = not determined

LCH = lentil lectin

Con A = Concanavalin A

* = Value reported in Lubrol PX

radius observed for neuronal pnAChRs (70-80 Å) is almost identical with that for muscle nAChRs.

The subunit structure reported for neuronal pnAChRs has however, been less consistent than its other properties. Seto et al (1981) and Norman et al (1982) both reported affinity purifications resulting in the observation of a single subunit pattern for rat brain (51,000) and chick optic lobe (54,000) pnAChRs, respectively. However, another group, also used chick optic lobes and found at least three subunits of 57,000, 35,000 and 25,000 by affinity labelling with ^{125}I-α BuTX followed by covalent cross linking (Betz et al, 1982). In a more recent study of the chick optic lobe pnAChR, Mehraban (1983) concluded that there were at least two subunits of 54,000 and 57,000, after ^{125}I-iodination of the pnAChR purified by affinity chromatography. In only one study has a 4 subunit pattern, analogous to the muscle nAChR, been found. Kemp et al (1980) reported that subunits of 44,000, 50,000, 56,000 and 62,000 were present in the rat brain pnAChR after affinity purification. These inconsistent findings for the pnAChR, are similar to early reports on purification of muscle nAChRs (Conti-Tronconi and Raftery, 1982). Problems of proteolysis were the cause of those discrepancies (Lindstrom et al, 1980b) and suggest that the neuronal pnAChR may also be a multisubunit oligomer.

One consistent finding however, has been the presence of a disulphide bond associated with the α BuTX binding site of the neuronal pnAChR (Lukas and Bennett, 1980a,b; Norman et al, 1982; Leprince, 1983). A disulphide bond is also known to be associated with the ACh binding site in muscle nAChRs (Karlin, 1969). On reduction of this disulphide with DTT, both the nAChR and neuronal pnAChR display changed affinities for agonists

(Lukas and Bennett, 1980a). After disulphide bond reduction, nAChR sulphydryls can be alkylated by radiolabelled affinity reagents such as 4-(N-maleimido) benzyltrimethylammonium (MBTA) or bromoacetylcholine (BAC) (Karlin et al, 1976; Wolosin et al, 1980). The observation that the purified neuronal pnAChR from chick optic lobe and chick brain also reacted with BAC after reduction, gives further support for the nAChR identity of this protein (Norman et al, 1982). The latter authors further showed that a subunit of 54,000 molecular weight was specifically labelled, since no labelling with BAC occurred in the presence of excess (+) tubocurarine or α BuTX, or without prior disulphide bond reduction.

1.5.6 Regulation and experimentally induced changes

In skeletal muscle, denervation induces a proliferation of extrajunctional nAChRs over the entire muscle fibre surface (review Fambrough, 1979). In a study on the superior cervical ganglion in rat, ganglionic denervation produced no apparent changes in the level of α BuTX binding (Fumagalli et al, 1976). Similarly, denervation studies in rat hippocampus found that denervating cholinergic synapses abolished nAChR activity, but had no effect on α BuTX binding (Dudai and Segal, 1978; Hunt and Schmidt, 1979). This was suggested to indicate that, in contrast to muscle nAChR regulation, loss of presynaptic input in brain had no marked effect on postsynaptic receptors, assuming that neuronal nAChRs were localized postsynaptically.

Different findings have been reported for the regulation of cholinergic pathways in the optic lobes of lower vertebrates. These pathways were lesioned by crushing the optic nerve or complete removal of the eye, and found to result in 30-60% loss

of α BuTX binding (Brecha et al, 1979; Schechter et al, 1979; Oswald et al, 1980). Subsequent regeneration of the optic nerve in goldfish, was observed to parallel the reappearence of α BuTX binding in the optic lobes (Schechter et al, 1979). These studies suggested that if α BuTX does bind to the neuronal nAChR, then denervation effects are not analogous to those in muscle.

In a recent study using chick ciliary ganglion neurons in culture, the sites responsible for ACh sensitivity and α BuTX binding, were suggested to be associated with separate membrane proteins (Smith et al, 1983). It was found that in neurons grown in the presence of embryonic eye extract, ACh sensitivity, measured electrophysiologically, was increased, whilst α BuTX binding was decreased, whereas neurons grown in medium containing high K^+ ion concentrations displayed the reverse. However, a similar study on cultured chick embryo retinal neurons, concluded that regulation of the α BuTX binding protein was analogous to regulation of the muscle nAChR (Betz, 1983).

1.5.7 Immunology

A possible alternative to α BuTX for identifying a pnAChR in neuronal tissues, is the use of anti-muscle nAChR antibodies. Patrick and Stallcup (1977a,b) reported that ACh-induced flux of $^{22}Na^+$ into PC 12 cells was blocked by an anti-eel electroplax nAChR antiserum, whilst α BuTX had no effect. They also found that the antiserum could not precipitate the α BuTX binding protein. Using a series of monoclonal antibodies (mAbs) to various muscle nAChRs, Swanson et al (1983) tested the possibility of cross reactivity with neuronal nAChRs. Several mAbs were found to specifically label in chick optic lobes, however, comparison with ^{125}I-α BuTX labelling, showed very

little overlap in the pattern of labelling. Similarly, Jacob et al (1984), found that muscle nAChR mAbs produced a different labelling pattern to that of α BuTX, in chick ciliary ganglion neurons. These reports all concluded that the neuronal nAChR was distinct from the pnAChR identified by α BuTX binding. However, similar reports by other authors indicating the opposite have also been made. Schwartz et al (1980), using anti-eel nAChR antiserum, found that the antibody and α BuTX binding patterns were identical, in cultured goldfish optic nerve and ganglia. They also observed a parallel decrease in binding of the antibody and toxin, after optic nerve crush. Also, rat brain α BuTX binding proteins have been shown to be immunoprecipitated by antisera to both electroplax nAChRs and rat muscle nAChRs. Block and Billiar (1979) found 60% of the α BuTX binding sites from solubilised rat brain hypothalamus was immunoprecipitated by anti-electroplax nAChR antiserum, whilst Mills and Wonacott (1984) observed immunoprecipitation of 75% of the α BuTX binding protein in rat brain by an anti-rat muscle nAChR antiserum. Interestingly, the latter antibodies were also able to precipitate 100% of electroplax nAChRs.

Similarly, two mAbs to chick muscle nAChR have been shown to crossreact with the pnAChR in chick optic lobes and chick brain, although only 15% of these could be immunoprecipitated (Mehraban et al, 1984).

1.6 The present study

The above review gives a clear indication of the lack of uniformity resulting from the various reports on the neuronal α BuTX binding protein relative to muscle nAChRs.

This study was initiated following the important findings

in this laboratory (Norman et al, 1982), that the pnAChR from chick optic lobes, could be purified to homogeneity, was sensitive to cholinergic ligands, and could be specifically labelled by BAC. This, together with the reports of α BuTX blocking the ACh response in retinotectal synapses of lower vertebrates (Freeman et al, 1980), suggested that this protein is a true nAChR.

The aim of this project was to elucidate further biochemical and structural information on the chick optic lobe pnAChR. The approach to determining the molecular weight of the pnAChR from optic lobe, entailed determination of its Stokes radius followed by its sedimentation coefficient, after correction for bound detergent (Chapter 2).

After purification by affinity chromatography, the subunit structure was analysed, followed by larger scale purifications to enable amino acid sequence analysis of the isolated subunits (Chapter 3).

Finally, expression of the pnAChR in oocytes microinjected with optic lobe mRNA was studied by immunoprecipitation and metabolic labelling (Chapter 4).

CHAPTER 2 OLIGOMERIC CHARACTERISATION OF THE CHICK OPTIC LOBE pnAChR

2.1 MATERIALS

Bungarus multicinctus venom was purchased from Miami Serpentarium, Florida, USA. ^{125}I-α BuTX, 200-300 Ci/mmol, was a gift from N. Ray, (synthesized by the iodine monochloride method of Vogel et al, 1972), or was purchased from Amersham International (230 Ci/mmol). All protease inhibitors, enzymes, deuterium oxide (D_2O), Lubrol PX and carbamylcholine chloride (carbachol) were purchased from Sigma. Other materials were Triton X-100, Rohm and Haas; Sepharose 4B, Pharmacia; Ultrogel, LKB; DE 81 discs, Whatman and CNBr, BDH. All other chemicals were of analytical grade. Chicks were obtained from local farms and Torpedo marmorata from Arcachon, France.

2.2 METHODS

2.2.1 Preparation of α BuTX

α BuTX from Bungarus multicinctus venom was routinely prepared in this laboratory by Mr. J. Skinner, using the procedure of Lee et al, (1972).

Crude venom was fractionated by cation exchange chromatography on CM-Sephadex C-50 followed by refractionation of peak 2 on CM-52 cellulose. The main peak, 2.1 (α BuTX), was pooled and checked for purity by isoelectric focussing (pH 9-11), SDS gradient gel electrophoresis and HPLC sizing column (Waters I-125 x 2).

2.2.2 Preparation of α BuTX-Sepharose

Pure α BuTX was covalently coupled to CNBr-activated Sepharose 4B by the method of March et al, (1974).

Cyanogen bromide (CNBr) dissolved in acetonitrile (2g/ml), was added (0.05 vol/vol of suspension) to a 25% (v/v) Sepharose 4B suspension in 1M Na_2CO_3. After 3 minutes of vigorous stirring the Sepharose was filtered, washed rapidly with,

(a) 25 bed volumes (b/vol) of 0.1M $NaHCO_3$ pH 9.5,

(b) 25 b/vol of distilled water and

(c) 10 b/vol of 0.1M $NaHCO_3$ pH 9.5,

then added to 1 b/vol of 0.1M $NaHCO_3$ containing α BuTX (1mg/ml).

The coupling mixture was roller shaken overnight (~16 hours) at 4°C, then filtered and resuspended in 2 volumes of 1M glycine, 0.1M $NaHCO_3$ pH 9.5 for 4 hrs to block any remaining active groups. The α BuTX-Sepharose was finally washed sequentially with

(a) 10 b/vol of 1M NaCl, 0.1M $NaHCO_3$ pH 9.5,

(b) 10 b/vol of 1M NaCl, 0.2M CH_3COONa pH 4.5,

(c) 20 b/vol of distilled H_2O

and stored at 4°C in 0.05M Na phosphate pH 7, containing 0.02% sodium azide (NaN_3).

Before use, α BuTX-Sepharose was washed with 50 b/vol of 0.5M NaCl, 0.05 M Na phosphate pH 7, and equilibrated in buffer A (2.2.4)

2.2.3 Preparation of DNase-1-Sepharose

DNase-1-Sepharose (1mg/ml) was prepared by CNBr activation as for α BuTX-Sepharose preparation, except for a coupling pH of 8.4.

2.2.4 Preparation of pnAChR from optic lobes

One day post-hatch chicks (White Leghorns) were decapitated, whole brain and optic lobes dissected and immediately frozen in liquid N_2.

Optic lobes were homogenized in 10 volumes of ice cold buffer A (Na phosphate 50 mM, EDTA 5 mM, EGTA 1 mM, PMSF 1 mM, benzamidine 1 mM, bacitracin 100 µg/ml, soybean trypsin inhibitor 25 µg/ml pH 7.5) by 10 passes through a Teflon pestle homogeniser. All subsequent steps were performed at 4°C. After centrifugation (100,000g, 30 minutes) of homogenate, the membrane pellet was rehomogenised in 5 volumes of buffer A containing 1% (w/v) Triton X-100. Membranes were solubilised for 1 hour, then recentrifuged as above, and the supernatant incubated on shaking rollers, with 0.01 volumes of α BuTX-Sepharose for 4 hours. The affinity resin was then packed into a column and washed sequentially with:

a) 20 b/vol of buffer A, 0.2% Triton

b) 100 b/vol of buffer A, 0.2% Triton, 1M NaCl

c) 40 b/vol of buffer A, 0.2% Triton

Finally, the resin was twice eluted with 1 b/vol of 1M carbachol in buffer A, 0.2% Triton for 2 hours. Carbachol eluates were pooled and, where indicated, incubated with 0.1 volumes of DNase-1-Sepharose for 30 minutes. Eluates were then dialysed extensively (5 x 2 litre changes over 24 hours) against 10 mM Na phosphate, 50 mM NaCl, 0.1% Triton X-100 pH 7.5. Dialysed eluate was used immediately or stored at 4°C for up to 1 day.

Preparation of pnAChR using Lubrol PX (5%, w/v) instead of Triton X-100, was carried out as above, except for a longer membrane solubilisation time of 2 hours.

2.2.5 Assay of soluble pnAChR

Receptor assays were performed by the method of Dolly and Barnard (1977) with small modifications. α BuTX binding was measured by incubating soluble samples (100-150 µl) in 10 nM ^{125}I-α BuTX for 1hr at 23°C. Aliquots (60-100 µl) were pipetted onto Whatman DE 81 discs (2.3 cm), left for 1-2 minutes, then washed (x3, 4 minutes each) in 300 ml of ice cold 25 mM Na phosphate, 0.2% Triton X-100 pH 7. Discs were dried under an infra-red lamp and counted in a gamma counter with counting efficiency of 45-50%. All assays were performed in triplicate. Non-specific binding was determined in the presence of 5 µM α BuTX, which was added 15 minutes before ^{125}I-α BuTX. Specific binding was defined as the total minus non-specific binding.

2.2.6 Assay of pnAChR in optic lobe membranes

The filtration apparatus used, consisted of a PVC filtration manifold, attached via a waste liquid trap, to an electric vacuum pump.

Optic lobe membranes (100-150 µl) were incubated with 10nM ^{125}I-α BuTX for 1 hour at 23°C, then filtered under reduced pressure through presoaked Whatman GF/C (2.4 cm) filters. After rapid washing with 3x5ml of cold 50mM Na phosphate pH 7, filters were dried under an infra red lamp and counted in an LKB Wallac gamma counter.

Non-specific binding was determined by pre-incubation of membranes with 5µM α BuTX for 15 minutes before addition of hot toxin, then filtered as above. Gamma counter counting efficiency was 45-50%.

2.2.7 Sucrose density gradient centrifugation

Linear gradients of 5-20% sucrose (12 ml) in buffer A (2.2.4) containing 0.05 M NaCl, 0.2% Triton X-100, were poured onto a 60% sucrose cushion (0.5 ml) using a Buchler gradient maker. Dialysed eluate samples (0.2 ml, ~8 pmol pnAChR) containing catalase (0.2 mg), were carefully layered onto the gradient meniscus, then centrifuged at 100,000g for 17 hours at 5°C in a SW40Ti rotor, with slow acceleration and deceleration. Fractions were collected with a Buchler gradient fractionator and 60-100 µl aliquots assayed for ^{125}I-α BuTX binding activity (2.2.5). For sedimentation coefficient ($s_{20,w}$) calibration of gradients, the soluble enzyme markers horse liver alcohol dehydrogenase, 4.8S (5 units), bovine liver catalase, 11.3S (0.2 mg) and E. coli β-galactosidase, 16S (10 units) were run in parallel gradients on the same rotor.

For calculation of the $s_{20,w}$, sedimentation analysis of the pnAChR was performed in sucrose/D_2O gradients. Centrifugation in D_2O was as above, except that D_2O gradients were made immediately before use, due to its hygroscopicity.

2.2.8 Gel filtration chromatography

An Ultrogel (ACA 22) column, 50 X 1.5 cm, was washed and equilibrated at 4°C in running medium (Na phosphate 50 mM, 0.5% Triton X-100, pH 7.5). Dialysed pnAChR samples (1 ml, ~20 pmol pnAChR) were loaded and 1 ml fractions collected (Gilson Microcol) at a flow rate of 20 ml/hour. Aliquots (0.15 ml) of each fraction were assayed for α BuTX binding activity (2.2.5).

Soluble enzymes, bovine thyroglobulin, E. coli β-galactosidase, bovine liver catalase, horse liver alcohol dehydrogenase and chicken ovalbumin were run under identical

conditions to produce a calibration curve for the column. Blue dextran (10µg) and ^{3}H-GABA (1µCi) were used to estimate the void volume (Vo) and total included volume (V_t), respectively.

2.2.9 Protein determination

Solubilised membrane protein concentrations were determined by the method of Lowry et al, (1951), as modified by Markwell et al, (1978).

To a stock solution of 2% Na_2CO_3, 0.4% NaOH, 0.16% Na tartrate, 1% SDS, was added 0.01 volumes of 4% $CuSO_4.5H_2O$. Samples (0.1 ml) were incubated for 45 minutes in 0.45 ml of the above mixture at room temperature, then 45 µl of Folin reagent, diluted 1:1 with water, was added. After vortexing thoroughly and further incubation for 45 minutes, the OD at 750 nm was measured. Bovine serum albumin (BSA) was used as the protein standard for obtaining a calibration curve.

2.2.10. Enzyme assays

The catalase assay was performed by measuring the decrease in OD at 240nm (Beers and Sizer, 1952), in the following medium: Na phosphate 50mM pH 7, H_2O_2 20mM. Other enzymes were assayed as described in Methods 7.2

2.3 RESULTS

2.3.1 Preparation of α BuTX-Sepharose

α BuTX-Sepharose was normally prepared sufficient to perform several experiments, as it was found to be stable for >5 months when stored in NaN_3 at 4°C. OD_{280} measurements of the α BuTX solution before and after coupling to CNBr-activated Sepharose gave a coupling efficiency of 98-100%, indicating an α BuTX concentration of 0.98-1mg/ml of Sepharose.

Biological activity of the resin was checked by incubating a small volume of resin with an excess of soluble nAChR prepared from Torpedo marmorata membranes (preparation as in Lo et al, 1982), and measuring the decrease in receptor concentration using ^{125}I-α BuTX (Dolly and Barnard, 1977). Values for biological activity of ~12nmol/ml Sepharose imply that only ~10% of the coupled α BuTX (~/mg/ml) is available for receptor binding. Similar biological activity values (~10 nmol/ml) were found for other identical preparations of 1 mg/ml α BuTX-Sepharose (S. Dunn, personal communication), and also for different batches of α BuTX. This low value could be due to coupling occurring at the binding site of the toxin or coupling in a sterically unfavourable position for specific interactions. The α BuTX concentrations used in affinity chromatography purifications however, were well in excess (~80 fold) of the pnAChR concentration solubilised from optic lobe membranes (2.3.3).

2.3.2 Assay of pnAChR

Soluble pnAChR-^{125}I-α BuTX complex (pI ~5) was measured by virtue of its electrostatic binding to positively charged diethyl aminoethyl (DEAE) derivatized cellulose discs (Schmidt and

Raftery, 1973). Excess ^{125}I-α BuTX (pI ~10) however, does not bind significantly and is removed by washing the discs in buffer.

Small modifications to the assay procedure used for muscle nAChR (Dolly and Barnard, 1977) were made. This was necessary after losses of up to 15% of specific ^{125}I-α BuTX binding to the optic lobe pnAChR were found, during prolonged washes at room temperature (Wang et al, 1978). Several short washes with large volumes of ice cold buffer was employed to reduce the loss caused by dissociation of specifically bound toxin. Combined with a change in washing buffer pH from 8.0 to 7.0, to minimise toxin binding to filters, this helped to improve the ratio of specific to non-specific binding.

Binding of ^{125}I-α BuTX to both membranes and solubilised extracts gave reproducible values for specific binding, with standard deviations of ~ ± 7% between assay triplicates. Blank controls, with no optic lobe membranes or extract present, were less than 1% of the total radioactivity added, indicating low levels of toxin binding to the Whatman DE 81 discs and GF/C filters. Levels of non-specific binding to solubilised extracts was 19-28% of total binding, whereas with membranes the value was 21-26%.

2.3.3 Preparation of pnAChR

The pnAChR was readily solubilised from optic lobe membranes in the nonionic detergents, Triton X-100 and Lubrol PX. The optimal concentration of 1% Triton and 5% Lubrol with solubilisation times of 1 and 2 hours, respectively, were used. To minimise proteolysis during preparation procedures (Lindstrom et al, 1980b) high levels of divalent cation chelators and

protease inhibitors were added to the homogenisation buffer.

Solubilised extracts generally gave ~15 pmols pnAChR /g of optic lobe tissue (wet weight). This represented 84% pnAChR solubilization efficiency (Table 2.1) when compared to the value of ~18 pmol/g found for optic lobe membranes. After 4 hours incubation with detergent extract, 75-85% of the pnAChR was bound to the affinity resin. However, yields of only 20-25% were obtained from carbachol elution of the resin. This low value could be an underestimate because, if there was incomplete removal of carbachol after dialysis, even very low levels could reduce the binding to ^{125}I-α BuTX, though more lengthy dialysis would probably not increase yields significantly, due to increased possibility for proteolysis to occur.

In initial experiments, the carbachol eluate was incubated in DNase-Sepharose before dialysis. This step had been shown to remove the actin that always copurified with muscle nAChR (Strader et al, 1980). The optic lobe pnAChR was found in this study not to contain any contaminating actin, therefore this step was omitted in subsequent experiments. Without this preincubation a slightly higher pnAChR yield of 25-30% was obtained from carbachol elution of the α BuTX-Sepharose (Table 2.1).

2.3.4 Sucrose density gradient centrifugation

Previous sedimentation studies in this lab (Norman, 1981), found the apparent sedimentation coefficient of the optic lobe pnAChR in Lubrol to be 9.1, whereas that for Triton was 11.8. It was necessary to further investigate this finding to enable choice of a suitable detergent in the subsequent determination of Stokes radius (S_r) and sedimentation coefficient ($S_{20,w}$).

Table 2.1 pnAChR yields throughout preparation procedure

	Source	% of total in optic lobe membranes	pmols
1.	OL membranes	100	391
2.	Triton extract	84	328
3.	Triton extract after incubation with α BuTX-Sepharose	12	47
4.	Bound to α BuTX-Sepharose (4 = 2-3)	72	282
5.	Carbachol eluate	16(22)	63
6.	Carbachol eluate - without DNase-Sepharose preincubation	19(26)	73

Typical preparation (2.2.4) of pnAChR from 21g of optic lobes from 1 day old chicks. Figures in parenthesis represent the % recovery of pnAChR from the α BuTX-Sepharose by carbachol elution (after dialysis).

Table 2.2 Hydrodynamic parameters of calibrating proteins

	Stokes radius (nm)	Sedimentation coefficient ($s_{20,w}$)	Molecular weight (kD)
Thyroglobulin	8.5	-	660
β Galactosidase	6.84	16.0	484
Catalase	5.2	11.3	240
Aldolase	4.8	-	160
Alcohol dehydrogenase	-	4.8	84
Ovalbumin	3.1	-	45

For calculation of $s_{20,w}$ for the pnAChR, a value of 0.735 ml/g was assumed for the partial specific volume of all calibrating proteins. Alcohol dehydrogenase (ADH) from horse liver was used, as opposed to the yeast ADH with MW of 160,000.

The carbachol eluate from Lubrol and Triton solubilised membranes was divided into two equal fractions, and one fraction incubated with DNase-Sepharose before dialysing. Samples were loaded onto sucrose gradients and centrifuged on the same rotor. Assays of the gradient fractions (2.2.5) for both Lubrol and Triton extracted pnAChR, displayed single peaks which corresponded to an identical apparent sedimentation coefficient of 10.5 ± 0.4 (Figs 2.1 and 2.2). The position of both peaks was completely unchanged by the DNase-Sepharose preincubation. Assay of marker enzymes (Table 2.2), centrifuged in parallel tubes, produced activity peaks which when plotted against their $s_{20,w}$ values, gave straight lines with correlation coefficients of 0.999. The activity peak of the catalase present in pnAChR sample gradients, was identical to that in marker enzyme gradients. These observations suggest that no significant size difference is present between Triton and Lubrol solubilised pnAChR, and actin is not a contaminant in the preparation method used. Further experiments, therefore, were all performed in Triton.

2.3.5 Calculation of sedimentation coefficient and partial specific volume.

Due to a significant amount of detergent binding to membrane proteins, centrifugation of membrane protein-detergent complexes in sucrose/H_2O gradients determines only the apparent sedimentation coefficient (S). However, simultaneous centrifugation in media of different densities, such as sucrose/H_2O and sucrose/D_2O gradients, allows calculation of the partial specific volume ($\bar{v}$) and $s_{20,w}$ of the membrane protein. This approach was employed for the optic lobe

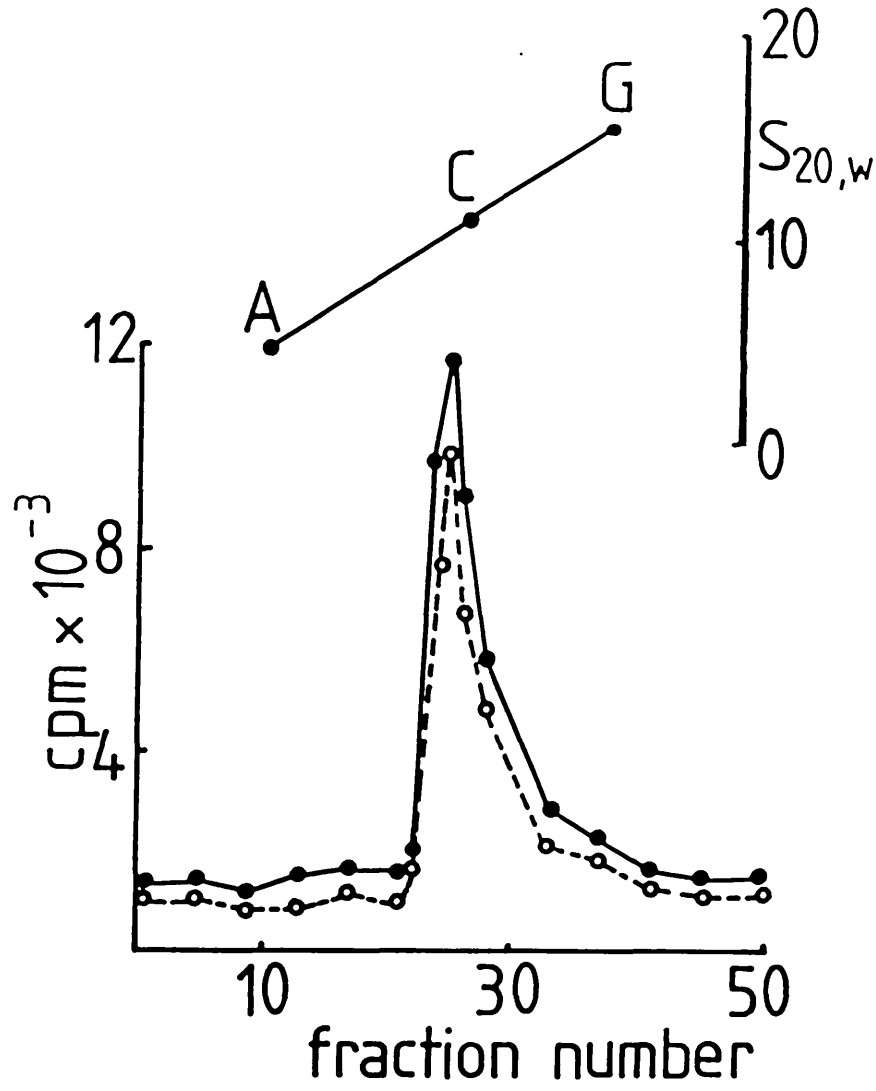

Figure 2.1 Sedimentation of pnAChR prepared in Triton X-100

Triton X-100 solubilised pnAChR from optic lobes was applied to sucrose density gradients prepared as described in Methods (2.2.4 and 2.2.7). Gradients were fractionated from the top and assayed for ^{125}I-α BuTX binding activity (2.2.5). Closed circles represent pre-DNase-Sepharose treatment, open circles represent post-DNase-Sepharose treatment.

Upper calibration curve shows the marker enzymes, alcohol dehydrogenase (A), catalase (C) and β-galactosidase (G) in order of increasing $s_{20,w}$. Correlation coefficient r=0.999.

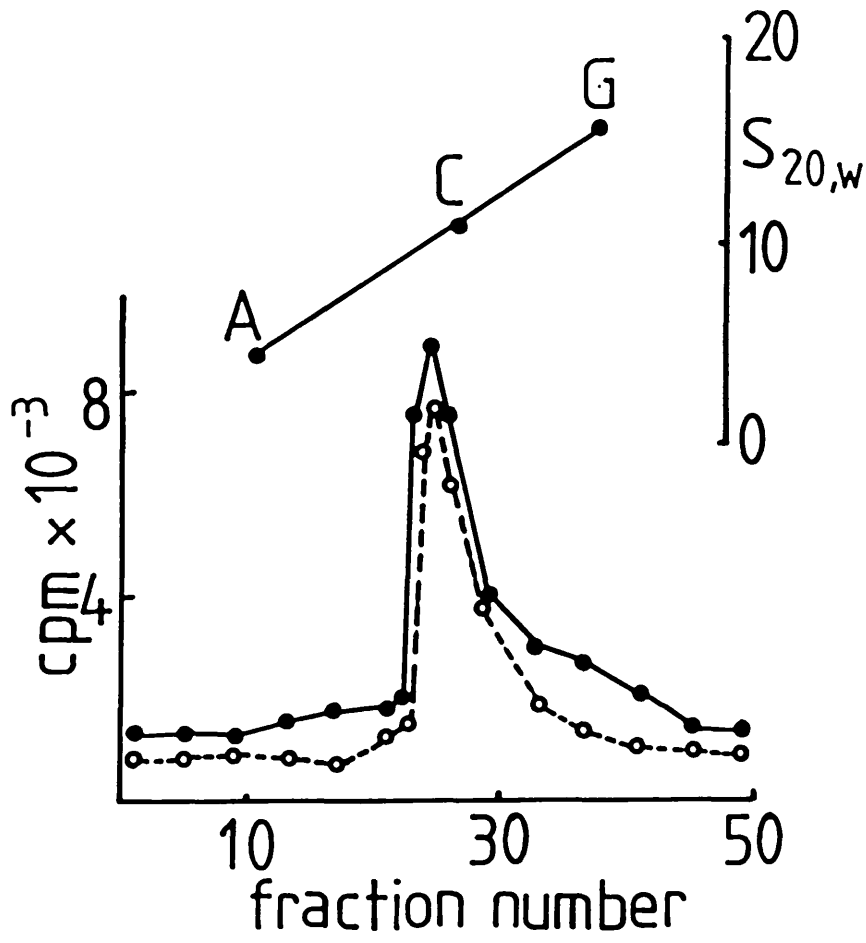

Figure 2.2 Sedimentation of pnAChR prepared in Lubrol PX

Lubrol PX solubilised pnAChR from optic lobes was applied to sucrose density gradients prepared as described in Methods (2.2.4 and 2.2.7). Gradients were fractionated from the top and assayed for ^{125}I-α BuTX binding activity (2.2.5). Closed circles represent pre-DNase-treatment, open circles represent post-DNase-treatment.

Upper calibration curve shows the marker enzymes, alcohol dehydrogenase (A), catalase (C) and β-galactosidase (G) in order of increasing $s_{20,w}$. Correlation coefficient r=0.999.

pnAChR-Triton X-100 complex.

From the sedimentation profile of pnAChR in sucrose /H_2O and sucrose/D_2O gradients, a marked shift in the peak of α BuTx binding activity was observed (Fig 2.3). This D_2O shift is the basis for $\bar{v}$ and $s_{20,w}$ calculation.

Martin and Ames (1961) have shown that the distance r travelled from the meniscus by any macromolecule in a given medium is

$$r = k\, s_{20,w}\, (1-\bar{v}p)$$

where k is a constant for the medium and p the density of the medium. From the sedimentation positions of marker enzymes of known $s_{20,w}$, k is calculated as the enzyme marker calibration slope in that medium (Fig. 2.4). p is the average density of the medium, usually measured by weighing a fixed volume of medium from the middle gradient fraction ($p_{½}$).

From the distance travelled by the pnAChR molecule in sucrose/H_2O and sucrose/D_2O gradients, two simultaneous equations can be obtained, containing the two unknowns, $\bar{v}$ and $s_{20,w}$.

$$r_D = k_D\, s_{20,w}\, (1-\bar{v}\, p_D) \qquad (1)$$

$$r_H = k_H\, s_{20,w}\, (1-\bar{v}\, p_H) \qquad (2)$$

where H = H_2O and D = D_2O.

Combining (1) and (2) to eliminate $s_{20,w}$

$$\frac{r_D}{k_D\,(1-\bar{v}\,p_D)} = \frac{r_H}{k_H\,(1-\bar{v}\,p_H)}$$

Substituting the values for r, k and $p_{½}$, the $\bar{v}$ and $s_{20,w}$ for the membrane protein can be found. For the optic lobe pnAChR the

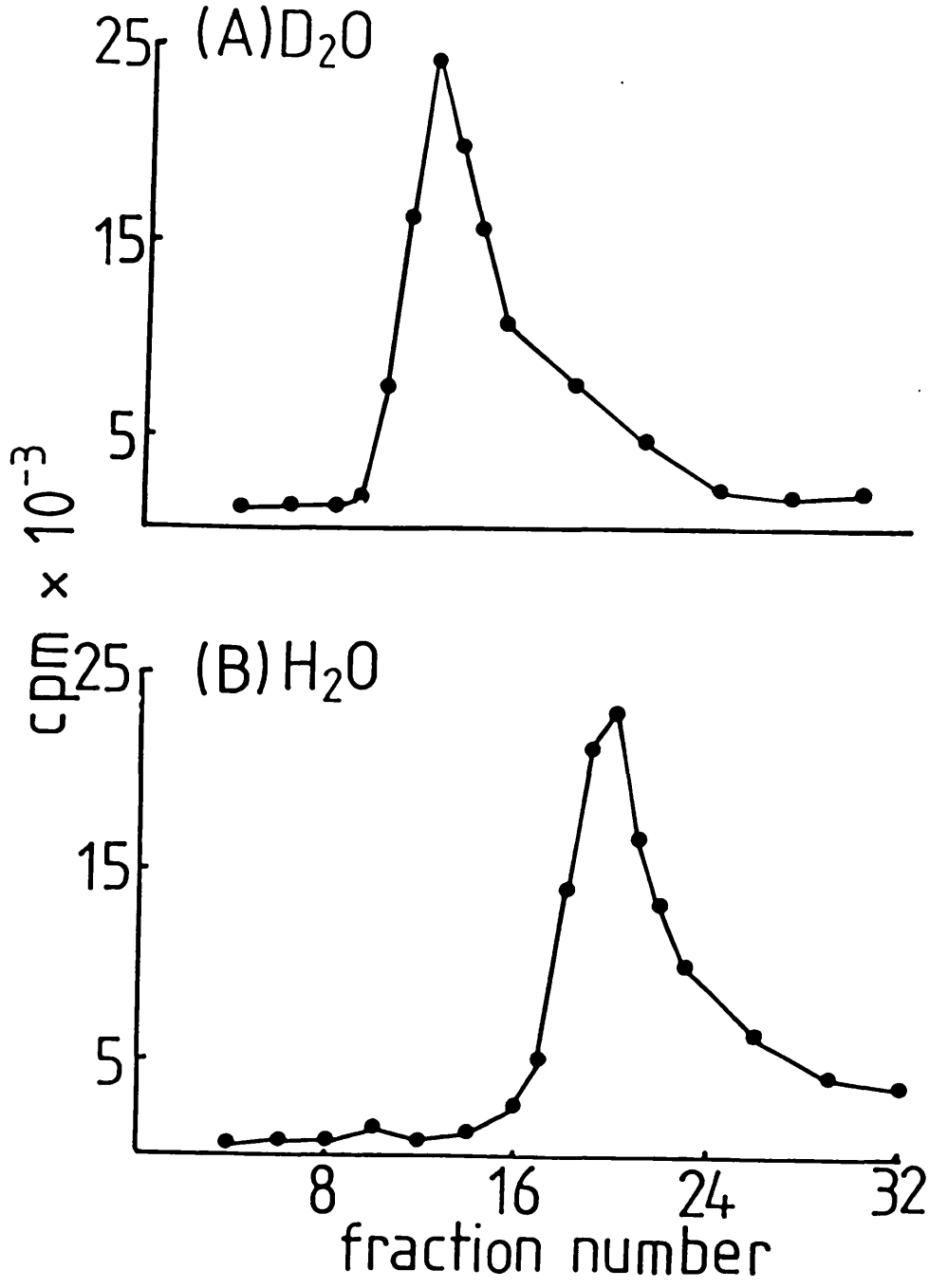

Figure 2.3 Sedimentation of the pnAChR in D_2O and H_2O

Triton X-100 solubilized pnAChR from optic lobes was applied to sucrose density gradients prepared in (A) D_2O, and (B) H_2O, as described in Methods (2.2.4 and 2.2.7). Gradients were fractionated from the top and assayed for ^{125}I-α BuTX binding activity.

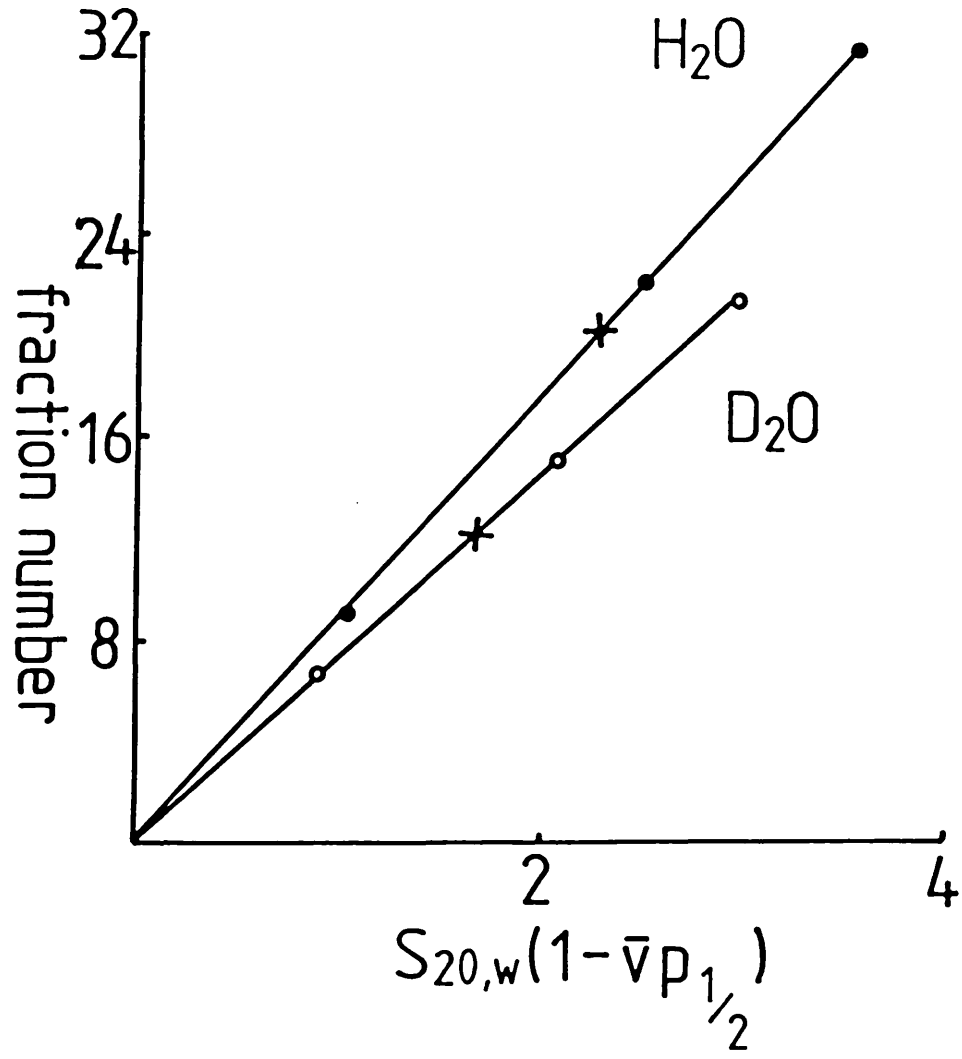

Figure 2.4 Calibration plot for sedimentation in D_2O and H_2O

Fraction number i.e. distance travelled by the protein, is plotted versus $s_{20,w}$ $(1-vp_{1/2})$ for sucrose density gradients prepared in D_2O and H_2O. The marker enzymes are alcohol dehydrogenase, catalase and β-galactosidase in ascending order of the x co-ordinate. The position of the pnAChR peak is indicated by an X. Correlation coefficient for both D_2O and H_2O plots, r=0.999.

mean $\bar{v}$ from 3 determinations was 0.766 ± 0.009 ml/g and the $s_{20,w}$ was 11.76 ± 0.29 (Table 2.3).

2.3.6 Gel filtration chromatography

For globular proteins, gel filtration (molecular exclusion) chromatography can accurately estimate protein size (Andrews, 1964). The actual value obtained for non spherical proteins is the Stokes radius, which can only give an apparent molecular weight when related to globular protein standards (Tanford and Reynolds, 1976). However, when combined with $\bar{v}$ and $s_{20,w}$ the Stokes radius can be used to determine actual molecular weight (2.3.7).

Gel filtration of the optic lobe pnAChR produced an elution profile with one broad peak of α BuTX binding activity between the peaks for thyroglobulin and β-galactosidase (Fig. 2.5). Approximately 50% of the applied activity was recovered in this peak. A smaller peak of aggregated pnAChR was always present, which eluted at a position corresponding to the void volume of the column (V_o), determined using blue dextran.

Soluble enzymes of known Stokes radius were used to obtain a calibration curve. These enzymes, which do not bind a significant amount of Triton (Clarke, 1975), were eluted under identical conditions. From their elution position the partition coefficient (K_{av}) was calculated (Laurent and Killander, 1964) from the equation

$$K_{av} = \frac{V - V_o}{V_t - V_o}$$

where V = elution volume of the protein

V_o = void volume

V_t = total volume

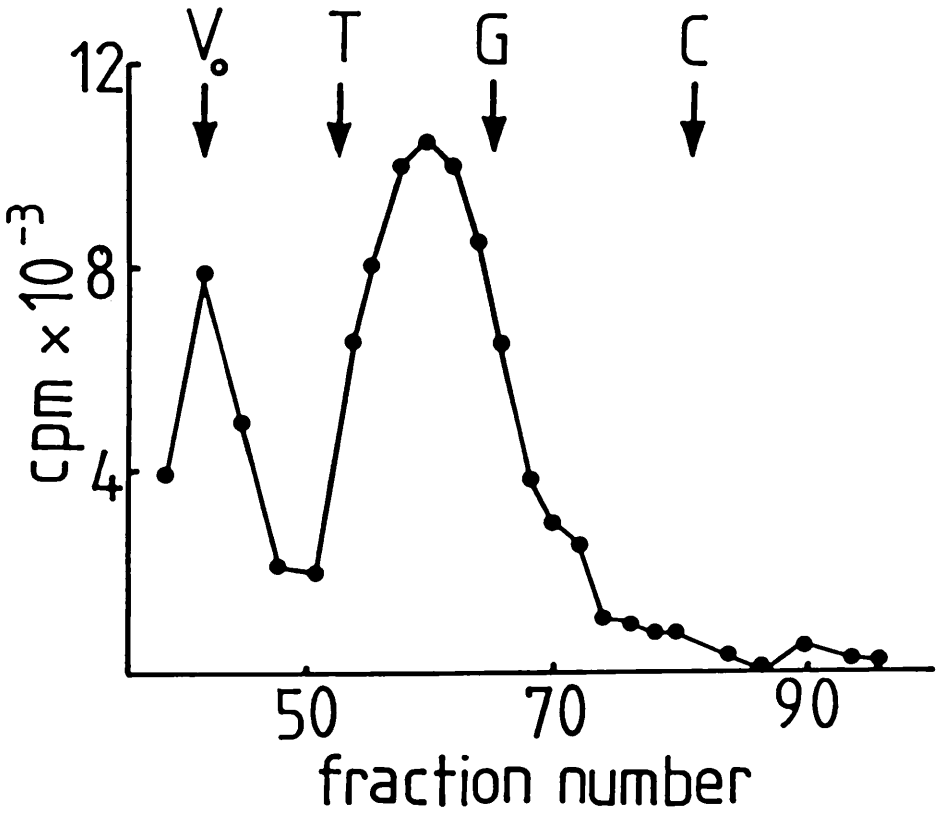

Figure 2.5 Gel filtration of the pnAChR

Solubilized pnAChR from optic lobes was prepared and applied to an Ultrogel column as described in Methods (2.2.4 and 2.2.8). Fractions were collected and assayed for ^{125}I-α BuTX binding activity (2.2.5). Arrows represent the position of the void volume (Vo), and the elution peaks of thyroglobulin (T), β-galactosidase (G) and catalase (C).

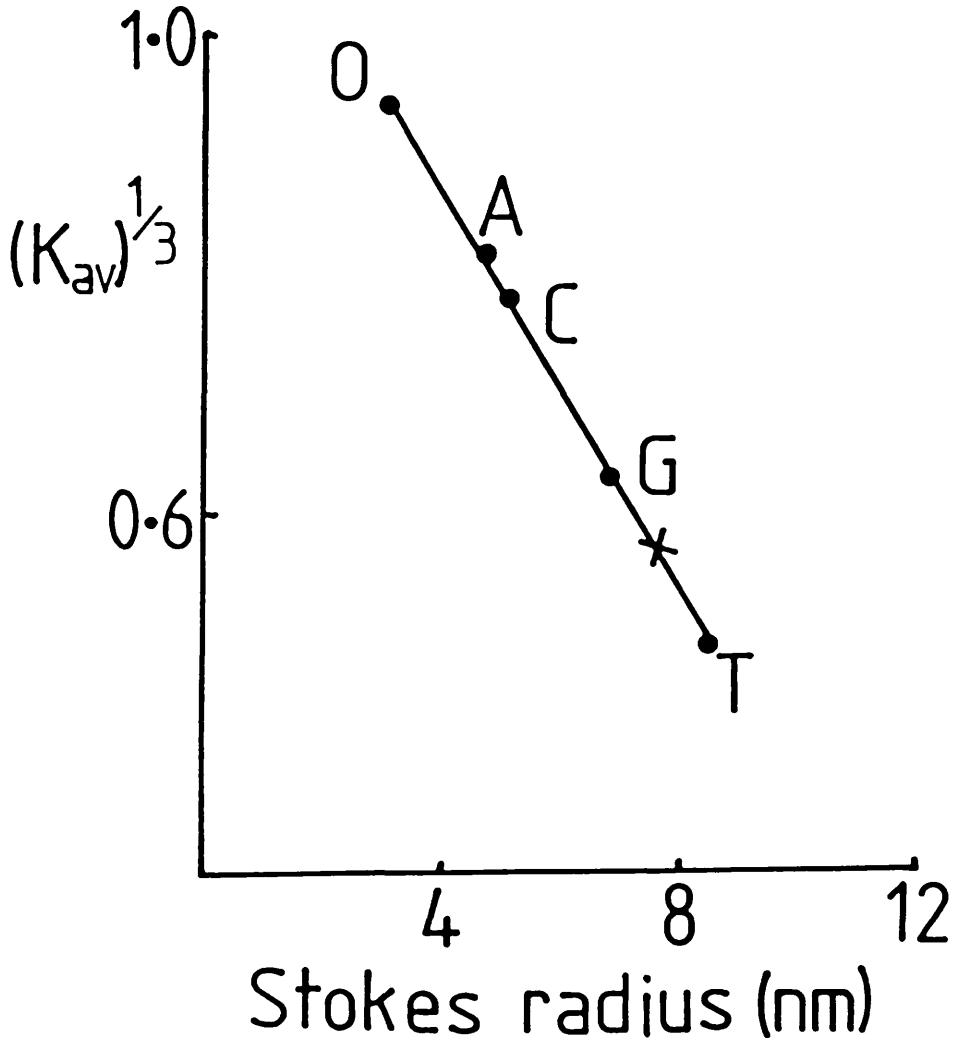

Figure 2.6 Calibration plot for partition coefficients versus Stokes radius

$(K_{av})^{1/3}$ is plotted versus the Stokes radius of the protein. The marker enzymes are ovalbumin, aldolase, catalase, β galactosidase and thyroglobulin in order of increasing Stokes radius (Table 2.2). The position of the pnAChR is indicated by an X. Correlation coefficient r=0.998.

From a plot of $K_{av}^{1/3}$ versus Stokes radius for the soluble enzyme markers, a straight line was obtained with a correlation coefficient of 0.99. Using this calibration plot the average Stokes radius for the pnAChR from 3 determinations was found to be 7.6 ± 0.2 nm.

2.3.7 Molecular weight calculation

Using the $\bar{v}$ and $s_{20,w}$ values determined by sedimentation analysis and Stokes radius by gel filtration, the molecular weight of the protein-detergent complex can be calculated (Meunier et al, 1972) from the equation

$$MW = \frac{6\pi n_{20,w} \cdot N \cdot S_r \cdot s_{20,w}}{1-\bar{v} P_{20,w}}$$

where MW = molecular weight of the complex

$n_{20,w}$ = viscosity of water at 20°C

N = Avogadro's number

S_r = Stokes radius

$s_{20,w}$ = Sedimentation coefficient

$\bar{v}$ = partial specific volume

$P_{20,w}$ = density of water at 20°C

The MW determined thus, is that of the protein-detergent complex. By calculating the weight fraction of the protein, ($\bar{X}$), the protein molecular weight can be obtained (Tanford and Reynolds, 1976)

$$\bar{X} = \frac{\bar{V}_c - \bar{V}_d}{\bar{V}_p - \bar{V}_d}$$

where $\bar{V}_c$ = partial specific volume of the protein-detergent complex

$\bar{V}_d$ = partial specific volume of the detergent

$\bar{V}_p$ = partial specific volume of protein

Table 2.3 Physical characteristics of the solubilized pnAChR protein

Data expressed as mean (± SEM, n=3)

Stokes radius (nm)	7.6 ± 0.2
Partial specific volume (ml/g)	0.766 ± 0.009
Apparent sedimentation coefficient (in H_2O)	10.5 ± 0.4
Sedimentation coefficient ($s_{20,w}$)	11.76 ± 0.29
Total molecular weight	430,000 ± 40,000
Weight fraction of protein (g/g)	0.823 ± 0.05
Molecular weight of protein	354,000 ± 33,000
Frictional ratio	1.49 ± 0.03

Partial specific volume and sedimentation coefficient were determined from sucrose gradient sedimentation analysis in Triton X-100 detergent, as described in 2.3.5. Stokes radius was determined from gel filtration as in 2.3.6. All other values were determined as in 2.3.7.

($\bar{V}_{\text{Triton X-100}} = 0.910$ and $\bar{V}_p = 0.735$)

Hence, molecular weight of the protein = MW x $\bar{X}$

Using the above parameters, the frictional ratio (f/fo), which indicates the degree of symmetry of the complex, can also be calculated

$$\frac{f}{f_o} = S_r \left[\frac{4\pi N}{3.MW.\bar{v}} \right]^{1/3}$$

Values obtained for the optic lobe pnAChR-Triton X-100 complex are summarised in Table 2.3.

CHAPTER 3 SUBUNIT CHARACTERISATION AND MICROSEQUENCING OF THE CHICK OPTIC LOBE pnAChR

3.1 MATERIALS

SDS was purchased from Biorad, 25K cut-off dialysis tubing from Spectrapor, activated charcoal and all electrophoresis reagents from BDH and β-mercaptoethanol from Sigma. All other chemicals were of analytical grade.

3.2 METHODS

3.2.1 Recrystallization of SDS

SDS (100g) was added to ethanol (450 ml) heated to 55°C, and hot glass-distilled water was added (~75ml) until all the SDS dissolved. Activated charcoal (10g) was added, and after stirring for 10 minutes, was removed by filtration under reduced pressure through Whatman No. 5 paper. The filtered solution was cooled to 4°C overnight, then to -20°C for 25 hours. Crystalline SDS was collected and washed with ethanol (400 ml) cooled to -20°C. The SDS was then recrystallized using the same procedure but without charcoal treatment. Purified SDS (2x SDS) was dried under vacuum overnight.

3.2.2 Preparation of pnAChR from optic lobe and whole brain

Preparation of pnAChR was the same as in Methods 2.2.4, except, instead of passing wash buffers through α BuTX-Sepharose packed into a column, rapid washing was achieved by successive washes in 30ml centrifuge tubes. In this modification, the toxin resin was:

(1) thoroughly vortexed in 10 b/vol of wash buffer,

(2) centrifuged for one minute at 1000g, and the supernatant removed by aspiration, then

(3) resuspended in fresh wash buffer, and the above steps repeated.

Volumes of wash buffer used here, were the same as described in 2.2.4.

Also, after the final wash of α BuTX-Sepharose with buffer A/0.2% Triton, the affinity resin was either:

(a) twice eluted with 1 b/vol of 1M carbachol in buffer A, 0.2% Triton for 2 hours at 4°C, then 2x SDS and β-mercaptoethanol added to the pooled eluates to concentrations of 3% and 5% (w/v) respectively, or

(b) twice eluted with 1 b/vol of buffer B (Tris-HCl 60 mM, pH 6.8, 5% w/v β-mercaptoethanol, 3% 2x SDS) for 1 hour at room temperature.

In later experiments, pnAChR elution was performed as in (a) above, except the eluting ligand carbachol, was replaced by nicotine, and elution time was reduced to 30 minutes. Eluates were immediately heated to 90°C for 3 minutes, after addition of SDS and β-mercaptoethanol.

The pooled eluates were in all experiments, dialysed against Tris-HCl 15 mM, pH 6.8, 0.05% 2x SDS for 48 hours with 5 x 2 litre changes. Dialysed eluate was then lyophilised in acid washed tubes and stored at -20°C.

In the preparations of pnAChR for amino-terminal amino acid sequence analysis (ATAS), from the carbachol or buffer B elution step onwards, only glass-distilled water passed through a Millipore filter was used. After dialysis, eluates were lyophilised overnight, and stored at -20°C before sending to

U.S.A. for amino-terminal sequence analysis (3.2.4).

Before use, the dialysis tubing (Spectrapor 25K cutoff) was washed for one hour at 45°C, first in 2% $NaHCO_3$, then 1% SDS and stored in 0.1% SDS containing 0.01% NaN_3. Assays of pnAChR were performed as in 2.2.5 and 2.2.6.

3.2.3 SDS-polyacrylamide gel electrophoresis

Electrophoresis was performed essentially as described by Laemmli (1970).

Slab gels (12 x 12 x 0.2 cm) of 9.75% acrylamide/ 0.25% N,N' methylene bisacrylamide were used, containing 0.375 M Tris-HCl pH 8.8, 0.1% SDS, 0.1% (v/v) TEMED and 0.05% ammonium persulphate. Stacking gels (12 x 4 x 0.2cm) of 3% acrylamide/ 0.08% N,N' methylene bisacrylamide contained 0.125 M Tris-HCl pH 6.8, 0.1% SDS, 0.1% (v/v) TEMED and 0.05% ammonium persulphate. For electrophoresis of purified α neurotoxins, gels containing 19.5% acrylamide/0.5% N,N' methylene bisacrylamide were used. Tris-HCl, SDS, TEMED and ammonium persulphate were as above, as was the stacking gel.

Samples were heated for 3 minutes at 90°C in sample buffer to give final concentrations of 2% SDS, 2% (w/v) β-mercaptoethanol, 10% (v/v) glycerol, 0.1 M Tris HCl pH 6.8 and 0.02% bromophenol blue (BPB).

Electrophoresis was at 150 V (constant voltage) until the BPB tracking dye reached the bottom (~6 hours) of the gel. Gels were stained for protein either with Coomassie dye or silver.

For Coomassie staining, gels were fixed and stained overnight in 50% (v/v) methanol, 10% (v/v) acetic acid containing 0.025% Coomassie Brilliant Blue R-250, then destained in 10% (v/v) methanol, 15% (v/v) acetic acid.

For silver staining, the method of Oakley et al, (1980) was used. After fixing in 10% (v/v) glutaraldehyde (30 minutes) and washing extensively with glass-distilled water, the gel was placed for 10 minutes in freshly made ammoniacal silver solution ($AgNO_3$ 0.08%, NaOH 0.075%, NH_4OH 1.4% v/v). After 2 x 1 minute water washes, the gel was placed in freshly made developer solution (HCHO 0.0175% v/v, CH_3OH 0.00375% v/v, citric acid 0.05%) until bands were visible, then transferred to glass-distilled water. To reduce background staining, gels were sometimes destained in 0.05% potassium thiosulphate, 0.05% potassium ferricyanide.

3.2.4 Amino-terminal amino acid sequence analysis

All procedures described in this section were carried out by Dr. B.M. Conti-Tronconi in the laboratory of Dr. M. Raftery, at the California Institute of Technology, U.S.A. Samples of purified pnAChR (3.2.2) were sent in dry ice, by airfreight to Los Angeles, U.S.A.

Lyophilised pnAChR subunits 200-400 pmols, were separated by preparative SDS gel electrophoresis (Conti-Tronconi et al, 1984), stained with Coomassie blue and the protein bands cut out and stored at -20°C. The separated subunits were recovered from the gel by electroelution and then electrodesalted (Conti- Tronconi et al, 1982b) and lyophilised. Purity of subunits was checked by SDS gel electrophoresis of ~1 pmol of each subunit followed by silver staining. Lyophilised purified subunit samples were dissolved in glass-distilled water, 30 µl (~20 pmols) was loaded on a polybrene-coated glass filter disc in a gas phase sequencer (Applied Biosystems) and submitted to amino-terminal sequence analysis by automated Edman degradation (Herrick et al, 1981).

The polybrene-coated disc had been precycled for 10 cycles of automated Edman degradation. Phenylthiohydantoin (PTH) derivatized amino acids were identified by HPLC using an IBM cyano column (Hunkapiller and Hood, 1983).

3.3 RESULTS

3.3.1 Purification of SDS and α BuTX

SDS was twice recrystallized in order to remove minor impurities present in commercially obtained sources. This was necessary to obtain a good signal to noise ratio in the microsequencing, which was performed on pmole amounts of purified protein. Use of commercially obtained SDS without prior recrystallization was found to produce low signal to noise ratios (B.M. Conti-Tronconi, personal communication).

Purification of α BuTX, was as described in 2.2.1. To verify the purity of the toxin, electrophoresis in a 20% polyacrylamide gel was performed. A single major band at MW ~8000 (8K) was observed, after Coomassie staining indicating a pure protein (Fig. 3.1).

3.3.2 Purification of pnAChR

The purification method used here, was a modified version of the previous method employed by Norman et al, (1982). The changes made were:

(a) All buffers contained increased concentrations of protease inhibitors, e.g. EDTA 5 fold to 5mM, PMSF 10 fold to 1mM, and STI 5 fold to 25μg/ml. The addition of 1mM benzamidine was also made.

(b) The nonionic detergent Triton X-100 (1%) was used, rather

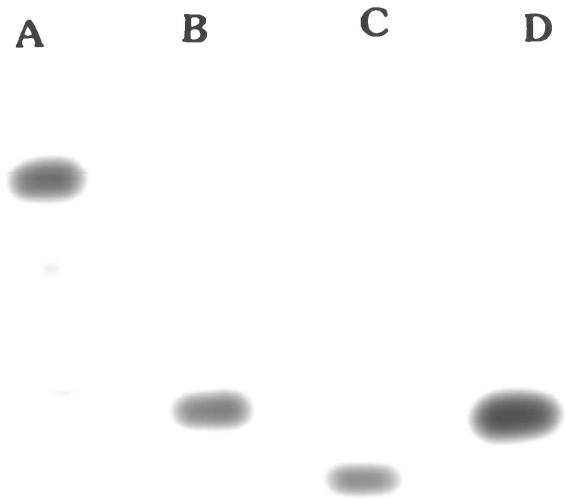

Figure 3.1 SDS-PAGE of α BuTX purified from B. multicinctus venom

α BuTX prepared as described in 2.2.1 (Track B), was subjected to electrophoresis in a 20% polyacrylamide gel (3.2.3), then stained with Coomassie blue dye. The molecular weight markers used were;

Track A - haemoglobin fragments,

Track C -k BuTX purified from B. multicinctus (6.5 K), and

Track D - DV 4.9.3 toxin purified from Dendroaspis viridis (8K).

than Lubrol PX (5%).

(c) The recycling elution method through α BuTX-Sepharose, then DNase-Sepharose, then lentil lectin-Sepharose followed by overnight glycoside elution, was omitted and replaced by a single rapid affinity purification step on α BuTX-Sepharose.

(d) The time from tissue homogenisation to addition of SDS/β-mercaptoethanol to the eluate was reduced from 3-4 days to 8-10 hours.

(e) Rapid washing in centrifuge tubes, replaced the slower column washing method.

(f) The volume of high salt wash used, was increased from 50 b/vol to 100 b/vol of α Butx-Sepharose.

The purification of pnAChR from chick optic lobes to a specific activity of 2590 nmol/g of protein (by α BuTX binding assay) is summarised in Table 3.1. A similar specific activity of 2485 nmol/g of protein, was obtained by assaying the protein eluted from the α BuTX-Sepharose by method (b) (3.2.2), and referring to the amount of pnAChR known to have bound to the resin. These very similar values of specific activity, calculated by separate methods, suggest that all the non-specifically bound protein was removed by the thorough washing of the resin in the high salt buffer. Although lower, the final specific activity achieved was similar to the specific activity (3095 nmol/g of protein) obtained by Norman et al (1982), but the subunit pattern observed in the preparation here was more complex.

SDS-polyacrylamide gels of the protein eluted from the α BuTX-Sepharose by method (b) (3.2.2), showed 3 major bands of MW 47K, 57K, and 72K (Fig. 3.2). Some high molecular weight protein, present at the top of the gel, probably represented

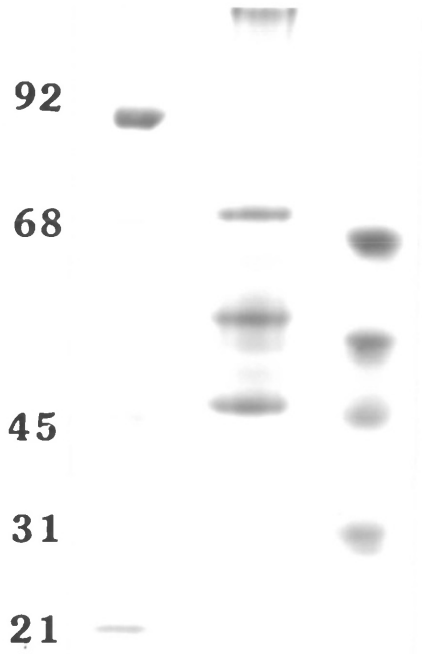

Figure 3.2 SDS-PAGE of pnAChR from chick optic lobes (1)

Affinity purified pnAChR, eluted by method (b) (3.2.2), was subjected to electrophoresis in a 10% polyacrylamide gel (3.2.3) then stained with Coomassie. The standard protein molecular weight markers were phosphorylase b (92K), bovine serum albumin (68K), glutamate dehydrogenase (55K), ovalbumin (45K), carbonic anhydrase (31K) and soybean trypsin inhibitor (21K). Optic lobe pnAChR =centre track.

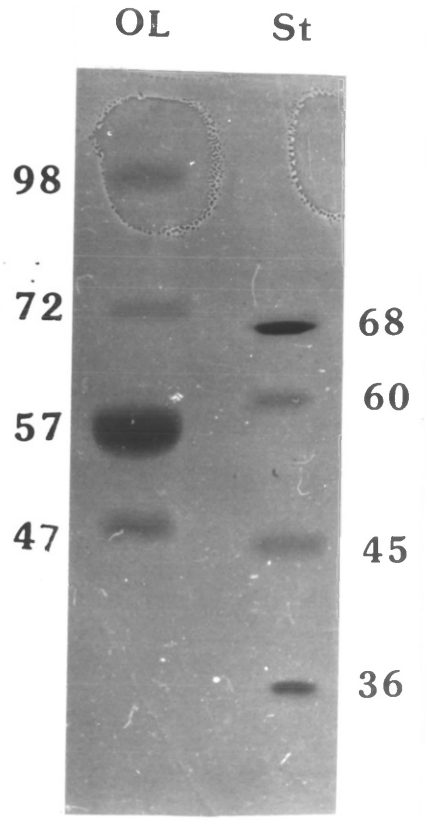

Figure 3.3 SDS-PAGE of pnAChR from chick optic lobes (2)

Affinity purified pnAChR was eluted with nicotine (3.2.2), and after addition of SDS and β-mercaptoethanol was immediately heated to 90°C. Following electrophoresis in a 10% polyacrylamide gel, proteins were visualised by silver staining. The standard molecular weight markers were bovine serum albumin (68K), bovine liver catalase (60K), ovalbumin (45K) and rabbit muscle lactate dehydrogenase (36K).

Table 3.1 Purification of the pnAChR from chick optic lobes

Stage	pnAChR (pmoles)	Specific Activity (nmoles/g protein)	Purification	Yield (%)
1. Membranes	352	0.18	1	100
2. Homogenate supernatant	16	0.03	-	4.5
3. Triton extract	302	0.55	-	86
4. Triton extract after incubation	57	0.11	-	16
5. α BuTX-Seph arose*	245	-	-	70
6. Nicotine eluate	96	2590	14390	27

Purification of the pnAChR from 20g of optic lobes from 1 day old chicks, by α BuTX affinity chromatography (3.2.2).

* Represents the amount of pnAChR bound to the α BuTX-Sepharose (differenc between 3. and 4.). Eluates were dialysed using Spectrapor 150K cutoff tubing.

non-denatured or aggregated protein.

In preparations eluted by method (a), identical patterns were seen, although bands were more diffuse, and a weakly stained band at MW 62K was often present (Conti-Tronconi et al, 1985). Later preparations in which the eluting ligand was changed to nicotine produced almost identical subunit patterns. Again, major bands of MW 47K, 57K and 72K were seen, however an additional band at MW ~98K was consistently found (Fig. 3.3). Its elution by nicotine suggests that this MW 98K protein may be a true subunit of the pnAChR. The reason why this subunit was seen only in these later preparations, may be due to the reduced elution time used and the immediate heat treatment of eluate after SDS and β-mercaptoethanol addition.

3.3.3 Amino-terminal amino acid sequencing

In the initial experiment, optic lobe pnAChR was prepared using the recycling method of Norman et al (1982). Very little protein was obtained, as a sample subjected to SDS-polyacrylamide gel electrophoresis did not reveal any bands after silver staining. Nevertheless, the remainder of the sample was submitted to ATAS. A short sequence was obtained which, after careful scrutiny, was identified as the sequence corresponding to the sequence for lentil lectin (B.M. Conti-Tronconi, personal communication). As a result of this, the purification method was changed, so that yields were maximised by reducing the number of steps involved in purification, and proteolysis minimised by increasing the level of protease inhibitors (3.3.2). Subsequent preparations using elution methods (a) and (b) in 3.2.2 yielded sufficient protein for sequencing, as shown by visualisation of bands after silver staining of SDS-polyacrylamide gels. The

major subunit seen at MW 57,000, as well as the other heavier subunits, when individually subjected to ATAS, all yielded no signal above the high background consistently present. This probably indicated the presence of blocked N-termini on these subunits. However, the lowest MW (47K) subunit, gave a readily identifiable single sequence (Fig. 3.4, Conti-Tronconi et al, 1985).

To determine whether the blocked N-terminus of the other subunits was caused by their isolation from SDS gels, intact optic lobe pnAChR preparations were submitted to simultaneous ATAS, without prior isolation of individual subunits. Only one signal above a high background was detected, which corresponded exactly to that previously found for the MW 47K subunit. Comparison of this sequence with the known amino-terminal sequences of Torpedo, Electrophorus, calf, chick and human muscle nAChR subunits, revealed that a small but definite homology existed (Fig. 3.5). The highest degree of homology is with the α subunits (Table 3.2), indicating that the divergence of peripheral nAChRs and this neuronal pnAChR, probably occurred very early during vertebrate evolution. This is shown by the construction of a phylogenetic tree (Fig. 3.6), using the method of Orcutt and Dayhoff (1975).

In two preparations of pnAChR from chick whole brains (minus the optic lobes), isolation of individual subunits was not attempted. This was due to the low levels of protein present, and the possible losses incurred by subunit isolation. Instead, intact whole brain pnAChR was submitted to ATAS. As for the optic lobe pnAChR, only one signal was present above a high background, indicating the presence of other proteins with blocked N-termini. The sequence obtained in both preparations

Sequence 1

1	5	10	15	20	25
X E F E T K L Y K E/F L L K N Y N X L E R X V A					

Sequence 2

1	5	10	15	20	25
X E F X X K L Y K E L L K N Y N P L X X P V A E D R/L					

Sequence 3

1	5	10	15	20	25
X E F E T K L Y K E L L K N Y N P L E R P V A E D R					

Overall Sequence

1	5	10	15	20	25
X E F E T K L Y K E L L K N Y N P L E R P V A E D R					

Figure 3.4 Amino-terminal sequence analysis of the 47K subunit from pnAChR

The sequences 1,2 and 3 were obtained by amino-terminal amino acid sequence analysis of the 47K subunit isolated from preparative SDS-PA gel of purified pnAChR (3.2.4). The standard amino acid one letter code is used, and X represents unknown residues.

	1				5				10				15				20				25	
Chick optic lobe and whole brain	X	E	F	E	T	K	L	Y	K	E	L	L	K	N	Y	N	P	L	E	R	P	V	A	E	D	R
Chick muscle	S		H			R		V	D	D		F	R	D		S	K	V	V			E	N	H		
Calf muscle	S		H			R		V	D	K		F	E	D			S	V	V			E	D	H		
Human muscle	S		H			R		V	A	K		F		D		S	S	Y	V			E	D	H		
Torpedo electroplax	S		H			R		V	A	N			E	N			K	V	I			E	H	H	T	
Electrophorus electroplax	S		D			R		V		L	N	F	S	G			K	V	V			N	H	F	K	
	1				5				10				15				20				25	

Figure 3.5 Comparison of the 47K subunit with muscle nAChR α-subunit amino terminal sequences

The amino-terminal sequence of the 47K subunit from optic lobe pnAChR was compared with the known amino-terminal sequence of muscle nAChR α-subunits from chick muscle (Barnard et al, 1983), calf muscle (Conti-Tronconi et al, 1982b), human muscle (Noda et al, 1983c), Torpedo electroplax (Raftery et al, 1980) and Electrophorus electroplax and muscle (Conti-Tronconi et al, 1982a; 1984). Gaps in muscle α-subunit sequences represent identity with the 47K sequence.

Table 3.2 Percentage identity between amino-terminal sequence of the 47K subunit and muscle nAChR subunits
(from Conti-Tronconi et al, 1985)

Subunit	Chick	Calf	Human	Torpedo	Electrophorus
α	35	39	39	48	43
β	38	35	-	30	39
	-	-	-	26	30
δ	28	-	-	32	24

References:

Chick α- Barnard et al, (1983).

Chick β and δ - Beeson et al, in press

Calf α and β- Conti-Tronconi et al, (1982b).

Human α - Noda et al, (1983c).

Torpedo - Raftery et al, (1980).

Electrophorus - Conti-Tronconi et al, (1982a).

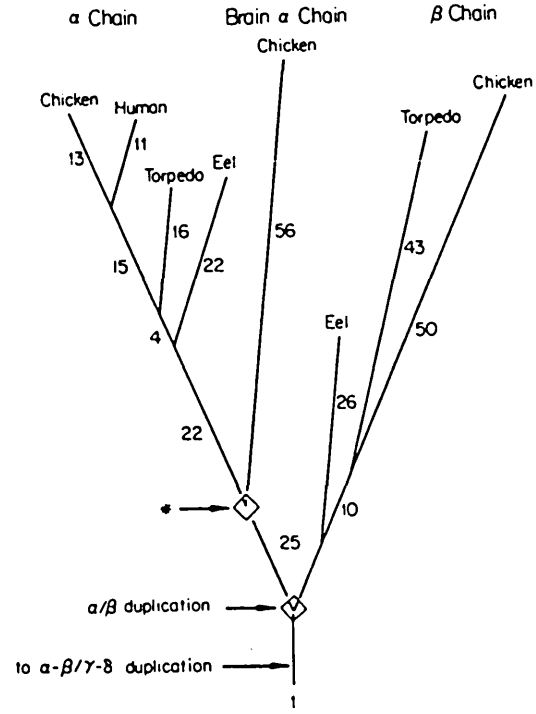

Figure 3.6 Phylogenetic tree of α- and β-subunits of muscle nAChRs (from Conti-Tronconi et al, 1985)

A phylogenetic tree generated from the amino-terminal sequence data of the known α- and β-subunits of muscle nAChRs (Orcutt and Dayhoff, 1975). The numbers associated with each branch length represent the "accepted point mutations" (PAMs) per 100 amino acid residues that occurred in generating the contemporary nAChR subunits.

The position of the α/β duplication is arbitrarily located along a 25-PAM segment separating the ancestral sequences of modern α- and β-subunits.

The * indicates the divergence of the α-subunit of the brain pnAChR from the ancestor of the muscle α-subunit.

was identical to that of the lowest MW component of the optic lobe pnAChR (Fig. 3.4).

CHAPTER 4 EXPRESSION OF mRNA FROM CHICK OPTIC LOBES

4.2 MATERIALS

Oocytes were obtained from the frog colony (Xenopus laevis) in this Department. Fertilized chick eggs were also from this Department.

Guanidinium isothiocyanate was purchased from Fluka, oligo(dT)-cellulose from Collaborative Research Inc., and ^{35}S-methionine from Amersham International. Nicotine and sodium lauryl sarcosinate were from Sigma, Autofluor from National Diagnostics, X-ray safety film from Fuji and Immunobeads from Biorad.

Rabbit anti-chick muscle nAChR anti-serum, normal mouse serum and rabbit anti-mouse IgG anti-serum were gifts from Dr. F. Mehraban, Imperial College, while chick muscle and chick fibroblast poly(A)$^+$-mRNA were gifts from Dr. D. Beeson, Molecular Genetics Department, Searle Research and Development, High Wycombe.

4.2 METHODS

4.2.1 Preparation of RNA from chick optic lobes

RNA was prepared by the guanidinium isothiocyanate (GTC) method of Chirgwin et al, (1979).

Chick optic lobes from 19 day old embryos were liquid N_2-frozen, ground into a fine powder with a liquid N_2-cooled mortar and pestle, and then Polytron homogenised (PCU 6, 30 seconds, speed 3) at 20°C in 10 volumes of GTC buffer (Tris-HCl 50 mM pH 7.6, GTC 4M, EDTA 10 mM, sodium lauryl sarcosinate, 2%

β-mercaptoethanol 1% v/v; buffer was passed through Nalgene nitrocellulose filter before use). Following removal of cell debris (1000g, 10 minutes), the supernatant was layered onto a 3ml cushion of caesium chloride 5.7M, EDTA 0.1M pH 7.5 and centrifuged at 100,000g for 18 hours at 20°C. The supernatant was aspirated and, after two superficial washes with 95% (v/v) EtOH, the RNA pellet was dissolved in 0.4ml of STE buffer (Tris-HCl 10mM pH 7.5, EDTA 5mM, SDS 0.1%). NaCl was then added to 0.1M followed by addition of 2 volumes of EtOH. After overnight storage at -70°C, the RNA precipitate was recovered by centrifugation (10,000g, 30 minutes), dissolved in 1ml of sterile H_2O and reprecipitated by addition of 2 volumes of EtOH. After centrifugation, the RNA pellet was washed and stored in 70% (v/v) EtOH at -70°C.

4.2.2 Purification of poly(A)$^+$-mRNA

Polyadenylated (poly(A)$^+$)-mRNA was separated from total RNA by chromatography on oligo(dT)-cellulose (Aviv and Leder, 1972).

A 1ml column of oligo(dT)- cellulose was prepared and washed sequentially with 10mls of

a) sterile H_2O,

b) 0.1M NaOH, 5mM EDTA,

c) sterile H_2O.

Total RNA (from 4.2.1) was dissolved in STE buffer, heated to 65°C for 1 minute, then cooled to room temperature, and NaCl added to 0.4M. The mixture was applied to the oligo(dT) column, and the flow-through collected and reapplied, after reheating to 65°C for 1 minute and cooling. After washing the column with 10mls of;

a) STE buffer containing 0.4M NaCl, and

b) STE buffer containing 0.1M NaCl.

The poly(A)$^+$-mRNA was eluted with 2ml of STE buffer. mRNA levels were monitored by measuring the OD_{260} of eluate throughout the elution procedure. The above procedures were then repeated using the same oligo(dT) column and, followed by addition of 2 volumes of EtOH to the STE eluate and overnight storage at -70°C. The poly(A)$^+$-mRNA precipitate was finally washed and stored in 70% EtOH at -70°C.

4.2.3 mRNA microinjection and assay of pnAChR in X. oocytes

Poly(A)$^+$-mRNA resuspended in sterile H_2O (1mg/ml), was microinjected into Xenopus laevis oocytes (40ng/oocyte) selected at stage 5/6 of their development (Gurdon et al, 1971), with the assistance of Dr. G. Bilbe, Imperial College.

Injected oocytes were incubated at 21°C for 48 hours in Barth's medium (Tris-HCl 50mM pH 7.5, NaCl 80mM, KCl 1mM, $NaHCO_3$ 2.4mM, $Ca(NO_3)_2$ 0.5mM, $CaCl_2$ 0.4mM, $MgSO_4$ 0.4mM) then homogenised, 10µl/oocyte, in buffer A (2.2.4) at 4°C, with a hand-held glass Potter homogeniser. Triton X-100 was added to 1% (w/v), and, after 1 hour incubation at 4°C, the extract was centrifuged at 10,000g for 20 minutes. The supernatant was taken for assay of ^{125}I-α BuTX binding activity using DE 81 cellulose discs or by immunoprecipitation.

Disc assays were performed as previously described (2.2.5).

For immunoprecipitation, a monoclonal antibody to the optic lobe α BuTX-binding protein (mAb 3a, Betz and Pfeiffer, 1984) was used. After incubation of 250µl oocyte extract in 10nM ^{125}I-α BuTX (1hr, 4°C), mAb 3a (1µl) in 10µl of normal mouse serum was

added. Following a 2 hour incubation at 4°C, the second antibody, rabbit anti-mouse IgG (100µl), was added and the extract left overnight at 4°C. The pellet obtained after centrifugation (10,000g, 20 mins) was twice washed with 1ml of buffer A, 0.1% Triton, and counted for radioactivity.

Preliminary immunoprecipitation experiments were performed using optic lobe membrane extracts and Immunobeads (rabbit anti-mouse IgG conjugated to polyacrylamide beads).

Microinjection experiments were also performed with poly(A)$^+$-mRNA isolated from embryonic (12 days in ovo) chick pectoral muscle and chick fibroblast tissue as positive and negative controls respectively, using a rabbit anti-chick muscle nAChR antiserum.

4.2.4 Purification of pnAChR in X. oocytes.

Poly(A)$^+$-mRNA and ^{35}S-methionine (1200 Ci/mmol) were coinjected (40ng, 0.2µ Ci/oocyte respectively) into Xenopus oocytes as described above (4.2.3). After Triton extraction of homogenised oocytes (as in 4.2.3), the supernatant was incubated with 0.2 ml of α BuTX-Sepharose (2.2.2) for 3 hours at 4°C. The beads were washed sequentially as in 3.2.2, then twice eluted for 30 minutes with 1M nicotine in buffer A, 0.2% Triton. After adding SDS to 3%, β-mercaptoethanol to 5% (v/v) and heating to 90°C, the eluate was dialysed using Spectrapor 25K cutoff tubing as before (3.2.2), then lyophilised and stored at -20°C. Samples were then subjected to SDS-PAGE followed by autoradiography.

4.2.5 SDS-PAGE and autoradiography

Polyacrylamide (10%) slab gels were cast and run as previously described (3.2.4). Gels containing ^{35}S-methionine

labelled proteins were stained with Coomassie Brilliant Blue R-250 and destained (3.2.4), in order to visualise the Bio-rad molecular weight marker lanes. After two 30 minute washes in distilled H_2O, the gel was immersed in Autofluor enhancing reagent for 2 hours, then placed on moistened filter paper, covered with cling-film and dried, in a Biorad gel-drier, under vacuum at 60°C. Preflashed X-ray film (1 msec) was then exposed to the dried gel at -70°C, until bands were visible after developing (~20-30 days).

4.3 RESULTS

4.3.1 Ontogeny of pnAChRs in chick optic lobes

Before preparation of RNA from chick optic lobes, the developmental profile of pnAChRs in optic lobes was obtained. This enables selection of the time period when optic lobes contain high levels of mRNA for the pnAChR protein, thereby improving its yield from RNA preparations.

Using optic lobes from 14 day old embryos onward, the concentration of pnAChR, relative to protein, was found to rise steadily with time, reaching a maximum at 19 days *in ovo*, after which it decreased to its adult level (Fig. 4.1). As a tissue comparison, the ontogeny of chick pectoral muscle nAChRs was also studied. In contrast to the optic lobe pnAChR, the maximal level of muscle nAChR was found in 12 day old embryos, after which a rapid decrease was observed. From these findings, optic lobes from 19 day old embryos were chosen for subsequent mRNA preparations.

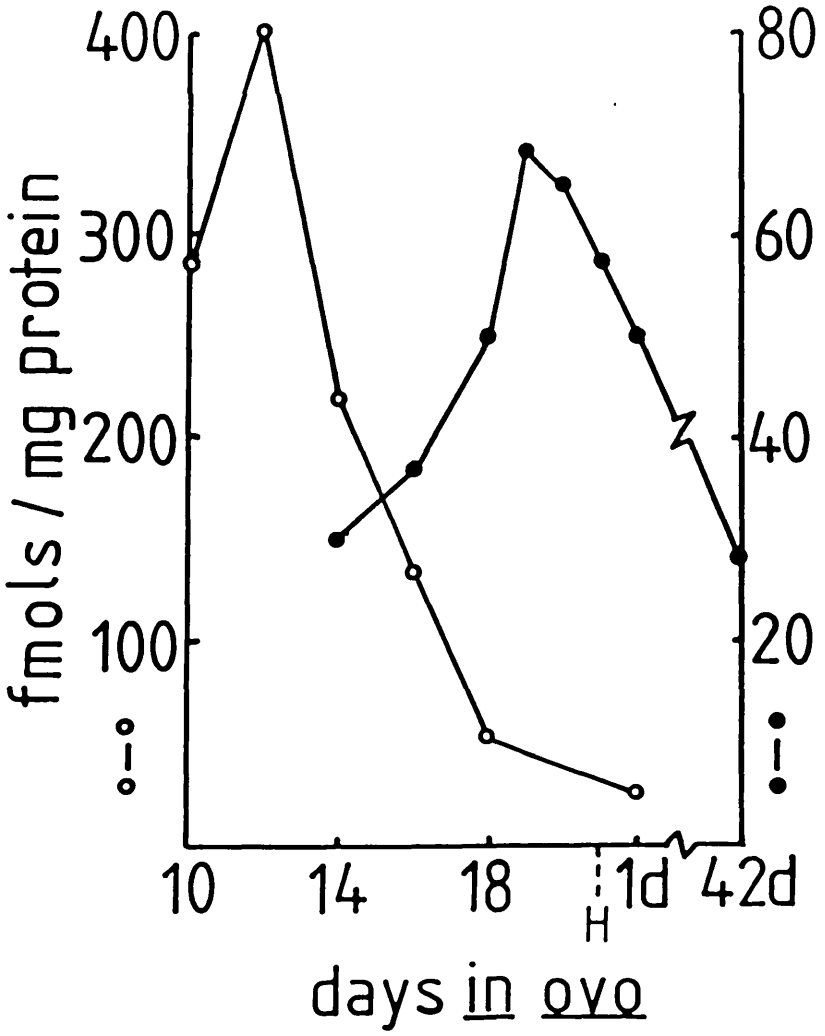

Fig. 4.1 Ontogeny of the nAChR in chick pectoral muscle and pnAChR in chick optic lobes

Tissue (~100mg) from chick pectoral muscle and chick optic lobes was homogenised in buffer A (2.2.4) containing 1% Triton X-100. After 1 hour at 4°C, the extract was centrifuged (10,000g, 20 minutes), and aliquots of the supernatant assayed for ^{125}I-α BuTX binding activity (2.2.5) and protein (2.2.9).

Closed circles represent optic lobe and open circles represent pectoral muscle. H indicates day of hatching (21), and d represents the number of days post-hatch.

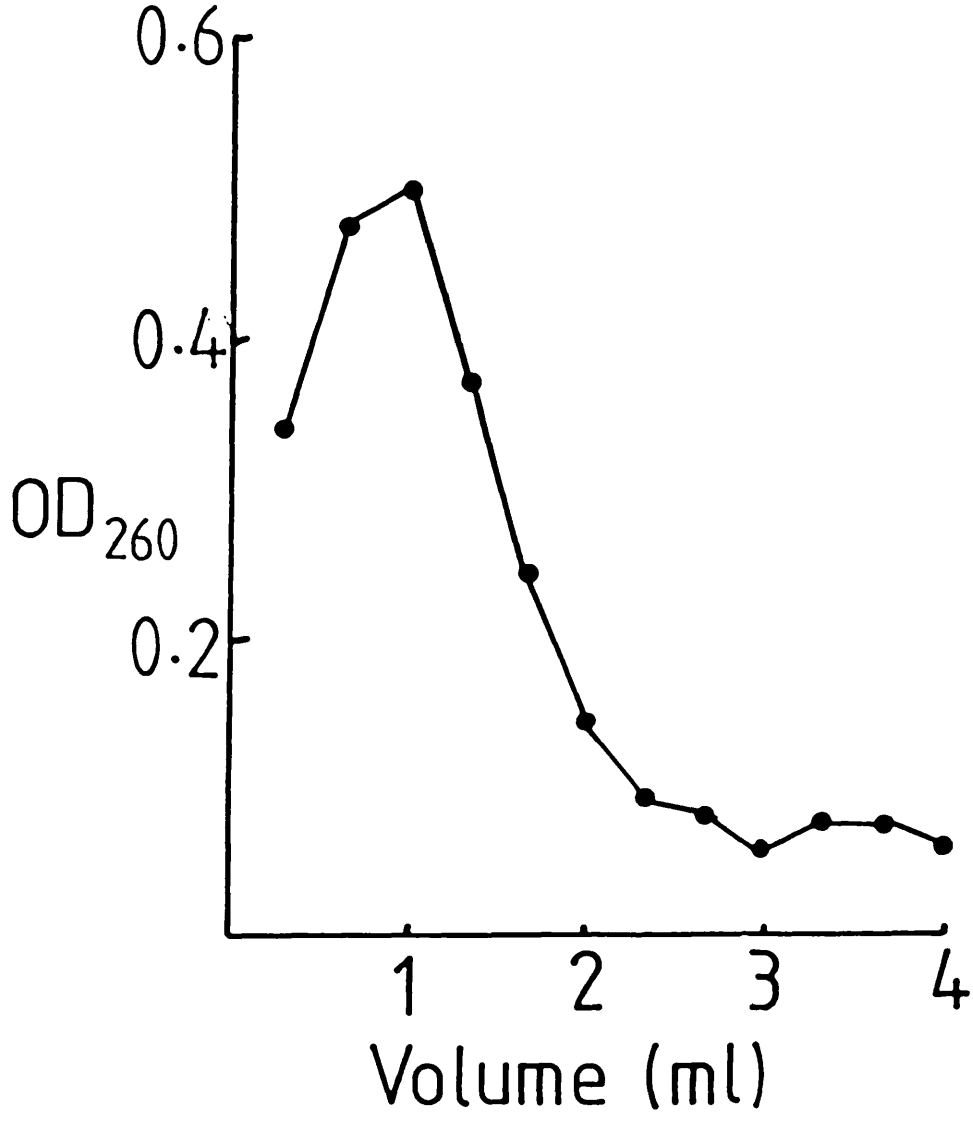

Fig. 4.2 Elution profile of poly(A)$^+$-mRNA

The elution of poly(A)$^+$-mRNA in STE buffer (4.2.2) was monitored by measuring the OD_{260} of the eluate.

4.3.2 Oocyte translation of optic lobe poly(A)$^+$-mRNA

(i) Measurement of AChE activity

In order to check that oocytes and poly(A)$^+$-mRNA preparations (Fig. 4.2) were capable of synthesizing new polypeptides, a sensitive radiometric assay for measuring AChE activity (Johnson and Russell, 1975) was employed to measure for AChE activity in microinjected oocytes. The two preparations tested using this assay, were found to give a positive response, indicating the presence of biologically active mRNA.

Before assaying, oocytes which had not survived micro-injection (10-20%) were removed from the incubation medium. Non-injected oocytes were used in control experiments in order to determine the level of non-specific activity and spontaneous AChE degradation. This value was always <10% of the total activity. Results obtained using different batches of oocytes (from different frogs), were often variable, with some oocyte batches expressing higher levels of AChE activity than others. However, within a particular batch, translation of the injected poly(A)$^+$-mRNA was consistent (Fig. 4.3).

(ii) Measurement of ^{125}I-α BuTX binding

Since the DE 81 disc assay was routinely used in the determination of ^{125}I-α BuTX binding (2.2.5), this method was initially employed in assaying for pnAChRs synthesized by oocytes.

A serious problem with results obtained from disc assays, was the presence of a very high background level of counts (Table 4.1). This appeared to be due to high levels of non-specific binding to the oocyte's intrinsic proteins and not to newly synthesized proteins, as non-injected oocyte controls also gave

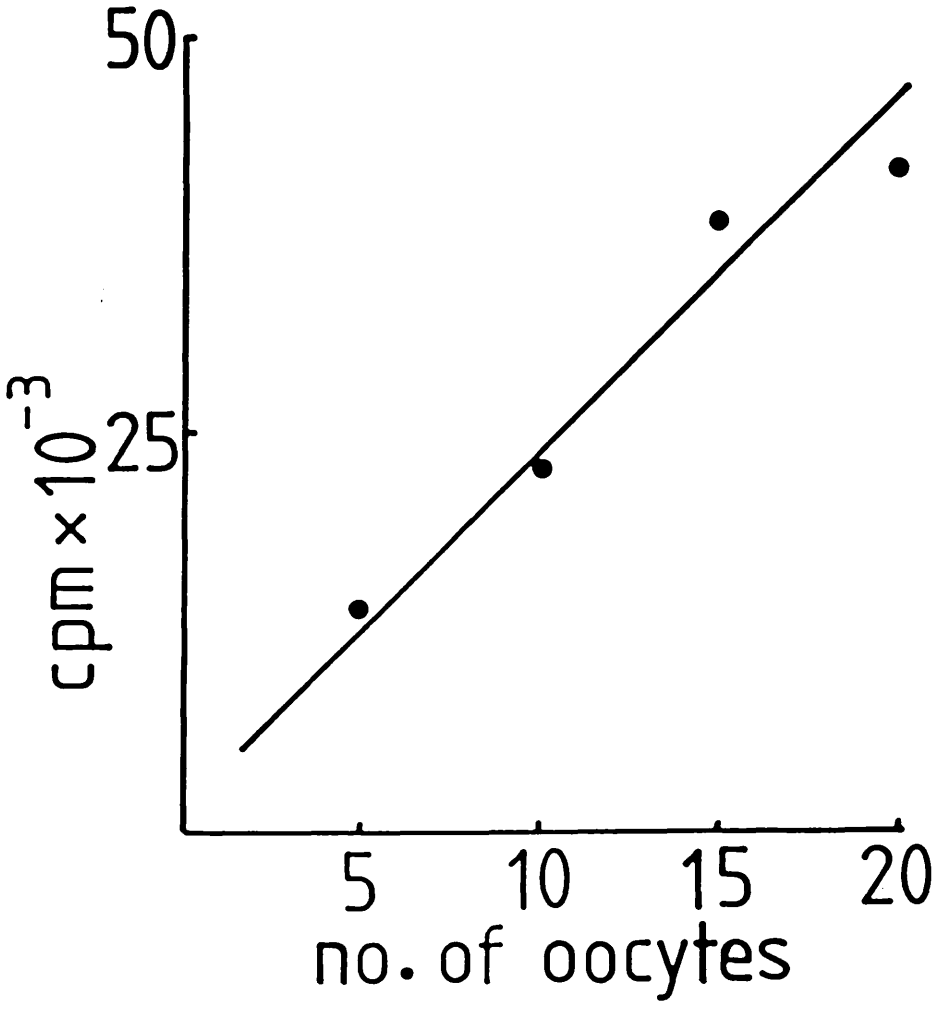

Fig. 4.3 AChE activity in oocytes after microinjection of chick optic lobe poly(A)$^+$-mRNA

Oocytes were microinjected with 40ng of optic lobe poly(A)$^+$-mRNA, incubated in Barth's medium for 48 hours at 21°C (4.2.3), then assayed for AChE activity (7.2.10). Correlation coefficient r = 0.97.

Table 4.1 α BuTX binding to oocytes after microinjection of poly(A)$^+$-mRNA

	cpm/10 oocytes			
Volume of oocyte extract	Total	Non-specific	Specific	% of total binding
Injected				
100µl	26670	25790	880	3.3
50µl	25631	25090	541	2.1
Non-injected				
100µl	24912	25215		
50µl	22604	22550		

Oocytes were microinjected with 40ng of chick optic lobe poly(A)$^+$-mRNA, incubated in Barth's medium for 48 hours at 21°C, then assayed for ^{125}I-α BuTX binding activity using DE 81 cellulose discs (4.2.3).

Non-specific binding was determined in the presence of 5µM α BuTX. Control experiments were performed using non-injected oocytes.

high backgrounds. The specific counts that were found, represented only 2-3% of the total counts, too low a level to reliably measure the small quantity of pnAChR synthesized by the oocytes. When additional washing of discs to reduce the level of non-specific binding was attempted, specific binding was not detectable.

(iii) Immunoassays with mAb 3a

The use of immunoassays was made in order to overcome the high background problem found using DE discs. This approach was facilitated by the use of a monoclonal antibody specific for the optic lobe pnAChR. The mAB 3a (obtained from H. Betz, Martinsried, FRG - Betz and Pfeiffer, 1984), was ideal for this purpose as it displayed a high titer, a low K_D and did not compete with ^{125}I-α BuTX (Table 4.2). Preliminary experiments using mAb 3a binding to the ^{125}I-α BuTX-pnAChR complex in optic lobe membrane extracts, employed as second antibody rabbit anti-mouse IgG coupled to polyacrylamide beads (Immunobeads). The advantages of Immunobeads over immunoprecipitation, are the shorter incubation period with antigen (2hr), and rapid separation of beads from the supernatant by centrifugation. However, experiments comparing the percentage recovery of ^{125}I-α BuTX-pnAChR complex, showed that the recovery using Immunobeads was much lower than that obtained by immunoprecipitation using rabbit antimouse IgG antiserum. An equivalent recovery by Immunobeads required 3-4 additions to the same extract (Fig. 4.4). Hence, the immuno- precipitation method was chosen in subsequent microinjection experiments. Control experiments in which oocytes were injected with poly(A)$^+$-mRNA fom chick muscle and chick fibroblast used a rabbit anti-chick

Table 4.2 Properties of mAb 3a

(from Betz and Pfeiffer, 1984).

Ig class[a]	IgG 2a
Titre[b]	1200nM
K_D	0.3nM
Inhibition of α BuTX binding[c] to:	
optic lobe membranes	(-)
detergent extract	(-)
Cross-reaction with detergent extract from PC12 cells	(+)

a Determined by immunodiffusion

b Determined by titrating a constant amount of antibody with different concentrations of ^{125}I-α BuTX-labelled detergent extract

c Membranes or detergent extracts were incubated with dilutions of mAb 3a then ^{125}I-α BuTX binding was determined

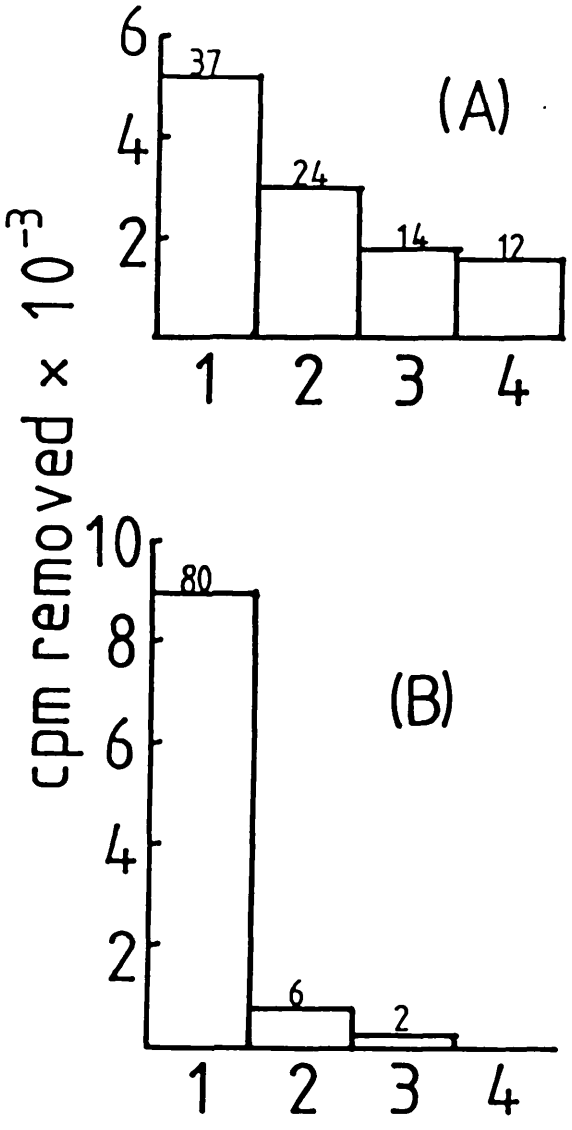

Fig. 4.4 Immunoassay of optic lobe pnAChR with mAb3a

(A) Immunobeads (10 fold excess over mAb 3a) were added to optic lobe extracts preincubated with ^{125}I-α BuTX and mAb 3a (4.2.3). After 2 hours incubation, the beads were pelleted (1000g, 5 mins), washed with 2x 1ml of PBS containing 1% Triton, then counted for radioactivity. Assays were repeated by further additions of Immunobeads to the remaining supernatant.

(B) Immunoprecipitation with rabbit anti-mouse IgG (100µl) was performed in 4.2.3. A second and third immunoprecipitation was made after readdition of normal mouse serum (10µl) followed by rabbit anti- mouse IgG (100µl).

muscle nAChR antiserum followed by goat anti-rabbit IgG antiserum for precipitation. These controls confirmed that high levels of nAChR were obtained from muscle, but not fibroblast mRNA.

Due to the minute levels of pnAChR synthesized, immunoprecipitations were performed on batches of 100 injected oocytes. Although the total specific counts obtained were low, they confirmed that the oocytes were capable of synthesizing the optic lobe pnAChR in a form containing both the αBuTX and mAB 3a binding sites (Table 4.3).

(iv) Purification of ^{35}S-methionine labelled pnAChR

Because of the low (femtomole) levels of pnAChR expressed by injected oocytes, purification of the pnAChR to determine its subunit composition was not feasible by silver staining of the protein. Instead, with coinjection of ^{35}S-methionine into oocytes, incorporation of radiolabel into the pnAChR subunits would allow their detection by fluorography, following incubation in enhancing reagents. Using an identical purification protocol to that in 3.2.2, the nicotine eluate from the α BuTX-Sepharose was found to contain several thousand counts. When analysed by SDS-PAGE followed by autoradiography, several subunits were apparent at MW 48K, 57K, 73K and 98K. These correspond identically to the subunit composition of the pnAChR protein purified from optic lobe membranes, with the 57K band being the most intense and the 73K and 98K bands relatively weak.

Table 4.3 Immunoprecipitation of nAChR and pnAChR from microinjected oocytes

mRNA source	cpm/100 oocytes	fmols/oocyte
chick embryonic 19 day optic lobe	2450	0.30
chick embryonic 12 day pectoral muscle	11167	1.35
chick fibroblast	127	0.003

Oocytes were microinjected with 40ng of poly(A)$^+$-mRNA, incubated in Barth's medium for 48 hours at 21°C, then assayed for nAChR or pnAChR by immunoprecipitation with ^{3}H-α BuTX and mAb 3a (4.2.3).

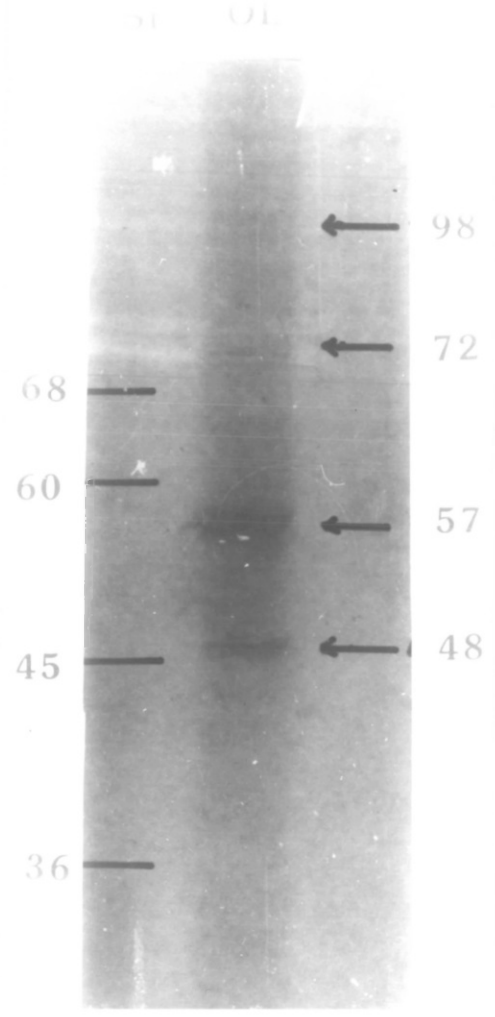

Fig 4.5 Autoradiogram from SDS-gel of ^{35}S-methionine labelled pnAChR

The labelled pnAChR from oocytes microinjected with optic lobe poly(A)$^+$-mRNA, was purified by affinity chromatography on α BuTX- Sepharose and subjected to SDS-PAGE (4.2.4). After drying, the gel was exposed to Fuji X-ray film at -70°C for 21 days.

OL represents the pnAChR track, and St the position of standards visualised by Coomassie staining (4.2.5).

CHAPTER 5 DISCUSSION AND CONCLUSIONS

5.1 Choice of tissue

By analogy to its extreme specificity for muscle nAChRs (Weber and Changeux, 1974), the snake venom neurotoxin, α BuTX, has been used for many studies of a corresponding putative neuronal nAChR (pnAChR). In all such studies, specific α BuTX binding sites have been observed in the membrane fraction of various neuronal tissues, such as vertebrate brain (McQuarrie et al, 1976; Lowy et al, 1976; Oswald and Freeman, 1979), invertebrate brain (Schmidt-Nielsen et al, 1978; Thomas et al, 1978), retina (Wang and Schmidt, 1976; Vogel and Nirenberg, 1976), parasympathetic (Ravdin and Berg, 1979) and sympathetic (Patrick and Stallcup, 1977a,b; Carbonetto et al, 1978) ganglia and cultured neurons. However, the equivalence of the neuronal α BuTX binding protein to a classical nAChR, has been a matter of great controversy in recent years, due to the ineffectiveness of α BuTX application on the known physiological response of nAChRs (see Chapter 1). Only in the optic tectum of the visual pathway of lower vertebrates, is there undisputed evidence for an electrophysiological blockade of nAChRs by α BuTX (Freeman, 1977; Barnard et al, 1979; Oswald and Freeman, 1981b). This region of the lower vertebrate brain, and its higher vertebrate homologue the superior colliculus, is also known to contain the highest levels of α BuTX binding (Table 1.1). In addition, the saturable binding of α BuTX to membranes and soluble preparations from chick optic lobes, which is specifically antagonised by nicotinic ligands, has already been demonstrated (Wang et al, 1979; Barnard et al, 1979). For these reasons, the present study chose this

source of neuronal tissue for further investigation, as well as for the easier dissection, facilitated by the relatively large size of chick optic lobes (compared to goldfish), and the commercial availability of large numbers of chicks.

5.2 Oligomeric characterization

In an earlier study from this laboratory, many molecular properties of the pnAChR from chick optic lobe were characterised (Norman et al, 1982). Although the oligomeric size had not been determined in the latter study, the apparent sedimentation coefficient (S value) of the pnAChR solubilised in the nonionic detergents Triton X-100 and Lubrol PX, had been obtained, giving values of ~9S and 11-12S respectively. The reason for these different S values was not obvious, although it was suggested that use of Triton X-100, has solubilised additional protein, which remained complexed to the pnAChR in detergent solution (Norman, 1981). This explanation was feasible, as it had been found that muscle actin always contaminated nAChR preparations from foetal calf muscle, and could only be removed by inclusion of a DNase-1-Sepharose step in the purification procedure (Strader et al, 1980).

Similarly, in a study which used several different detergents to solubilise muscarinic AChRs from rat brain, Berrie et al (1984), also found a smaller S value in Lubrol PX when compared to other detergents used, although this contrasts with the finding for the bovine brain GABA/benzodiazepine receptor that the S value was unchanged in both Lubrol PX and Triton X-100 (Chang and Barnard, 1982).

Evidence obtained in this study however, implied actin was not present as a contaminant (Chapter 2). It was clearly shown

that after incubation of the pnAChR preparation in DNase-1-Sepharose, the S value was unchanged. Further treatment of the used DNase-1-Sepharose with SDS/β-mercaptoethanol, and subjecting the eluate to SDS-PAGE, did not reveal any bands corresponding to the molecular weight of brain actin (MW 45K, Pardee and Bamburg, 1979). In addition, simultaneously performed experiments found that both Lubrol and Triton solubilised pnAChR gave identical S values of 10.5 S. Previous findings could have been caused by the fact that the Lubrol PX had partially denatured the protein, as was found by Berrie et al, (1984) for the mAChR, thus causing altered hydrodynamic properties. It was concluded that no real difference in the pnAChR's oligomeric size existed.

As described by Fish (1975), direct measurement of a membrane protein's true sedimentation coefficient ($s_{20,w}$), by interpolation from the sedimentation rates of globular proteins of known $s_{20,w}$ (Martin and Ames, 1961), is invalid. The globular proteins have a lower affinity for detergent than the membrane protein, which in turn will alter the ratios of their buoyant density factors and the sedimentation coefficent obtained is that of the membrane protein-detergent complex (S value). Thus, for membrane proteins, sedimentation in sucrose/D_2O gradients, to enable a correction for bound detergent, is required (Tanford et al, 1974). This method in addition, allows calculation of the membrane protein's partial specific volume ($\bar{v}$). Such studies have been performed on the pnAChR from goldfish optic lobes, and resulted in a $s_{20,w}$ value of 11.45 (Oswald and Freeman, 1979). This is similar to the $s_{20,w}$ of 11.76 obtained for the chick optic lobe pnAChR in this study, and suggests that the increased $s_{20,w}$ value, relative to muscle nAChRs, may be a common property of all neuronal pnAChRs.

Correspondingly, the $\bar{v}$ of the chick (0.766 ml/g), as well as the goldfish optic lobe pnAChR (0.786) ml/g), are both greater than the $\bar{v}$ found for muscle nAChR (0.75 ml/g). Since the average protein $\bar{v}$ is 0.735 ml/g, and additional carbohydrate moieties can result in an increased $\bar{v}$, the higher value for neuronal pnAChRs may thus reflect an increased level of glycosylation. This possibility is supported by the presence of sugar residues, found on the pnAChR from chick optic lobe (Norman et al, 1982), goldfish optic lobe (Oswald and Freeman, 1979) and rat brain (Salvaterra et al, 1977) by their retention on lectin-Sepharose columns. Using several such columns, the presence of mannose, N-acetyl glucosamine, and galactose, but not fucose, residues has been confirmed (Salvaterra et al, 1977).

Since membrane proteins require detergent for solubilisation in aqueous solvents, their molecular weight (MW) cannot be obtained directly by comparison with a partition coefficient calibration plot of soluble proteins after gel filtration chromatography (Fish, 1975). The Stokes radius which is obtained, can however, be combined with results from sedimentation experiments, to allow calculation of MW (Tanford et al, 1974). This method has been found to give an accuracy of ± 7% (Pitts et al, 1974). The MW of 354K calculated by the above method for the chick optic lobe pnAChR, is very similar to the 357K found for rat brain (Salvaterra and Mahler, 1976), and 340K for goldfish optic lobe (Oswald and Freeman, 1979) pnAChR.

All these are significantly larger than the 285K MW ofthe muscle nAChR. It should be noted that the 354K for chick pnAChR, was obtained using the calculated $\bar{v}$ value of 0.766ml/g, hence this is an average MW including any carbohydrate moieties, whereas the 340K found for the goldfish pnAChR assumed a $\bar{v}$ of

0.735ml/g (Oswald and Freeman, 1979). If this $\bar{v}$ was also assumed for the chick pnAChR the MW would be 314K. Because the $s_{20,w}$ and Stokes radius values determined are for the whole oligomeric complex, including any carbohydrate moieties, the calculated $\bar{v}$ should be the more appropriate one for MW calculations. It should be noted also, that the MW calculation by the above method relies on the degree of accuracy obtained in two sets of different experimental determinations ($s_{20,w}$ and Stokes radius), therefore a combination of two possible sources of errors could be introduced. Only by complete sequencing of the protein, for example, as achieved in the case of muscle nAChR by cDNA cloning (Noda et al, 1982, 1983a,b), can the exact protein MW be determined. The method used here does indicate however, that the chick optic lobe pnAChR is larger than the muscle nAChR. This increase could be explained by the presence of more and complex regulatory sites for modulation of function, possibly by the neuronal transmitter ligands, on this putative nAChR.

While the pnAChRs have a larger $s_{20,w}$ and calculated MW than the muscle nAChR, in rat brain, the pnAChR has been found to co-chromatograph with the T. californica nAChR, upon gel filtration (Lowy et al, 1976). Also from the Stokes radius value of 7.6nm for the pnAChR from chick optic lobe, and the 7.4nm found for rat brain, mouse brain and goldfish optic lobe (Salvaterra and Mahler, 1976; Seto et al, 1977; Oswald and Freeman, 1979), it appears that there is only a slight increase over the 7.3nm Stokes radius for the muscle nAChR (Meunier et al, 1972b).

With a knowledge of the pnAChR MW, its extent of deviation from a globular structure can be estimated by calculation of its frictional ratio. In dilute buffer, the value for a globular

protein is 1-1.3 · (Tanford, 1961). The observation of a frictional ratio of 1.49 for the chick optic lobe pnAChR, indicates a significant deviation from a globular structure and is consistent with either a prolate ellipsoid or an oblate ellipsoid. Similarly, high frictional ratios have also been observed for other membrane proteins, such as 1.45 for the goldfish optic lobe pnAChR (Oswald and Freeman, 1979), 1.46 for the bovine brain GABA/benzodiazepine receptor (Stephenson et al, 1982) and 1.52 for the β-BuTX binding protein in chick brain (Rehm and Betz, 1984).

5.3 Subunit characterisation

In early purification studies from various laboratories, purified preparations of the muscle nAChR were obtained, which yielded apparently identical values of sedimentation coefficient, toxin binding sites per gram of protein (specific activity), and activity in reconstitution experiments. However, the same preparations were also reported to contain widely different subunit patterns after SDS-PAGE (Conti-Tronconi and Raftery, 1982). Although a major band called α (38-44K), was always found, sometimes, variable ratios of heavier subunits termed β (48-53K), γ (57-60K) and δ (64-67K), were also present.

After several recent major advances (1.4.3), the muscle nAChR subunit structure has been clearly established, and is known to comprise an oligomer of 5 subunits with a stoichiometry of $\alpha_2\beta\gamma\delta$ (Mishina et al, 1984). The reasons for the variability of early SDS-PAGE patterns of purified nAChR is now clearly understood (Popot and Changeux, 1984). Due to their susceptibility to proteolytic attack and the presence of a high concentration of endogenous proteases in homogenized tissue

extracts, cuts, or nicks, in the β, γ and δ subunits had occurred throughout the purification procedure (Vandlen et al, 1979; Lindstrom et al, 1980b). Most of the small polypeptides produced, remained associated with the nAChR oligomer until the SDS denaturation step, thus explaining why the identical oligomeric properties were found. In addition the α subunit, which is present twice per oligomer and contains the ACh and α BuTX binding sites, was shown to be relatively protease resistant (Bartfeld and Fuchs, 1979; Klymkowsky et al, 1980), hence its ubiquitous presence in all preparations.

Similarly, a purification protocol of a pnAChR was reported by Norman et al, (1982) which had a specific activity for α BuTX binding of ~3000 nmol/g of protein, and revealed a single band of 54K on SDS-PAGE. Presence of only one subunit on SDS gels is a cause for concern, since the specific activity achieved, corresponds to a pure protein with a MW of ~330K per α BuTX binding site. The following two explanations are compatible with the above findings:

1) the pnAChR exists as a pentameric/hexameric oligomer of 54K subunits, with some form of functional non-equivalence between the 5/6 subunits such that only one toxin molecule is bound per oligomer or,

2) due to nicking of the oligomer by proteases, loss of integral pnAChR subunits of different molecular weights occurred during purification, resulting in a single band of 54K. Supporting this possibility some preparations (in Triton X-100) were reported to contain several minor bands in addition to the 54K subunit. Also the 54K subunit is known to possess the ACh binding site, by its specific labelling with ^{3}H-BAC, as well as the α BuTX binding site (Norman et al, 1982). This suggests that

the 54K subunit, by analogy to the muscle nAChR α subunit, could be the most protease resistant subunit of a pnAChR hetero-oligomer.

The approach taken in this study was to preserve the pnAChR as well as possible, by reducing the time needed for purification, and also by increasing the level of protease inhibitors present. Significant reduction in the time required for purification was achieved through several modifications;

a) incubation with α BuTX-Sepharose was reduced from 18 hours to 4 hours, since it was already known that maximal percentage binding to the affinity gel was reached after ~3 hours,

b) washing the affinity gel in a column was exchanged for a more rapid centrifugation method,

c) the DNase-1-Sepharose incubation step was omitted, as brain actin was found not to have been removed by it, and

d) the GTP-agarose and lentil lectin-Sepharose steps were also omitted.

As a result of these modifications, two additional subunits of 47K and 72K were observed as well as a 57K (close to ~54K) subunit. Since determination of muscle nAChR subunits by a number of laboratories has shown that the apparent MW often varies slightly, depending on the gel system and the particular conditions employed during electrophoresis (Froehner and Rafto, 1979; Nathanson and Hall, 1979; Shorr *et al*, 1981), it is very likely that the 57K subunit is the same as the 54K subunit found by Norman *et al* (1982). Although the presence of the two other subunits of 47K and 72K were previously undetected, their specific elution from α BuTX-Sepharose by carbachol, suggests that they are specific to the pnAChR. The precise mechanism for the elution of nAChRs from α-toxin columns by carbachol is

unknown, but it has been proposed by Maelicke et al (1977), that in the presence of high concentrations of cholinergic ligands, unstable ternary complexes are formed, which eventually results in the release of bound nAChR. Also by using a high concentration of competing cholinergic ligand, any reinteraction of the eluted nAChR with α-toxin, is reduced to a minimum.

In further preparations for amino-terminal sequence analysis of purified subunits, carbachol elution was replaced with SDS elution, as the identical gel patterns suggested that all non-specifically bound proteins had been removed from the affinity gel.

Attempts to establish the subunit composition of other pnAChRs, using a variety of ligands, have also been reported. Seto et al (1981) purified a pnAChR from mouse brain by affinity chromatography on Naja naja kaouthia α toxin-Sepharose, followed by gel filtration and ion-exchange chromatography. After radioiodination of the purified product, only a single major subunit of 51K was seen. This subunit was further shown to specifically bind α BuTX from crosslinking experiments. However, purification of the rat brain pnAChR by affinity chromatography using Naja naja siamensis α toxin, has found evidence for four subunits (Kemp et al, 1980), although this preliminary result (abstract) has not yet been more fully reported. The same laboratory was able to achieve a final specific activity of 3000nmol/g protein (Morley and Kemp, 1981).

In a study employing a nicotine-Sepharose, rather than α toxin-Sepharose, column (Abood et al, 1983), affinity purification of a nicotine binding protein from rat brain, resulted in observation of a major subunit of 56K, with minor amounts of other subunits from 47-83K. The final specific

activity of the protein, by nicotine binding, was >2500 nmol/g protein. This specific activity, together with the similar values reported by Morley and Kemp (1981) and Norman et al, (1982), corresponds to the purification of a protein of 330-400K. The presence of a major band of 56K in nicotine eluates, like the 57K subunit found here for the chick optic lobe, suggests that this is a pnAChR α subunit. In addition, the presence of a 47K subunit, which is also found in the chick optic lobe pnAChR, implies possible subunit similarities between the pnAChR from these two sources. Due to its presence as a minor component, it was suggested that the 47K band may represent a breakdown product of the 56K subunit (Abood et al, 1983). However, the specific activity obtained suggests otherwise, and presence of these additional components is strong evidence for the existence of other integral pnAChR subunits. Why only one subunit of 51K was observed for mouse brain pnAChR is unclear (Seto et al, 1981), although it now appears likely that where only one subunit was observed, other subunits had probably been lost due to proteolysis. The reason why subunits other than α are much more susceptible to proteolysis is not yet understood, although Lindstrom et al (1980b) have reported that in preparations of eel nAChR, the δ subunit was preserved only when iodoacetamide, a thiol-blocking proteinase inhibitor, was present.

Previous reports that nicotine and (+) tubocurarine were the two most potent inhibitors of α BuTX binding (Table 1.2),in addition to the report by Abood et al, (1983), prompted the use of nicotine as an eluting ligand. However, in addition to the same three subunits found on elution with carbachol or SDS (47K, 57K and 72K), the gel pattern revealed an additional band at ~98K (approximate value because no MW markers above 68K were present).

The presence of this higher MW band was unexpected, since it had never been previously observed in carbachol elutions, although its elution by nicotine strongly suggested that it was specific. Possible explanations which may account for the appearance of the ~98K band are:

i) a dimer of the 47K or 57K subunits was present during purification and was incompletely dissociated before electrophoresis,

ii) two populations of α BuTX binding proteins exist, and carbachol elutes one, whereas nicotine elutes both, with the additional eluted protein accounting for the ~98K subunit, and,

iii) the immediate heat treatment of nicotine eluates and/or the shorter elution time used, both of which were modifications introduced simultaneously with elution by nicotine, may have effectively reduced proteolysis such that an additional, highly protease susceptible pnAChR subunit was revealed.

Without other evidence, the first explanation appears the most unlikely, since samples were denatured twice (immediately after elution and again before SDS-PAGE). In support of the second possibility, evidence has been found in rat brain (Lukas, 1984) and goldfish optic lobe (Oswald and Freeman, 1979), for a low affinity (K_D 400nM) binding site for α BuTX, in addition to the high affinity site (K_D 5nM). However, as they copurified after sedimentation on sucrose gradients, it was suggested more likely that the two sites were probably interconvertible sites on the same macromolecule. Similarly, only a single peak was found after sedimentation of the chick optic lobe pnAChR in this study. Although it is possible that the single gradient peaks contain two similar sized proteins, no evidence for this has yet been shown. For these and the following additional reasons, it

appears that the last explanation is, at present the most feasible;

1) the higher yield of pnAChR obtained by nicotine elution, resulted in increased protein concentration in SDS gels, thus improving staining intensity of the separated subunits,

2) although relatively faint, the ~98K subunit was also observed in the pnAChR metabolically labelled with ^{35}S-methionine in Xenopus oocytes, and,

3) in preliminary studies using a DV 493 toxin-Sepharose affinity gel, purification of pnAChR exactly as with α BuTX, produced an identical subunit pattern, with 47K, 57K, 72K and ~98K bands. DV 493, an α-toxin isolated from Dendroaspis viridis (Shipolini et al, 1973) specifically displaces α BuTX binding to the chick optic lobe pnAChR (Barnard et al, 1979) and muscle nAChR (Patrick et al, 1980). It has also been shown to block cholinergic transmission in the frog spinal cord (Miledi and Szcepaniak, 1975).

A further possibility, that the ~98K subunit is a peripheral, as opposed to integral pnAChR, subunit is exemplified by the recent observation of a high MW subunit in the purified glycine receptor from mammalian spinal cord (Betz et al, 1985). In this case, after one step purification on a strychnine affinity column, three polypeptides of 48K, 58K and 93K were obtained. Using mAbs raised to each subunit, cross-reaction was observed between mAbs specific for the 48K and the 58K subunits, but not with the 93K subunit (Graham et al, 1985). In addition, electron microscopic studies using immunogold staining methods, showed that whilst the 48K mAb bound to the outer face of the synaptic membrane, the 93K mAb was situated on the cytoplasmic face. It was postulated that the 93K subunit may be a peripheral

membrane-anchoring protein, but associated specifically with the glycine receptor.

Several studies using DV 493 have found evidence for a different α BuTX binding stoichiometry between rat brain pnAChR and muscle nAChR. In Torpedo nAChR membranes, the ratio of DV 493 to α BuTX binding sites was 1:1, whereas in rat brain membranes it was 2:1 (Hanley et al, 1978). Since the pharmacological and sedimentation behaviour of both sites were identical in both tissues, this implied that, in contrast to the two α BuTX binding sites known to exist in muscle nAChR, only one such site existed in rat brain pnAChR. In addition, when MBTA, an affinity reagent for the ACh binding site, was used at a concentration sufficient to reduce specific α BuTX binding to 50% in muscle nAChR, binding in rat brain was totally abolished (Morley and Kemp, 1981; Lukas and Bennett, 1980b), suggesting that in pnAChRs, an α BuTX site overlaps with only one of the two ACh sites. The latter explanation would correlate with the lack of effect on function found for many neuronal nAChRs, after application of α BuTX. Supporting evidence has also been found in studies using the affinity reagent BAC (Damle and Karlin, 1978; Wolosin et al, 1980). Moreover, these studies are also consistent with the reported specific activity of ~3000nmol/g protein achieved in various pnAChR purifications (Morley and Kemp, 1981; Norman et al, 1982; Abood et al, 1983), since this specific activity corresponds to a MW of 333K per α BuTX binding site, similar to the MW values obtained for pnAChRs from various sources (Salvaterra and Mahler, 1976; Oswald and Freeman, 1979). Assuming one α BuTX binding site on the 354K chick optic lobe pnAChR (Chapter 2), the pure pnAChR protein would be expected to display a specific activity of 2800 nmol/g protein. The actual

specific activity obtained experimentally (2590nmol/g protein Table 3.1), suggests that a purity of >92% was achieved.

5.4 Amino-terminal sequence analysis

In initial peptide mapping studies performed on muscle nAChR, no striking similarity between the subunits was apparent (Froehner and Rafto, 1979; Nathanson and Hall, 1979). It was surprising therefore, when immunological cross-reaction between the α and β subunits and γ and δ subunits was clearly demonstrated with mAbs (Tzartos and Lindstrom, 1980; Tzartos et al, 1981), and when extensive homologies between all four subunits were revealed by amino-terminal microsequencing of purified Torpedo (Raftery et al, 1980) and Electrophorus (Conti-Tronconi et al, 1982a) nAChR subunits. Recently, synthesis of radiolabelled oligodeoxyribonucleotides corresponding to these amino-terminal sequences, have enabled the cloning and sequencing of the corresponding cDNAs for all four subunits (Sumikawa et al, 1982b; Claudio et al, 1983; Noda et al, 1982, 1983 a,b,c). Alignment of the cDNA-deduced amino acid residues of nAChR subunits from T. californica, confirmed the earlier microsequencing studies and convincingly showed the existence of considerable homology between subunits (Noda et al, 1983b). These sequence homologies have suggested that the four nAChR subunits evolved by duplication and reduplication of a primordial gene, before the divergence of primitive vertebrates into Chond-richthyes and teleosts approximately 400 million years ago (Raftery et al, 1980).

Similarly, in this study, amino-terminal sequence analysis was used in an attempt to reveal further evidence for a similarity between the chick optic lobe pnAChR and muscle nAChRs (Chapter 4; Conti-Tronconi et al, 1985). After isolation of

subunits from preparative SDS gels, most of the polypeptides were found to be blocked at the amino-terminus. Reasons why all subunits except the 47K were blocked, are not clear, although similarly blocked subunits were found in purified preparations of the GABA/benzodiazepine receptor (F.A. Stephenson, personal communication). Chemical modification of the subunit amino-terminals during purification is conceivable, although sequencing of intact preparations suggested that the blockage preexisted subunit isolation by electrophoresis. Alternatively, the presence of intrinsically blocked subunits is also plausible. Omission of N-ethyl maleimide and iodoacetamide from all buffers during purification was without effect, suggesting that the latter explanation is more likely. Presence of a blocked 57K subunit was also further evidence that the 47K subunit is a distinct subunit and not, as had been suggested, a breakdown product of the 57K subunit (Abood et al, 1983). The obvious amino-terminal sequence homology on comparison of the 47K subunit with nAChR α subunits established that the pnAChR is indeed similar to the nAChR from muscle, and further indicated that, although encoded by different genes, the subunits originated from the same ancestral gene. Since the similarity between this sequence and the muscle α subunit was much less than between muscle α subunits from different animals, it may be concluded that the muscle nAChR and neuronal nAChR diverged very early during vertebrate evolution. This divergence from an ancestral common structure, could explain the significant overlap of pharmacological and biochemical characteristics observed. One apparent incongruity however, is the specific binding of both α BuTX and cholinergic affinity ligands to the 57K rather than 47K (putative α) subunit. This phenomenon could be interpreted as

resulting from an evolutionary divergence of the agonist binding site, from the 47K (putative α) to the 57K (putative β) subunit in neuronal nAChRs, and would concur with the previously inferred existence of only one α BuTX binding site as well as the relative inefficacy of α BuTX on neuronal nAChR function (Morley and Kemp, 1981). However, proof from further amino acid sequence information on the blocked subunits, especially the 57K, is required, since this might display an even higher α subunit homology than the 47K subunit. This would be feasible, by isolating and sequencing CNBr fragments from each subunit, and eventually by cloning and sequencing the subunit cDNAs. Further studies, possibly by production of mAbs to each subunit and electron microscopic localization (Betz et al, 1985), are also required to elucidate the relationship between the ~98K subunit and the pnAChR.

5.5 Recent studies

Recently much interest has focussed upon an α-toxin of low abundance, isolated from Bungarus multicinctus venom (Chiappinelli, 1984). Designated variously as kappa-bungarotoxin (k BuTX), 3.1 toxin or P15 toxin (Chiappinelli, 1983; Ravdin and Berg, 1979; Gotti et al, 1985), this α-toxin was shown to block nicotinic transmission at nanomolar concentrations, in sympathetic (Chiappinelli and Dryer, 1984; Gotti et al, 1985) and parasympathetic (Ravdin and Berg, 1979; Chiappinelli, 1983) neurons, but not at neuromuscular synapses (Grant and Chiappinelli, 1985). These findings suggested that k BuTX could be a highly specific probe for neuronal nAChRs. Structural characterisation of this toxin found it to contain 10 cysteine residues (Grant and Chiappinelli, 1985), indicating that it

should be classified as a "long" α-toxin (1.3), but the total amino acid sequence of only 66 residues was less than the 74 present in other long toxins, such as α BuTX. Although a significant sequence homology of 47% with α BuTX was found, the unique effectiveness of k BuTX on neuronal nAChRs was suggested to be due to its tendency to spontaneously associate into dimers under physiological conditions (Chiappinelli and Lee, 1985). Evidence that the k BuTX site is situated on the α BuTX binding protein has been found in a study on rat superior cervical ganglia (Gotti et al, 1985). In this case, addition of 10^{-6}M k BuTX, was able to completely displace specific α BuTX binding, and addition of α BuTX prevented the blockade of ganglionic transmission by k BuTX.

In an approach to testing this toxin on the pnAChR from chick optic lobes, k BuTX was purified in this laboratory by an improved method, with an overall yield from crude venom of 0.5% (R. Shipolini, personal communication). Preliminary studies showed that k BuTX could effectively block the binding of pnAChR to α BuTX-Sepharose, suggesting that similar sites for both toxins were present on the pnAChR. Since previous attempts to obtain a ^{125}I-iodinated k BuTX preparation which still retained its biological activity were unsuccessful (M.A. Smith, personal communication), the toxin was immobilised on Sepharose beads by CNBr activation, in experiments directed towards purifying the k BuTX binding protein. This would enable subunit comparison with the pnAChR purified using α BuTX-Sepharose. However, the k BuTX appeared to lose its biological activity after coupling, since no reduction of α BuTX binding in the eluate was evident. This suggested that the alteration of native k BuTX may have caused dissociation of the dimer and loss of the specific configuration

required for interaction with the neuronal nAChR. Further studies are therefore still required to further elucidate the relationship between the pnAChR and the k BuTX-sensitive neuronal nAChRs.

Presently, there are two situations which could explain the effect of k BuTX. Either, two neuronal k BuTX binding proteins exist, one of which is a functional nAChR and the other an α BuTX binding protein of unknown function, or, both k BuTX and α BuTX bind to specific sites which are coincident on a neuronal nAChR. Evidence for the latter possibility and demonstration of a blockade of retinotectal transmission by k BuTX in chick optic lobes is needed, and would further support arguments favouring use of α BuTX in studying neuronal nAChRs in the chick optic lobe.

The probable existence of more than one CNS nAChR, has been shown in a recent study comparing the distribution of agonist and antagonist binding in rat brain (Clarke et al, 1985). Using high resolution autoradiography to produce detailed maps, the relationship between ^{3}H-ACh, ^{3}H-nicotine and ^{125}I-α BuTX binding regions were analysed. The maps of high affinity agonist labelling were strikingly concordant, but both were quite different to the pattern of high affinity ^{125}I-α BuTX binding. However, a significant finding was the notable overlap of dense α BuTX and agonist binding in the superior colliculus (homologue of optic tectum in lower vertebrates) and the cerebral cortex (layer 1). This overlap suggests that only in these regions, do the nAChRs labelled by agonists also bind α BuTX, and thus further justifies the present study with chick optic lobes. In the absence of a toxin or other ligand specific only for the nAChRs which do not bind α BuTX, determination of the structure of these

receptors, relative to the pnAChR, cannot be achieved. However, evidence from the similar subunit pattern obtained by purification of nAChRs from whole rat brain using immobilised nicotine (Abood et al, 1983), suggests that these receptors are structurally similar to the pnAChR, and distinct functional changes, perhaps in the subunits(s) which binds ACh, may account for the lack of α BuTX binding, as well as for different affinities of various ligands. One simplifying speculation which accords with the above study, would be the possible equivalence of the low affinity binding sites for α BuTX shown by Lukas (1984), to the high affinity agonist binding sites localised by Clarke et al, (1985), which do not overlap with α BuTX sites.

Note added in proof

Results recently reported by Boulter et al (1986), have given further evidence supporting the presence of neuronal nAChRs functionally insensitive to α BuTX. By using a cDNA clone coding for the mouse muscle nAChR α subunit, a cDNA clone coding for a putative neuronal nAChR α subunit in PC12 cells was isolated by low-stringency DNA/DNA hybridisation. The clone encoded a mature protein of 474 amino acids corresponding to a MW of ~55K, and contained the 4 cysteines, at positions 128, 142, 192 and 193, characteristic of muscle nAChR α subunits, and thought to be involved in agonist and α-neurotoxin binding (Numa et al, 1983; Kao et al, 1984). The potential asparagine-linked glycosylation site at position 141, found in all subunits of muscle nAChRs was also present, as well as the 4 hydrophobic and one amphipathic helix sequence thought to form the transmembrane and ion channel regions respectively (Finer-Moore and Stroud, 1984; Guy, 1984).

Although the 4 cysteines are conserved, the sequences surrounding them are not. Of the 4 substitutions found between Cys 128 and Cys 142, two are not conservative changes, with a lysine for a glutamate at position 129 and an aspartate for an isoleucine at position 130. Both these positions are conserved in all reported α-subunit sequences (Boulter et al, 1985). More significantly, the sequence between Cys 142 and Cys 192, which has been suggested to be involved in α-neurotoxin binding (Wilson et al, 1986), appears to be one of the least conserved. Only one out of the 19 residues between positions 153 and 172 is common with the mouse muscle nAChR α-subunit sequence, and at 8 of the 19 positions, non-conservative substitutions have replaced uncharged residues with charged residues. This major difference between muscle and the putative neuronal α subunit in this critical region, could easily account for the fact that α BuTX blocks muscle nAChRs but have no effect on neuronal nAChRs.

5.6 Concluding remarks

The pnAChR from chick optic lobes has been purified and extensively characterised. In common with other pnAChRs it displays an oligomeric size greater than muscle nAChRs, although its biochemical and pharmacological properties indicate significant similarities. The structure of the pnAChR is almost definitely a heterooligomer with subunits of 47K, 57K and 72K, and a ~98K protein which may be a specific, but peripheral, component. The stoichiometry of the subunits is unknown since amino-terminal sequencing was feasible only for the 47K subunit. A structure comprising 2x47K, 57, 72K and 98K subunits, a total of 321K, which does not include carbohydrate residues (~5%), is proposed. The observations made in this study, support the

designation of the pnAChR as a true nAChR. However, conclusive evidence that this protein contains an agonist gated ion channel is still required. Further studies to clone and sequence the pnAChR subunit cDNAs (which are in progress in this laboratory), would enable a clearer understanding of their functional roles.

SECTION II

CHAPTER 6 INTRODUCTION

In the early 1920's and 30's, experiments conducted by Hussey and Thompson (1923), Crowther (1924) and Northrop (1934), showed that enzymes in solution were inactivated by strong ionizing radiation sources, such as X-rays and radioisotopes. Although the survival of enzyme activity was found to be a logarithmic function of total radiation dose, attempts to use such a relation to determine inactivation volumes were unsuccessful. The reason became clear when Fricke (1934) later showed, that water itself was chemically activated by ionizing radiation, and the free radicals produced, could diffuse in solution and were the main cause of inactivation. It was not until the 1940's that Lea et al (1944), first related the direct action of ionization to the target size or molecular weight, with a hypothesis now known as target theory (Fig 6.1), and used this relationship to estimate the sizes of a wide variety of biological macromolecules (Lea, 1946). Subsequently, the technique, target size analysis by radiation inactivation, was employed in the 1950's to determine target sizes of many water-soluble enzymes (Serlin and Fluke, 1956; Norman and Ginoza, 1958). However, results obtained with enzymes were, in some cases, not in agreement with their molecular weights as determined by other methods, such as gel filtration or sedimentation analysis (Pollard et al, 1952; Setlow, 1952). The smaller target sizes obtained, usually corresponded to the size of one or more subunits of the molecule (review Kempner and Schlegel, 1979). Hence, for water soluble enzymes, target size measurement was not considered to be superior to the other conventional methods, and its use diminished in the 1960's. Only

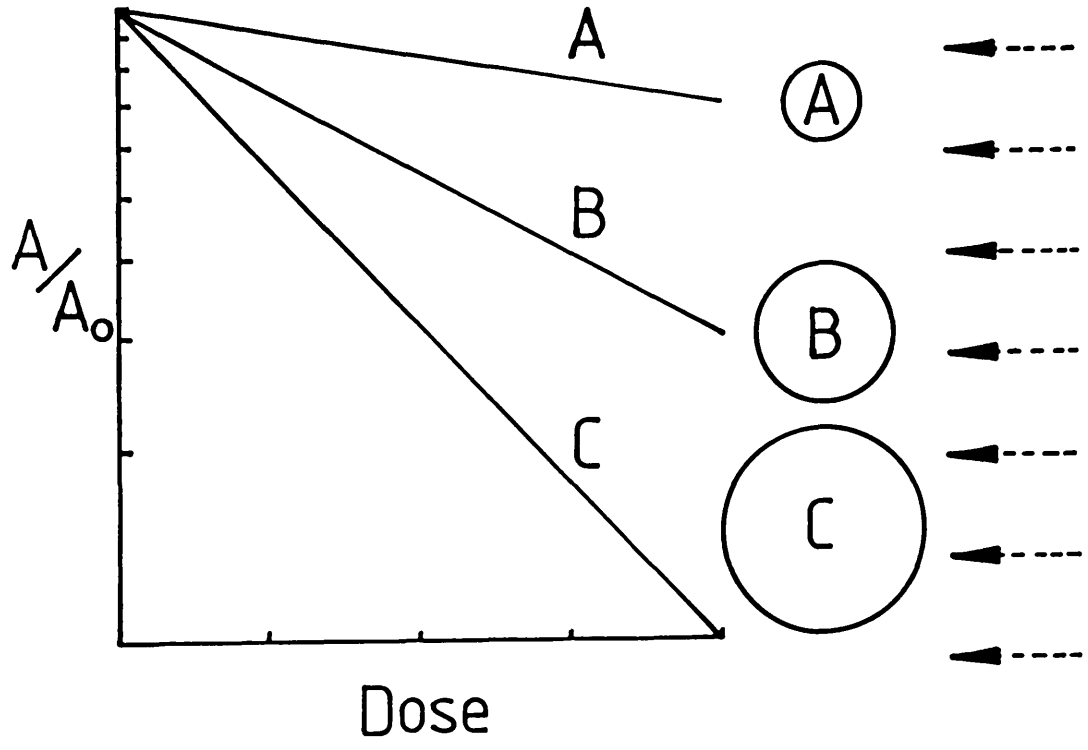

Fig 6.1 Simplified diagram illustrating the principle of target theory

A,B and C are hypothetical structures of biological molecules each with different target sizes. According to target theory, exposure to ionising radiation (arrows) reduces the activity in different sized targets at different rates (see text for more details).

more recently, with the importance of membrane proteins increasingly realized, and the possibility of studying them *in situ* by radiation inactivation, has interest in the method revived (Ellory, 1979).

6.1 Interactions of ionizing radiation with matter

The ionization of atoms is produced exclusively by high energy radiation such as X-rays, α-, β- and γ-radiation, protons and neutrons (Bichsel, 1966). High energy radiation, passes through free space unabated, but on interaction with matter, all can produce fast charged particles and hence, are called ionizing radiations. For example, X-rays and γ-rays produce fast electrons, and α-particles and neutrons produce fast protons.

In general, the various types of fast charged particles can be classified into the following two groups: fast electrons and fast heavy charged particles. For both types of particle, it is possible to separate their major interactions with matter into three broad groups: interactions with the electrons of atoms, interaction with the nuclei of atoms, and interaction with the atom as a whole. The latter occurs only for electrons and heavy charged particles with low energies, and will not be considered in this text.

The fundamental difference between fast electrons and fast heavy charged particles is that, due to its small mass, the main interaction of fast electrons is with the atomic electrons, to which most of its energy is transferred. Fast heavy charged particles in contrast, lose little of their energy to atomic electrons, and interact mainly with the atomic nucleus, producing additional fast heavy particles and often resulting in the formation of relatively unstable isotopes.

The rate of energy loss along the path of any charged particle traversing biological material, is referred to as its linear energy transfer (LET), and is measured in units of keV/μm. Although protons and α-particles have a much higher LET (i.e. are more effective ionisers) than electrons, their maximum range is too low for effective ionisation throughout the sample volume (Table 6.1). For these reasons the majority of target size studies utilise fast electrons.

6.2 Mechanism of radiation inactivation

Exposure of biological material to ionizing radiation initiates a complex series of reactions, which eventually result in the inactivation of biological function (Andrews, 1974). The first event is the physical absorption of radiation energy, causing ionization and excitation of atoms, which takes place in less than a picosecond. The second event is the formation of free radicals and ion pairs, which occurs in several milliseconds, and finally, due to the presence of highly reactive radicals, changes in molecular structure and subsequent loss of biological function occurs within seconds (Dartinger and Jung, 1970).

a) In the ionization process, the energy deposited by fast charged particles is so great, and localised to so few atoms, that valence orbital electrons are completely removed from the atom. This transfer of energy to the target material, occurs in discrete bursts to produce primary ionizations. In each primary ionization about 66 eV of energy is transferred to the target (Pollard, 1959; Kepner and Macey, 1968), corresponding to ~6300 kJ /mol (Tables 6.2 and 6.3).

Table 6.1 Properties of electrons, protons and α-particles with energy of 1 MeV, traversing through biological material.

	Electron	Proton	α-particle
LET (keV/μm)	1	25	260
Density of ionisations (ionisations/μm^3)	30	750	5000
Distance between each ionisation (Å)	1000	25	2
Maximum penetration (range) into sample (μm)	4000	20	5

Table 6.2 1st ionization energies of the main biological elements (kJ/mol)

Carbon	1100
Hydrogen	1300
Oxygen	1300
Nitrogen	1400
Phosphorus	1050
Sulphur	1000

Table 6.3 Average bond energies between the main biological elements (kJ/mol)

	H	C	N	O	S
Hydrogen	435	414	389	464	347
Carbon		347	305	360	272
Nitrogen			163	222	
Oxygen				197	
Sulphur					251

Fast electrons ejected by primary ionizations can produce further secondary ionizations, usually within a 20 Å radius, and this often results in a cluster of 2 to 3 ionizations. In the excitation process however, electrons are not completely removed from the atom, but are raised to higher energy levels. In dissipating this energy, the excited molecule undergoes a reorganisation of its valence electrons, which itself can lead to bond rupture and subsequent ion pair formation (Augenstein et al, 1964).

b) The ionisation and excitation step leads into the "initial chemical reaction", characterised by the production of free radicals and ion pairs. Free radicals, having unpaired or odd electrons, and ion pairs, are highly reactive chemical species and both capable of initiating covalent reactions within the molecule, resulting in a substantial change in molecular structure.

c) The disruption of chemical bonds and covalent changes produced, causes significant alterations in the secondary and tertiary structure of the target material. Changes in the functional site(s) present within the target subsequently lead to total loss of its biological function.

6.3 Target theory

The application of target theory requires the following assumptions to be made regarding the interaction of ionizing radiation with matter:

a) Primary ionisations are discrete and highly localised events within the target.

b) One primary ionisation occurring within a target totally inactivates the function associated with that target; partial inactivation does not occur.

c) Primary ionisations occur randomly in the path of the radiation; due to the large deposition of energy, there is no preferential ionisation of particular atoms.

d) No indirect inactivation by secondary effects of ionizing radiation occur; free radicals from solvents such as water are eliminated.

The probability of n primary ionisations occurring in a given unit follows a Poisson distribution

$$P(n) = \frac{e^{-x}.x^n}{n!} \qquad \ldots(1)$$

where x is the average number of primary ionisations occurring per unit.

The only activity remaining after radiation exposure is due to units which have totally escaped ionisation i.e. when n = 0

$$P(0) = e^{-x} = e^{k.D} \qquad \ldots(2)$$

The average number of primary ionisations per unit, x, is given by kD, where D is the radiation dose and k is a constant, characteristic of the particular biological unit being measured, and proportional to its mass. Since the remaining biological activity measured after irradiation is directly proportional to the fraction of units which escaped radiation damage

$$\frac{A}{A_o} = e^{k.D} \qquad \ldots(3)$$

where A is the number of active units surviving after a given radiation dose, and A_o the number of active units before irradiation, i.e. the non-irradiated control.

An expression relating the constant k to radiation exposure, can be derived when $D = D_{37}$, where D_{37} is the radiation dose (in primary ionisations/cm^3) responsible for reducing activity

to 37% of that in the non-irradiated control

i.e. $\frac{A}{A_o} = 0.37 = e^{k.D_{37}}$

$$\ln 0.37 = -1 = -k.D_{37}$$

Hence $$k = \frac{1}{D_{37}} \quad \ldots (4)$$

The approach employed by Kepner and Macey (1968), was to relate the constant k to the molecular weight (MW) of the target

$$MW = p.N.k$$

where p is the density (g/cm^3) and N is Avogadro's number

$$\frac{MW}{p.N} = \frac{1}{D_{37}} \quad \ldots (5)$$

From a collection of radiation data in the literature they derived an empirical formula for calculating the target molecular weight from its D_{37} (in rads).

$$MW = \frac{6.4 \times 10^{11}}{D_{37} \text{ (in rads)}} \quad \ldots (6)$$

This empirical formula, although widely used since its introduction, depends crucially on accurate determination of the radiation dose delivered. Often, due to experimental design, it is very difficult to measure the actual amount of radiation received by the sample, due to varying degrees of radiation quenching by materials such as the sample coolant and sample container.

A more practical approach, introduced recently by Lo *et al* (1982) in this laboratory, has bypassed the necessity for determining the absolute radiation dose given to each sample.

This method makes use of a calibration curve between relative molecular weight and relative radiation sensitivity, constructed from irradiation data of several marker proteins of known molecular weight. If the radiation sensitivity of a protein of unknown molecular weight, co-irradiated with several marker proteins is determined, then its molecular weight can be calculated from the calibration curve.

N.B. Many reports in the literature refer to the determination of the "target volume", which can, if taken literally, be misleading. The actual parameter determined experimentally is the target mass - the radiation sensitive mass whose function is destroyed by absorption of ionizing radiation - the shape and volume of the target are not factors entering into the molecular weight calculations (Lai et al, 1984; Schlegel and Kempner, 1984).

6.4 Radiation Source

In principle, any high energy radiation is suitable for target size measurements. However, as described above, the use of fast heavy particles is problematical, hence various sources of high energy electrons are most commonly employed. High energy X-rays and γ-rays can also be used, as both these forms of electromagnetic radiation produce fast electrons on interaction with matter, but for safety and practical reasons they are not often utilised.

The two main sources of high energy electrons are the Van der Graaf electron generator or the linear electron accelerator (linac). For sample thicknesses of less than 2mm, electron energies of $\sim$1.5 MeV from a Van der Graaf generator are sufficient, but for thicker samples, higher MeV electrons from a

powerful linac are required. Linacs are most commonly used in large hospitals to produce X-ray beams for radiotherapy, but can also produce fast electrons in the 5-20 MeV range when the experimental beam is utilised. As they were the source of high energy electrons used in this study, a brief description of its mode of action will be given (Fig 6.2).

Electrons produced by heating an electron gun (tantalum disc) are accelerated initially by a pulsed potential, then injected into a long evacuated, corrugated waveguide. Within the waveguide, which consists of an array of irises, each electron gains energy equivalent to being accelerated by a potential difference of millions of volts. The electrons gain their energy from a radio-frequency wave with a phase velocity which is intially equal to that of the injected electrons, but which increases along the length of the waveguide to match the increase in electron velocity. The electrons are grouped into bunches, so that they emerge in pulses rather than as a constant current. After acceleration to very high energy, the electrons pass out of the linac through a thin titanium foil window, in the form of a pencil-shaped beam, several millimetres in diameter (review, Karzmark and Pering, 1973).

6.5 Radiation dosimetry

Radiation dose in rads (a rad = deposition of 100 ergs of radiation energy/cm^3 of material) can be measured either directly, using calibrated cavity ionization chambers, or indirectly from physical or chemical changes produced in a well defined reference system.

Ionization chambers can measure radiation dose very accurately, although they are extremely sensitive to temperature

Fig 6.2 Simplified diagram of a linear electron accelerator.

a electron gun

b focussing coils

c centering coils

d bending magnet

e window for X-ray beam

f diffuser/ scattering foil

g bellows

h sample chamber

j total dose/ rate monitor

k target block

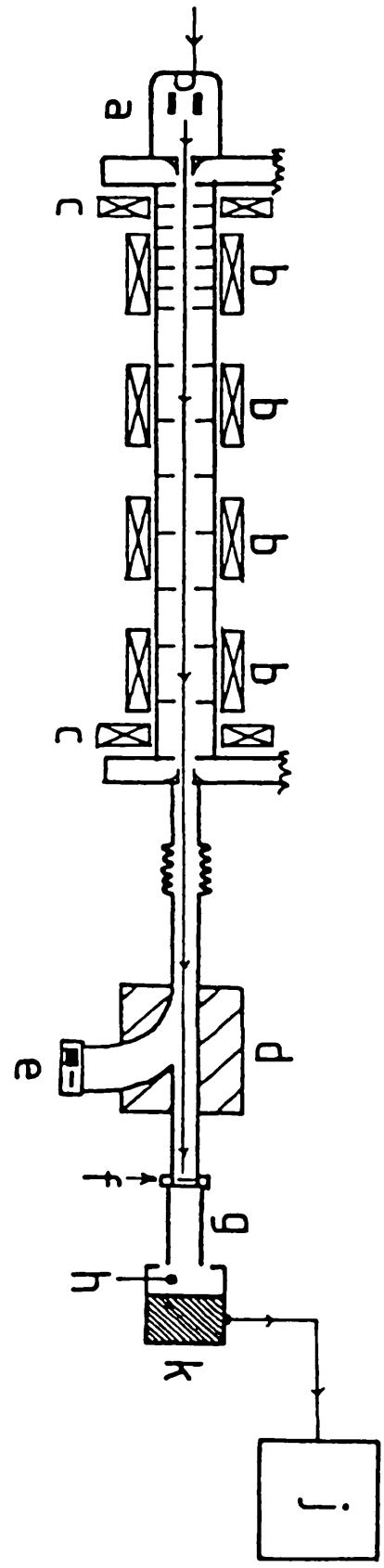

and pressure, requiring accurate barometer and thermometer readings, and also need to be calibrated regularly. The dose is derived from the Bragg-Gray relation by measuring the ionization produced in a gas filled cavity (review, McLaughlin, 1966).

Indirect dosimetry methods using solid state integrating dosimeters are generally more widely used (review, Fowler and Attix, 1966). For example, the change in the optical density at 292 nm, on irradiation of polymethylmethacrylate (clear Perspex, ICI) and comparison with precalibrated samples is a simple and extensively used method (Berry and Marshall, 1969). The absorption peak at 292 nm increases linearly with dose and is independent of radiation dose rate. The optical density does fade with time due to the inward diffusion of atmospheric oxygen, but is generally less than 1% a day. Blue Cellophane (Du Pont), containing dimethoxy-diphenyl-bisazo-8-amino-1-naphthol-5,7-disulphonic acid dye is another widely used chemical dosimeter, with an absorption peak at 655 nm (Henley, 1954).

Another simple procedure makes use of photographic X-ray film, in which the film darkening caused by radiation exposure is measured by a densitometer, although this method is more useful for electron beam uniformity measurement (Dutreix and Dutreix, 1968). The last major method of dosimetry, relatively more complex, but insensitive to the temperature of irradiation, is the thermoluminescent dosimeter (TLD) method. This makes use of stable compounds such as LiF and CaF_2 which, on irradiation, results in excitation of their electronic systems into energy states that are stable at room temperature, but which when heated rapidly to certain temperatures (220-230°C), causes de-excitation, with emission of light in the form of a glow curve. Dose received is then related to the integrated glow curve area (Karzmark et al, 1964).

Electron beam field uniformity is another important parameter to determine, since in most cases, several samples are irradiated simultaneously in the electron beam, and a uniform dose across all samples is required. To obtain uniform dose the electron beam is diverged by placing a scattering foil, usually made of a transition metal, at the beam window. Higher atomic number materials are generally more efficient scatterers than those with low atomic number.

The relative dose across the beam is easily obtained by placing a thin sheet of perspex or photographic X-ray film, at a set distance in front of the scattering foil, and measuring the change in optical density after radiation exposure.

6.6 Factors affecting the radiation inactivation of proteins

a) Physical state

The physical state of the sample during irradiation can be an important factor in results obtained by radiation inactivation. Due to the need to eliminate indirect inactivation by irradiation in solution, samples must be in a frozen or lyophilised state. In general, results obtained in both states are very similar. However, it has been found that irradiation of an enzyme as an ammonium sulphate precipitate yielded half the target size obtained when irradiated frozen in buffer (Kempner *et al*, 1980). Also, proteins whose functions are not resistant to lyophilisation can only be irradiated in the frozen state.

b) Temperature

Although not theoretically predicted, it was found that when several enzymes were irradiated at different temperatures, different D_{37} values were obtained (Setlow and Doyle, 1953; Fluke, 1966,1972). The sensitivity to radiation was reduced at

low temperatures and increased with higher temperatures. The effect was observed in both frozen and lyophilised samples. Subsequent studies showed that the radiation sensitivity ratio at +30°C relative to -110°C, was similar for many different enzymes, and this factor of (approximately) 2.8, was used in their calculations to determine target size (Schlegel et al, 1979; Kempner and Schlegel, 1979). A more recent report by Kempner and Haigler (1982), using temperature insensitive dosimeters, has shown that the actual radiation dose received by a sample was unchanged by temperature. They also found that a logarithmic relationship existed between radiation sensitivity and sample temperature during exposure. Although the majority of studies concur with the existence of temperature sensitive inactivation (Vollmer and Fluke, 1967; Pollard et al, 1952; Pauly and Rajewsky, 1956), a few studies have claimed no such dependence (Kagawa, 1969; Ostrovskii et al, 1969; Cuppoletti et al, 1981). However, the specific molecular processes which are influenced directly by temperature have not yet been fully clarified.

c) Energy transfer

According to classical target theory, ionizing energy absorbed at any one point in a target protein destroyed the function of that protein. For a monomeric protein, the target size is expected to be that of the single polypeptide chain. However, many proteins and enzymes consist of two or more polypeptide chains in an oligomeric structure, with no covalent bonds between them. Surveys of the literature showed that in many cases, the target sizes determined corresponded to the entire oligomeric structure, whilst other cases showed single subunit target sizes (Kempner and Schlegel, 1979). Hence, no generalisation that target analysis determines a monomeric or multimeric structure could be made.

6.7 Radiation inactivation of membrane proteins

Since the early report by Kepner and Macey (1968) on radiation inactivation of membrane ATPases, the technique has been applied to a large number of membrane proteins.

In 1973, Levinson and Ellory (1973) determined a 229K target size for the "tetrodotoxin (TTX) binding component" from pig brain membranes, using a relatively difficult bioassay for measuring TTX concentrations. This early value was similar to that found later by Barhanin et al (1983), in which the loss of binding activity of ^{3}H-TTX was used to determine a 260K target size for the voltage-sensitive Na^{+} channel in rat brain synaptosomes. In the same study (Barhanin et al, 1983), two other radiolabelled toxins, both of which interact specifically with the Na^{+} channel, were also found to bind to a protein with a molecular size of 266K and 270K, determined using radiation inactivation and covalent crosslinking techniques, respectively. From these results, they suggested that all three toxins bound to distinct sites, but which resided on different parts of the same macromolecule.

Separate studies in 1980, both using human erythrocyte membranes, determined the target sizes of two important integral membrane transport proteins. Using cytochalasin B, a potent inhibitor of glucose transport, Jung et al (1980), determined the size of the glucose transport protein to be ~200K, from the loss of specific binding of ^{3}H-cytochalasin B. Jarvis et al (1980) determined the size of a nucleoside transport protein to be 122K, using the specific nucleoside transport inhibitor, ^{3}H nitrobenzylthioinosine, which at the time represented the "first molecular information" on the physical properties of this protein. Recently many more studies on membrane proteins have been reported .

6.8 Studies on adenylate cyclase

Some membrane-associated biological functions involve a macromolecular assembly consisting of two or more mutually interacting species. A good example of such is the hormone receptor-adenylate cyclase system (Rodbell, 1980). The system includes at least three interacting proteins, the hormone receptor (R), a GTP binding protein (G) and the adenylate cyclase catalytic unit (C), which exist in equilibria between various states of assembly. Hormones, on binding to the receptor, are believed to induce a shift in the equilibria of molecular assembly which results subsequently in adenylate cyclase activity (Rodbell et al, 1975; Tolkovsky and Levitzki, 1978). In the hope of elucidating the structural changes involved in adenylate cyclase activation, target size analysis was applied to this complex system (Houslay et al, 1977; Martin et al, 1979; Schlegel et al, 1979; Nielsen et al, 1981). From the target inactivation data obtained, it was proposed (Nielsen et al, 1981) that, in the ground state, the adenylate cyclase system consisted of a tightly bound tertiary complex (R.G.C), which immediately dissociated on binding of hormone to its receptor, to release an activated C unit - the precoupled model. However, this is in complete contrast to kinetic evidence, which suggests that hormone binding to an initially uncoupled receptor, leads to the formation of a hormone.R.G complex, which is responsible for activation of the adenylate cyclase - the pre-uncoupled model (Swillens and Dumont, 1980). Due to the contradictory data presented, the target size evidence for the precoupled model was subsequently reanalysed by Simon et al (1982), who suggested that the target analysis data was overinterpreted. They showed that, even for a simple model system with two interacting proteins, the results obtained are

greatly affected by several equilibrium parameters and the ratios of each protein involved. They concluded that, as the sole method, target analysis could not discriminate between the two models.

The controversy over the use of target analysis on the adenylate cyclase system has not, however, hindered an increase in the use of target size analysis for studying other membrane proteins. Many of the more recent studies have made use of the increasing availability of specific radiolabelled ligands, which bind with high affinity to the various membrane receptors (Lai et al, 1984; Crause et al, 1984; Nielsen et al, 1984b; Bardsley and Roberts, 1985), although some studies of membrane located enzymes have also used reliable enzymic activity assays in their target size determinations (Suarez et al, 1984; Hymel et al, 1984).

6.9 The present study

At the beginning of this study (1981), the technique of target size analysis by radiation inactivation had been applied to relatively few membrane proteins. This situation has since been rapidly altered, by the growing number of reports in the literature of membrane protein target sizes, but which has also resulted in studies being made during the course of this project, subsequently to find the publication of similar work from other laboratories (Kempner and Haigler, 1982; Ott et al, 1983; Hymel et al, 1984; Lummis et al, 1984).

The present study was initiated to confirm and extend the previous application by workers in this laboratory (Chang et al, 1981; Lo et al 1982), of enzymes as molecular weight standards in membrane protein target size determination. After performing the necessary initial dosimetry measurements, the effects of physical

state and temperature on target size were determined. A series of enzymes were then used to produce a calibration plot, and was followed by determination of several mitochondrial membrane-associated enzyme target sizes, to show the general validity of this approach. Following the report by Fewtrell et al (1981), a study of the target sizes for the F_c and F_{ab} functions in a monoclonal IgG, and the heavy 20S form of acetylcholinesterase from chick muscle, was made. Subsequent studies focussed upon integral membrane proteins, the first of which was the Ca^{2+}/Mg^{2+}- ATPase from rabbit muscle , followed by the opioid receptor subtypes from rat brain. The target size of the GABA/ benzodiazepine receptor complex in bovine brain was also investigated as well as the putative nicotinic acetylcholine receptor from chick optic lobe.

CHAPTER 7 RADIATION DOSIMETRY AND RADIATION INACTIVATION STUDIES ON ENZYMES, IgG AND AChE

7.1 MATERIALS

All enzymes and substrates used were the purest grades from Sigma. Clear perspex was from ICI Ltd, and Perspex Red 400 was a gift from Mr. J. White, Department of Medical Physics, St. Bartholomew's Hospital Medical College, London EC1. Pyrex sample irradiation tubes (12x100mm) were purchased from Corning Glass Ltd. The sample holder for irradiation was made by the workshop in this department, and protein A-Sepharose 4B, monoclonal antibodies 3C4 and 419, Staphylococcus aureus membranes and SV80 extracts were gifts from Dr. D. Lane of this Department. All other reagents were of analytical grade.

High energy electron sources were the linear electron accelerators at MRC Cyclotron Unit, Hammersmith Hospital, London W12 and Medical Physics Department, St. Bartholomew's Hospital Medical College, London EC1. Preliminary experiments were carried out using the linear accelerator at the University of Cambridge Radiotherapeutics Department, Addenbrooke's Hospital, Cambridge.

METHODS

7.2.1 Radiation dosimetry and beam uniformity measurements

Routine radiation dose calibration of high energy electron beams was performed by measuring optical density changes of polymethyl methacrylate (clear Perspex) discs of 10mm diameter and 3mm thickness after irradiation (Berry and Marshall, 1969).

OD change at 292nm was measured and compared to standardised irradiated perspex samples obtained from the National Physical Laboratory (NPL), Teddington, Middlesex. Immediately before a series of irradiations, an attenuated electron beam was monitored with a Baldwin-Farmer cavity ionization chamber (calibrated by NPL regularly), and the actual radiation dose delivered, was measured and used to calculate the dose rate.

Electron beam uniformity at the St. Bartholomew's linac was determined using Perspex Red 400 sheets of 20x20x0.3cm (Day and Stein, 1951). After irradiating with a 1 Mrad dose of electrons, OD scans (630nm) across the sheet were performed to measure the uniformity of radiation-induced darkening (Perkin-Elmer spectro- photometer). Uniformity of the Hammersmith Hospital linac beam was determined by exposing photographic X-ray film (Ilford Ltd.) to a 100 Krad dose and measuring the film darkening with a densitometer.

7.2.2 Design of sample holder for irradiation

A sample holder was designed after consideration of the parameters affecting the radiation dose distribution, such as choice of scattering foil, electron energy, beam field area and sample tube thickness. Aluminium was the material chosen, and used to construct the holder, of 12cm width and height, and 24cm length (Fig. 7.2). The base, side and back walls were of 2.4mm aluminium with a front irradiation face of 0.8mm aluminium. A slide-out double rack was included for holding 12mm diameter sample tubes, and was positioned by guides attached to the inside side-wall.

7.2.3 Preparation of soluble enzymes and irradiation protocol

Thick-walled, 12x100mm Pyrex tubes were acid-washed, rinsed and oven-dried before use. Soluble enzymes (2-5 enzyme units/tube) were added to degassed 5mM NH_4HCO_3 pH7, 5mg/ml bovine serum albumin, then 200µl aliquots were transferred into sample tubes and frozen immediately in a dry ice slurry. Frozen samples were flushed with N_2 gas then sealed with an oxygen flame torch.

For experiments on effect of lyophilisation and temperature, the frozen samples were lyophilised overnight (Virtir freeze-drier) and sealed while under vacuum (<0.2mm Hg), as above.

Samples, including non-irradiated controls, were transported in dry ice to the site of irradiation. Sample tubes were placed in the slide-out double rack of the holder with the sample end flush against the irradiation face (Fig. 7.2). A dry ice/acetone slurry (-78°C), ice/H_2O mixture (0°C) or warm water (+40°C) was poured into the holder and left for 10 minutes to equilibrate. The holder was aligned in front of the electron beam port with premarked lines on an adjustable platform, before commencing irradiation.

Irradiation with 8 MeV electrons at the Hammersmith Hospital linac (dose rate 0.4 Mrad/min.) was monitored with electron collectors above and below the sample area, to determine total dose and dose rate, respectively. Total dose of 12 MeV electrons from the St. Bartholomew's machine (dose rate 0.2-0.4 Mrad/min.) was measured similarly. Irradiated sample tubes were stored at -70°C until opened for assay.

7.2.4 Assay of soluble enzymes

Irradiated samples were thawed, then diluted (frozen) or

reconstituted (lyophilised) in Tris-HCl or phosphate buffer, 50mM, pH7 and immediately assayed for enzyme activity using a Cecil 212 spectrophotometer at 23°C. Final assay concentrations were as follows:

a) E. coli β galactosidase EC 3.2.1.23

MW 464K, Fowler and Zabin, (1977). Assay, Craven et al, (1965).

Na phosphate, pH 7.5	0.1M
β mercaptoethanol	0.1M
o-Nitrophenyl β-D-galactopyranoside	3mM
$MgCl_2$	3mM

Measure OD change at 405nm.

b) Rabbit muscle pyruvate kinase EC 2.7.1.40

MW 238K, Warner, (1958). Assay, Beisenherz et al, (1953).

Tris-HCl, pH 7.5	50mM
KCl	100mM
$MgSO_4$	20mM
Phospho-enol pyruvate	1mM
ADP	3mM
NADH	0.2mM
LDH	3U/assay

Measure OD change at 340nm.

c) Rabbit muscle aldolase EC 4.1.2.13

MW 158K, Sia and Horecker, (1968). Assay, Taylor, (1955).

Tris-HCl pH 7.6	50mM
Fructose-1,6-diphosphate	1mM
NADH	0.2mM
Glycerol-3-phosphate dehydrogenase	1U/assay
Triose phosphate isomerase	3U/assay

Measure OD change at 340nm.

d) Rabbit muscle glyceraldehyde-3-phosphate dehydrogenase EC 1.2.1.12

MW 145K, Jaenicke et al, (1968). Assay, Velick and Furfine, (1963)

Tris-HCl pH 7.6	50mM
$MgSO_4$	2mM
ATP	1mM
Glycerate-3-phosphate	3mM
NADH	0.2mM
3-Phosphoglycerate kinase	13U/assay

Measure OD change at 340nm.

e) Rabbit muscle lactate dehydrogenase EC 1.1.1.27

MW 140K, Jaenicke and Knof, (1968). Assay, Beisenherz et al, (1953).

K phosphate pH 7.4	100mM
Na pyruvate	1mM
NADH	0.2mM

Measure OD change at 340nm.

f) L. mesenteroides glucose-6-phosphate dehydrogenase

MW 102K, Olive and Levy, (1975). Assay, Olive and Levy, (1971).

Tris-HCl pH 7.8	50mM
$MgCl_2$	3mM
NAD	2mM
Glucose-6-phosphate	2mM

Measure OD change at 340nm.

g) Horse liver alcohol dehydrogenase EC 1.1.1.1

MW 80K, Drum et al, (1967). Assay, Vallee and Hoch, (1955).

Na pyrophosphate pH 8.8	10mM
Ethanol	100mM
NAD	1mM

Measure OD change at 340nm.

h) Bovine pancreas carboxypeptidase A EC 3.4.2.1

MW 34K, Smith and Stockell, (1954). Assay, Folk and Schirmer, (1963)

Tris-HCl pH 7.5	50mM
Hippuryl-phenylalanine	1mM

Measure OD change at 254 nm.

7.2.5 Preparation of rat liver mitochondrial membranes for irradiation

Rat liver was homogenised (5ml/g) in ice-cold buffer C (sucrose 0.25M, Tris-HCl 10mM, EDTA 1mM, pH 7.6) by 7 passes of a glass-teflon homogeniser. All subsequent steps were then performed at 4°C. After centrifugation of homogenate for 10 minutes at 600g, the pellet was discarded and the supernatant was recentrifuged at 12,000g, 10 minutes. The mitochondrial pellet was resuspended and centrifuged with two washes of buffer C.

Mitochondria were then lysed by resuspending in water and the membranes collected as above. Pelleted mitochondrial membranes were resuspended in 2 volumes of 5mM NH_4HCO_3 pH 7, degassed, soluble enzymes were added and 200µl aliquots made into irradiation sample tubes and frozen immediately in dry ice. Sealing and lyophilisation were carried out as in 7.2.3.

7.2.6 Assay of mit ochondrial membrane-associated enzymes

Samples were processed as in 7.2.4 and assayed for activity of various enzymes. Soluble enzymes were assayed as in 7.2.4.

a) Glutamate dehydrogenase EC 1.4.1.3

MW 336K, Hucho and Janda, (1974). Assay, Buttery and Rowsell, (1971).

Tris-HCl	50mM
NH_4Cl	10mM
Na α-Ketoglutarate	5mM
NADH	0.2mM

Measure OD change at 340nm.

b) Isocitrate dehydrogenase (NADP-linked) EC 1.1.1.42

MW 150K, Illingworth and Tipton, (1970). Assay, Williamson and Corkey, (1969).

Tris-HCl pH 7.5	50mM
$MnCl_2$	0.2mM
Na isocitrate	10mM
NADP	0.4mM

Measure OD change at 340nm.

c) Succinate dehydrogenase EC 1.3.99.1

MW 97K, Davis and Hatefi, (1971). Assay, Hatefi and Stiggal, (1978).

Na phosphate pH 7.5	50mM
Na succinate	20mM
EDTA	0.2mM
2,6-Dichloroindophenol	0.1mM
Phenazine methosulphate	1mM

Preincubate sample in 20mM succinate, 10 min., 37°C before assay.

Measure OD change at 600nm.

d) Malate dehydrogenase EC 1.1.1.37.

MW 70K, Murphey et al, (1967). Assay, Sottocasa et al, (1967).

Tris-HCl pH 7.5	50mM
Na oxalacetate	10mM
NADH	0.2mM

Measure OD change at 340 nm.

7.2.7 Preparation of IgG for irradiation

An ^{125}I-radiolabelled monoclonal IgG, (3C4), specific for the T protein coded by the SV40 virus (Harlow et al, 1981), was used.

^{125}I-3C4, (22µCi/ml) was initially dialysed for 4hrs, 4°C against 5mM NH_4HCO_3 pH 7.5 with 2x1 litre changes. Soluble enzymes were added and 100µl aliquots made into irradiation sample tubes. After freezing in dry ice the samples were lyophilised overnight and sealed under vacuum as previously described (7.2.3.).

7.2.8 Assay of the F_{ab} and F_c binding domains of IgG

Irradiated samples were resuspended in 10mM Na phosphate pH 8 and assayed for F_{ab} and F_c binding activity as follows;.

a) Antigen binding activity was measured by incubating 50µl aliquots of reconstituted irradiated ^{125}I-3C4 with 50µl of SV80 extract (source of T protein) in 10mM Tris-HCl pH 7, 120mM NaCl, 1mM EDTA. An excess (100µl) of a second monoclonal to the T protein, 419, was added and incubated overnight at 23°C. The complex was then precipitated by addition of 30µl of a 10% suspension of Staphylococcus aureus membranes (source of Protein A), incubation for 2 hours and centrifugation for 20 minutes at 10,000g. The membranes were washed (2x1ml) with 10mM Na phosphate pH 8, then counted in a gamma counter.

b) Protein A binding activity was measured directly by incubating overnight, 50µl aliquots of irradiated ^{125}I-3C4 with 50µl of 50% (v/v) suspension of Protein A-Sepharose in 10mM Na phosphate pH 8. The beads were centrifuged, washed as in a) above , then counted in a gamma counter.

7.2.9 Preparation of chick muscle membranes for irradiation

Pectoral muscle from 1 day old chicks was homogenised (5ml/g) with a Polytron homogeniser (PCU 6, 1 minute) in buffer D (Na phosphate 10mM pH 7, EGTA 5mM EDTA 5mM, bacitracin 1mg/ml, benzamidine 2mM, N-ethyl maleimide 5mM, leupeptin 40µg/ml, pepstatin 20µg/ml, soybean trypsin inhibitor 100µg/ml). After initial centrifugation for 10 minutes at 1000g and the pellet discarded, membranes were collected (100,000g, 60') and resuspended in buffer D, then degassed and soluble enzymes added. Aliquots (200µl) were made into irradiation sample tubes and immediately frozen in dry ice.

In two additional experiments, the membranes prepared as above, were extracted for 1 hour with buffer D containing 1M NaCl and 1% Triton X-100. After centrifugation to remove insoluble material, the soluble extract was loaded onto 5-20% sucrose gradients (see 2.2.7), and the 20S peak fractions of AChE activity (7.2.10) pooled. After degassing, soluble enzymes were added and aliquots were taken and frozen as above.

7.2.10 Assay of AChE

Irradiated membrane samples were thawed and extracted with 1M NaCl and 1% Triton X-100 for 1 hour at 4°C. After centrifugation at 12,000g for 20 minutes, the supernatant was

assayed for AChE activity with acetylthiocholine, as previously described by Lyles et al, (1979).

Experiments with 20S AChE employed a more sensitive radiometric assay (Johnson and Russell, 1975), which measured the production of ^{3}H-acetate from ^{3}H- acetylcholine.

Aliquots of the irradiated sample were incubated with 0.75mM ACh in 0.1ml extraction buffer (D) containing ^{3}H-ACh(1.5µCi/ml) for 1 hour at 23°C. Scintillant cocktail (4ml) was added and the ^{3}H-acetate measured by counting in an Intertechnique scintillation spectrophotometer. AChE preparation and assays were performed with the assistance of Dr. J. Lai, of this department.

7.3 RESULTS

7.3.1. Design of irradiation sample holder

The design of the sample holder must be considered together with the penetration properties of the high energy electrons used for irradiation. Of particular importance is the spatial distribution of dose as a function of depth. For this reason, the percentage maximum dose with depth profile of 8 MeV electrons (produced by the MRC linac), was first determined. This profile was required, to estimate the amount of dose received at various depths within an irradiated sample.

The profile was obtained by irradiating a thin perspex sheet end on, and measuring the change in OD at 292 nm with distance from the irradiated face (Fig 7.1). Following calculation of the penetrability of high energy electrons through aluminium, glass and biological material, relative to that of perspex (J.A. Sylvester, MRC Cyclotron Unit, personal communication), the

maximum depth of biological sample that would receive ≥95% of the maximum dose could be determined. Assuming the use of a sample holder with a 0.8 mm aluminium face, the maximum depth was found to be ~8mm (Fig 7.1, S_1 to S_2).

In order to save exposure time during experiments, several samples could be irradiated simultaneously. Also, a large capacity to hold sample coolant material was required, to maintain constant temperature during irradiation. All these considerations were important factors in the final design of the sample holder, which consisted of a large rectangular aluminium box with a thin-walled front irradiation face (Fig 7.2, for dimensions, see 7.2.2). All joined edges were seam welded to ensure it was leakproof, and an indented slide-out sample rack was used to allow free mixing of coolant material. The sample holder allowed for a maximum of nine samples to be coirradiated.

In all experiments, the maximum sample depth never exceeded 6mm.

7.3.2 Beam uniformity measurement

Due to the irradiation protocol adopted (7.3.1), achieving a uniform electron beam across the sample field area was of great importance. Therefore, an investigation into the degree of uniformity obtainable under various conditions was made.

The main problem was in the choice of a suitable metal scattering foil, as higher atomic number material, although more efficient scatterers, can produce significant energy loss. An aluminium scattering foil, 0.25 mm thick, was chosen initially, as aluminium causes minimal energy retardation. However, although electron energy reduction was only 0.1 MeV, irradiation of perspex through this foil produced a curved OD profile after

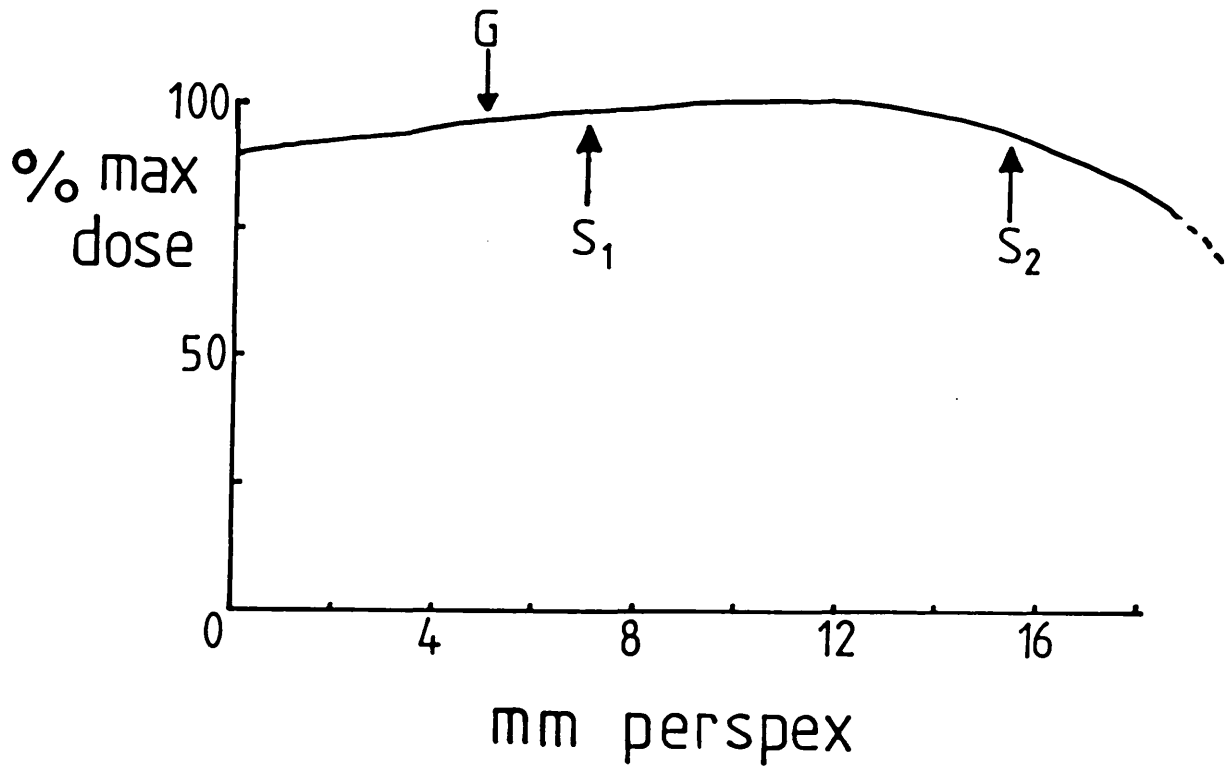

Fig 7.1 % maximum dose versus depth curve

A 3mm thick Perspex sheet was irradiated end-on (2 Mrads) with 8 MeV electrons at the MRC linac, and the decrease in OD at 292nm with distance was measured.

Arrows G to S_1 represents the glass tube thickness and S_1 to S_2 the maximum sample depth.

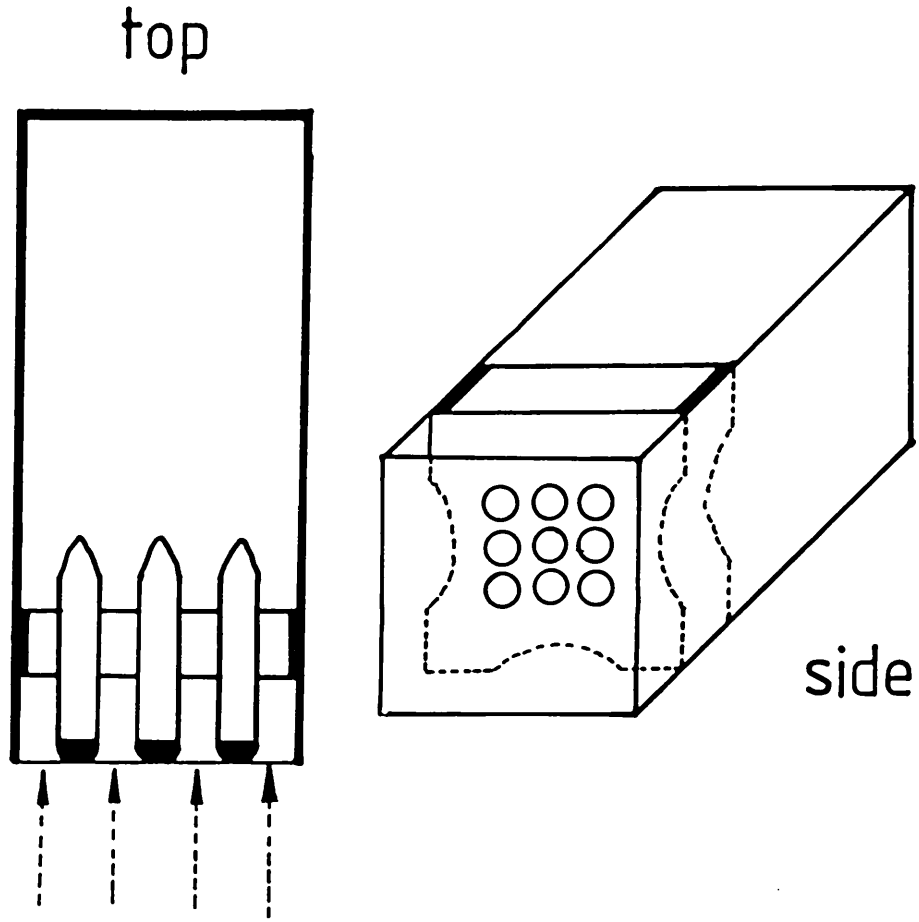

Fig 7.2 Irradiation sample holder

top - View of sample holder from above

side - Side view of sample holder

scanning, indicating an irregular beam.

Following tests using a variety of foils, a double scattering foil comprising titanium (0.2 mm) and tantalum (0.1 mm) was found to give the best results. This combination gave sufficient dose uniformity over the area required (Fig. 7.3), without causing a major loss of electron energy (<0.25 MeV).

Measured by photographic X-ray film dosimetry, the variation in beam uniformity across the sample area was ± 2%, for the MRC linac. The value for the St. Bartholomew's linac was ± 3%, measured using perspex dosimetry (Fig. 7.3).

7.3.3 Treatment of irradiation data

In all target analysis experiments described in this text, the data were obtained and treated in the following way:

a) Activity of each sample was measured at least in duplicate, often in triplicate.

b) The activity in non-irradiated tubes was determined in each experiment, as the mean of a minimum of three samples not subjected to irradiation, but otherwise treated identically (A_0).

c) Two to four samples were irradiated at each radiation dose of an experiment.

d) For each experiment, the mean activity (A), binding or enzymatic, after a particular radiation dose was normalized with respect to the mean activity in non-irradiated samples (A_0). The A/A_0 value was then plotted on semi-log graph paper versus radiation dose (A/A_0 on log scale, radiation dose on linear scale).

e) The inactivation slope from data obtained as above, was determined with a calculator programmed for unweighted regression

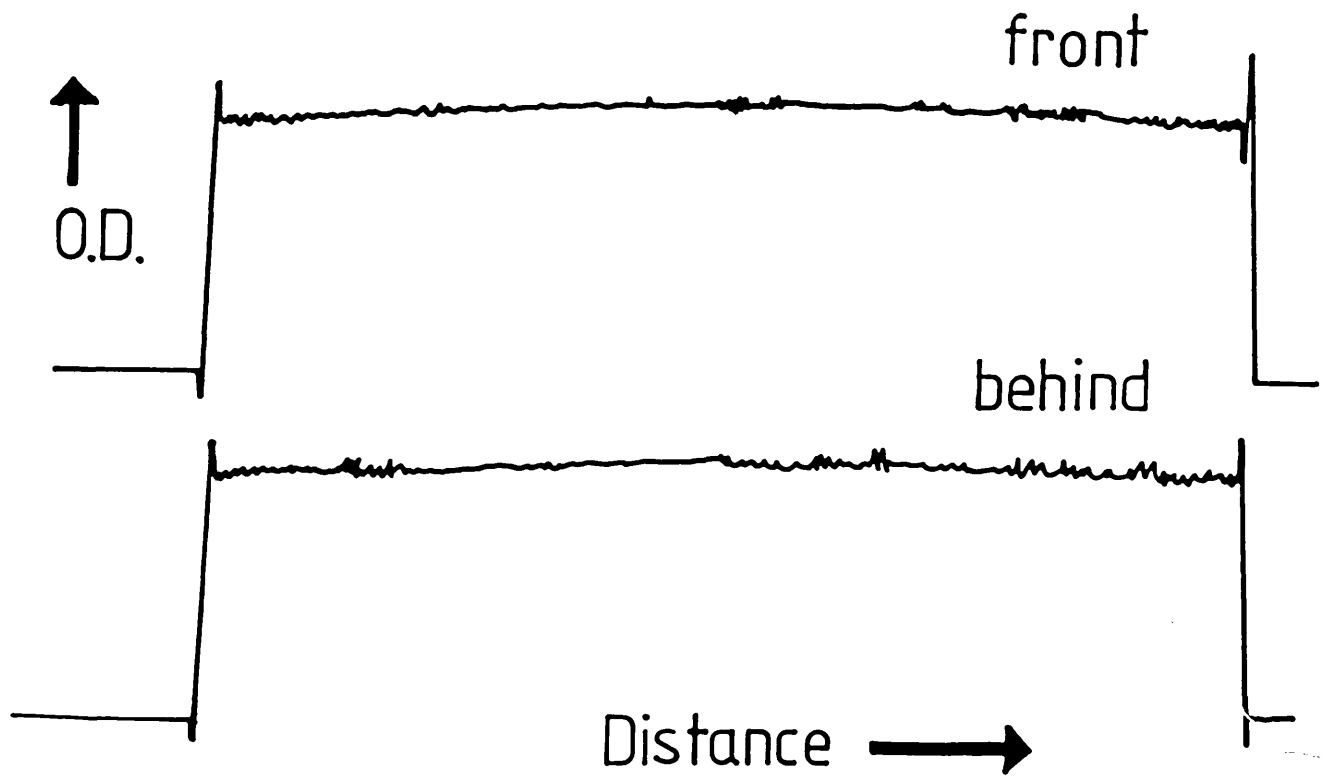

Fig 7.3 Electron beam uniformity measurement

OD scans at 630nm of 3mm Perspex Red 400 sheets irradiated with 12 MeV electrons at the St. Bartholomews linac. Sheets were placed in front of and behind the sample holder irradiation face

analysis and used in the logarithmic mode (Casio fx-180P).

f) The regressed curve produced by the irradiation data points, was not constrained to pass through the origin ($A/A_0 = 1$). Linear correlation coefficients (r) for all experiments were usually > 0.97; the few experiments with r values below this, were discarded.

7.3.4 Irradiation of soluble enzymes

7.3.4.1 Effect of lyophilisation on enzyme activity

The successful use of soluble enzymes for irradiation in the lyophilised state requires that there is no loss of activity on freezing and drying. In order to demonstrate this, enzymes (10 units), dissolved in phosphate buffer (50 mM), were individually frozen or lyophilised in glass tubes, then thawed or resuspended with water to their original volume and their activity measured. Essentially no activity loss was found for frozen samples. However, with most lyophilised samples, a variable but significant loss of activity, between 20 and 50% was found. This was at first thought to be explained by the presence of buffer salts; their presence during the lyophilisation process, could cause the irreversible inactivation of a fraction of the enzymes, most of which were relatively pure with high specific activities. In further experiments, the buffer was changed to utilise the volatile property of ammonium bicarbonate, but, even with low concentrations (5mM) of this salt the results were unchanged.

One notable exception in all these experiments, was horse liver alcohol dehydrogenase (hlADH). This unusually, had a low specific enzyme activity, with a relatively large amount of carrier protein, since only 1.2 units of enzyme activity was present per milligram of protein. The finding suggested, that

either the presence of excess carrier protein had helped protect against inactivation by lyophilisation, or, that hlADH itself was resistant to this type of inactivation. Evidence supporting the former idea was given, when other enzymes were mixed with hlADH and found also to retain >90% activity after lyophilisation. Similar experiments were then performed using bovine serum albumin (BSA) as the carrier protein, and these also showed that essentially all (>94%) enzymatic activity was retained after lyophilisation in the presence of 5 mg/ml BSA (Table 7.1). Hence, in all subsequent irradiation experiments, BSA was routinely added to enzyme preparations to be lyophilised.

7.3.4.2 Effect of temperature on radiation sensitivity

An earlier study in this laboratory on the effect of irradiating samples immersed in liquid nitrogen (Lo, 1981), suggested that the large decrease in sensitivity to radiation (3.5 fold), could be attributed to substantial radiation quenching by the liquid nitrogen and glass container holding the samples. This possible explanation could not be tested however, as removal of the suggested cause of radiation quenching, liquid nitrogen, would also change the irradiation temperature. With the new irradiation system designed in this study, it was possible to reinvestigate the question of temperature-dependent radiation sensitivity.

Using lyophilised enzyme preparations, the radiation sensitivity of PK, LDH and hlADH was investigated at -78°C, 0°C and +40°C, using as sample coolant, dry ice/acetone, ice/water, and warm water (maintained at +40°C with a water bath heating element and thermostat), respectively. The results showed clearly, that under otherwise identical conditions, there was a

Table 7.1 Effect of freezing and lyophilisation on soluble enzymes

Enzyme	Frozen	Lyophilised
β-galactosidase	98 ± 3	95 ± 4
pyruvate kinase	100 ± 2	97 ± 3
aldolase	98 ± 2	96 ± 4
glyceraldehyde-3 phosphate dehydrogenase	99 ± 4	95 ± 3
lactate dehydrogenase	100 ± 2	97 ± 4
glucose -6-phosphate dehydrogenase	98 ± 4	95 ± 2
alcohol dehydrogenase:		
horse liver	100 ± 3	98 ± 4
yeast	97 ± 2	95 ± 3
carboxypeptidase-A	98 ± 4	96 ± 3

Values are expressed as the mean % (± S.D.) of 4 determinations of enzyme activity of enzyme freshly prepared in 5mM NH_4HCO_3, 5mg/ml BSA. Activities were measured as described in 7.2.4.

significant decrease in radiation sensitivity with decreasing temperature (Fig. 7.4). The enzyme inactivation slopes at the three temperatures were normalized to the slope at +40°C (Table 7.2) and plotted against temperature. A linear relationship was found between the logarithm of the normalized slopes and temperature (Fig. 7.5). Although the data points in Fig. 7.5 were derived from only three different temperatures, the general result was subsequently validated by the report from Kempner and Haigler (1982), of essentially identical data from their own experiments. Also, the value of 2.8 for the ratio between inactivation at +30°C and -110°C, determined by Schlegel et al (1979) and used as a "correction factor" in their experiments, was similar to the ~2.9 value determined by extrapolation from Fig. 7.5.

7.3.4.3 Irradiation in the frozen state

Lyophilisation of samples for irradiation requires prolonged periods of drying (overnight), hence the feasibility of irradiating in the frozen state was considered. This approach was not possible in previous studies in this laboratory, since the experimental irradiation design only allowed for dry ice-cooled air as the coolant (Lo, 1981). With the new irradiation protocol, it was possible to maintain samples frozen, at a constant temperature below freezing point, using a dry ice/acetone slurry.

The presence of gases did not pose a problem for lyophilised samples, as they were sealed *in vacuo* before irradiation. However, in frozen samples, the presence of dissolved oxygen was found to have a significant effect on enzyme radiation sensitivity, with a very large inactivation seen at low doses of

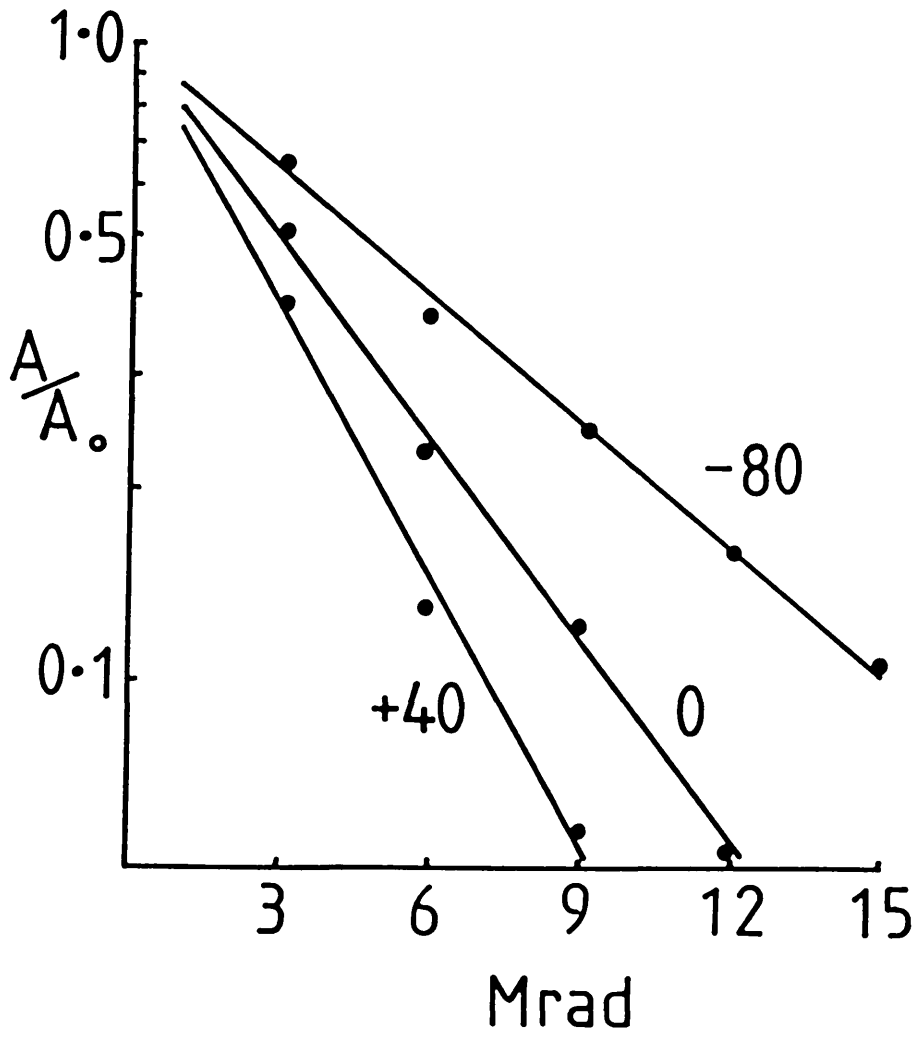

Fig 7.4 Temperature dependence of radiation inactivation

Samples containing PK were lyophilised and irradiated as in 7.2.3. The inactivation slopes show the enzyme activity of PK irradiated at different temperatures (°C).

Table 7.2 Effect of temperature on radiation sensitivity

Enzyme	Temperature(°C)	Inactivation slope $x10^2$	$\frac{E_T}{E_{40}}$
PK	-78	-6.58 ± 0.15	0.470
LDH	-78	-3.51 ± 0.11	0.438
ADH	-78	-1.88 ± 0.19	0.464
PK	+4	-10.7 ± 0.21	0.764
LDH	+4	-6.07 ± 0.10	0.758
ADH	+4	-3.16 ± 0.16	0.780
PK	+40	-14.00 ± 0.20	1.0
LDH	+40	-8.01 ± 0.12	1.0
ADH	+40	-4.05 ± 0.11	1.0

Values expressed as the mean (± S.D.) of 3 determinations.

E_T/E_{40} column represents the inactivation slope ratio of that enzyme at temperature T to that at +40°C.

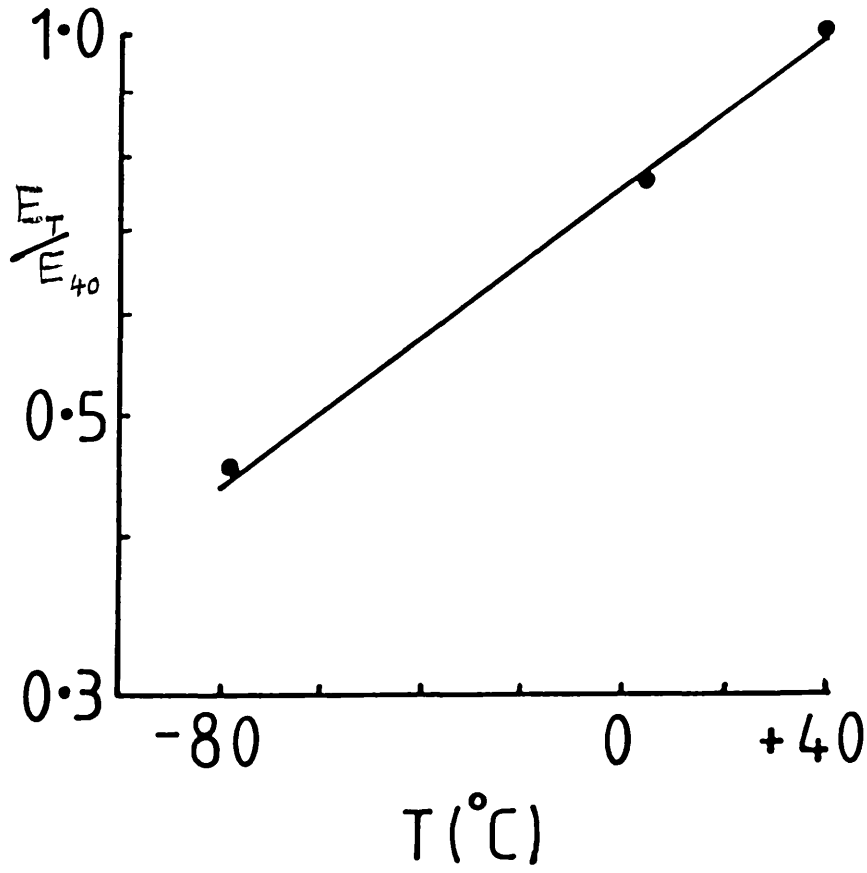

Fig 7.5 Effect of temperature on relative radiation sensitivity

The averaged values of relative radiation sensitivity from Table 7.2 are plotted on a log scale versus the temperature of irradiation. r=0.99

radiation (Fig. 7.6). Although the effect seen in Fig. 7.6 was greatly exaggerated, due to samples being bubbled with pure oxygen prior to freezing, all subsequent experiments with frozen samples, were routinely degassed, frozen immediately and air in the sample tube displaced with a jet of nitrogen gas (O_2 free) before sealing.

With the determination of a standard protocol and temperature (-78°C) for both lyophilised and frozen irradiations, a study of a series of enzymes in both states was performed, in order to compare the effect on their inactivation rates (Fig. 7.7). Almost all the soluble enzymes used were found to have similar slopes for inactivation in the frozen and lyophilised state (Table 7.3). This indicated, that at least for the enzymes used, the target size was unchanged in the two totally different conditions in which the sample was prepared. However, there was a surprising result seen for the tetrameric enzyme β-galactosidase (β-gal). It appeared to have a substantially smaller inactivation slope when irradiated frozen, with the value in the lyophilised state almost twice that in frozen samples. The result for aldolase was also anomalous, as its inactivation slope was similar to that for hlADH, approximately half of the value expected from its 158K molecular weight.

7.3.4.4 Calibration plots using soluble enzymes

Analysis of the enzyme inactivation slopes (Table 7.3) revealed that, as well as the anomalous reduction in the frozen state, the slope obtained for β-gal in the lyophilised state was similar to that of PK. When compared to other enzymes, it was apparent that the inactivation slope value for PK, but not β-gal, correlated to the others. Therefore, PK was used as the reference enzyme, i.e. the one to which other enzymes were

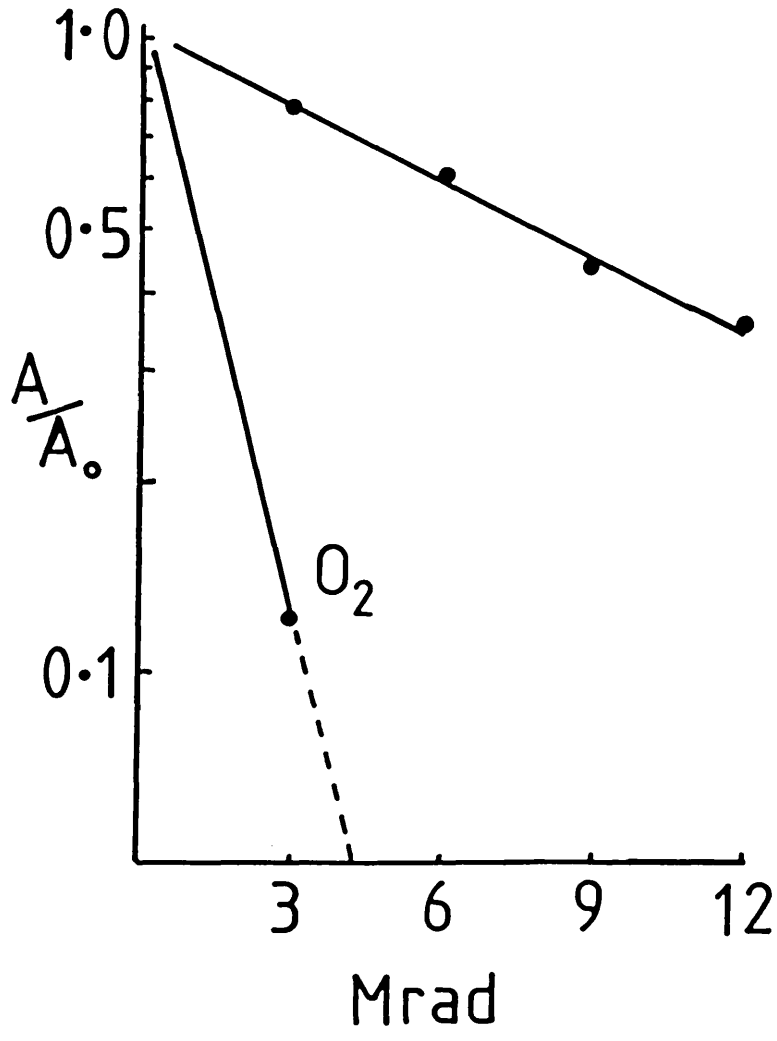

Fig 7.6 Effect of O_2 on the radiation sensitivity of LDH

LDH samples prepared as in 7.2.3 were irradiated after:

a) degassing before freezing, or,

b) bubbled with O_2 for several seconds before freezing (O_2)

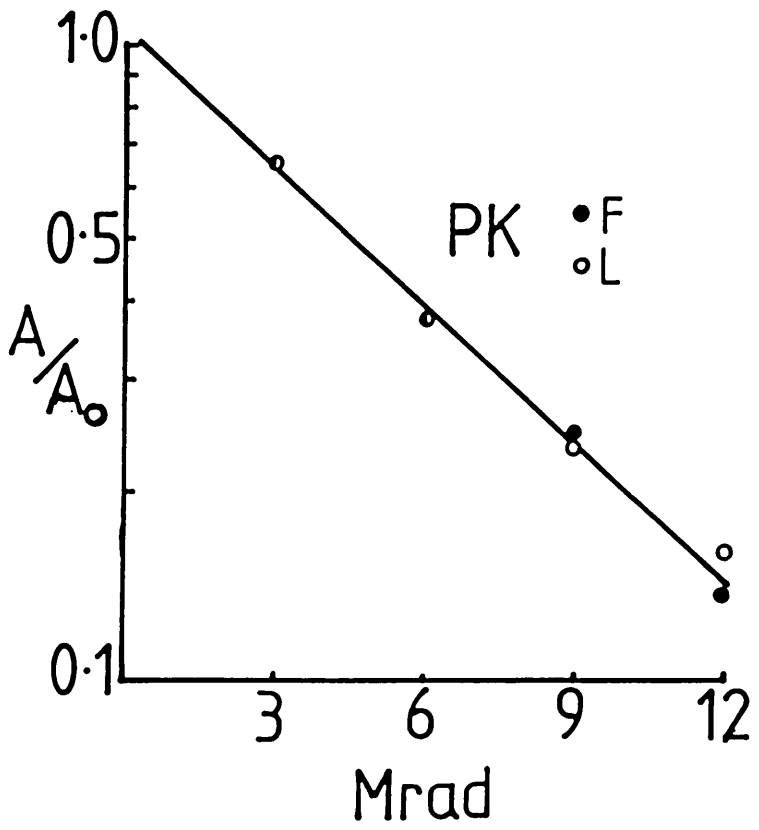

Fig 7.7 Radiation inactivation of lyophilised and frozen PK

Samples containing PK were prepared as in 7.2.3 and lyophilised (L,r=0.99), or frozen (F,r=0.99) before irradiation

Table 7.3 Radiation inactivation of soluble enzymes

Enzyme	Inactivation slope $x10^2$ Lyophilised	Frozen
β-galactosidase	-5.82 ± 0.22	-3.05 ± 0.17
pyruvate kinase	-6.21 ± 0.16	-6.35 ± 0.18
aldolase		-2.23 ± 0.15
glyceraldehyde-3-phosphate dehydrogenase	-4.36 ± 0.24	-4.63 ± 0.21
lactate dehydrogenase	-3.76 ± 0.18	-3.82 ± 0.16
alcohol dehydrogenase		
horse liver	-2.24 ± 0.22	-2.15 ± 0.20
yeast	-4.50 ± 0.20	
carboxypeptidase-A	-0.88 ± 0.19	-0.94 ± 0.25

Values are from irradiations at -78°C and are expressed as the mean (± S.D.) for 4 determinations

normalized. I_{PK} was defined as the inactivation slope ratio, and M_x/M_{PK} as the molecular weight ratio, both relative to PK.

From the inactivation ratios of the range of soluble enzymes studied (Fig. 7.8), a calibration curve was constructed. With the omission of both β-gal and aldolase, a linear relationship between inactivation ratio and molecular weight ratio was found. The correlation coefficients for both lyophilised and frozen enzyme calibration curves were good, 0.99 and 0.98, respectively (Fig. 7.9 and 7.10).

7.3.5 Irradiation of mitochondrial enzymes

With the completion of an enzyme calibration plot, target size analysis of mitochondrial enzymes was employed as a general test of validity of the enzyme marker approach. The enzymes selected for study were malate dehydrogenase (MDH), isocitrate dehydrogenase (ICDH), glutamate dehydrogenase (GDH) and succinate dehydrogenase (SDH), the former three all membrane-associated, and the latter an integral membrane protein.

On analysis of irradiation data for lyophilised membranes, inactivation curves for each enzyme were found, by extrapolation, to pass the A/A_0 axis at ~0.7 (Fig. 7.11). This puzzling phenomenon was reproducible. The data obtained did, however, show that on comparison with the enzyme calibration plot, the relative target sizes of the mitochondrial enzymes corresponded fairly well with their accepted molecular weights (Table 7.4). The single obvious exception was SDH which gave a target size (238 K) approximating a dimer of the literature molecular weight (97 K, Davis and Hatefi, 1971). Due to similar problems with the A/A_0 intercept of soluble enzymes added to the mitochondrial

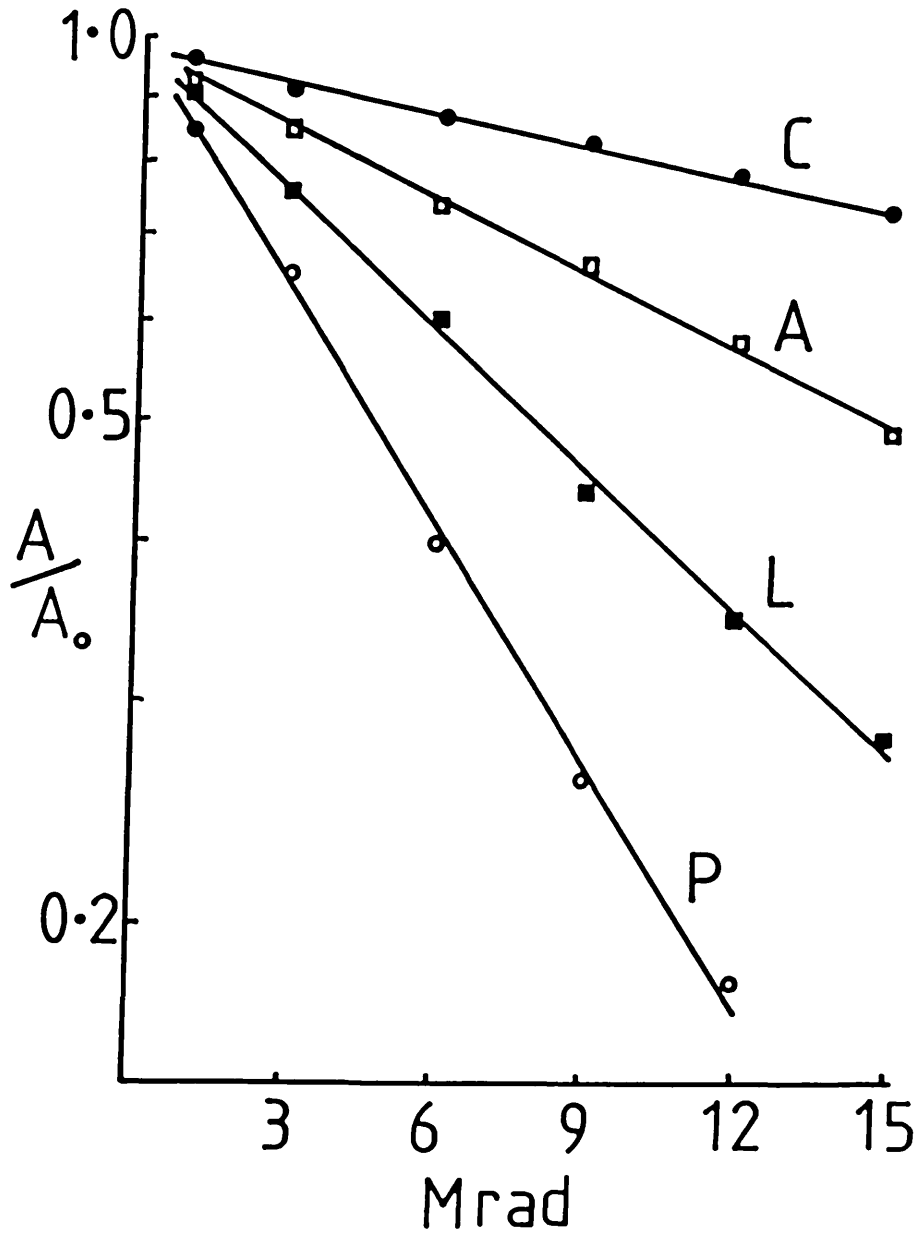

Fig 7.8 Radiation inactivation of enzymes

Lyophilised samples containing a mixture of enzymes were irradiated, then assayed for remaining activity (7.2.4). C-carboxypeptidase A, A-alcohol dehydrogenase (horse liver), L-lactate dehydrogenase and P-pyruvate kinase (All r=0.99)

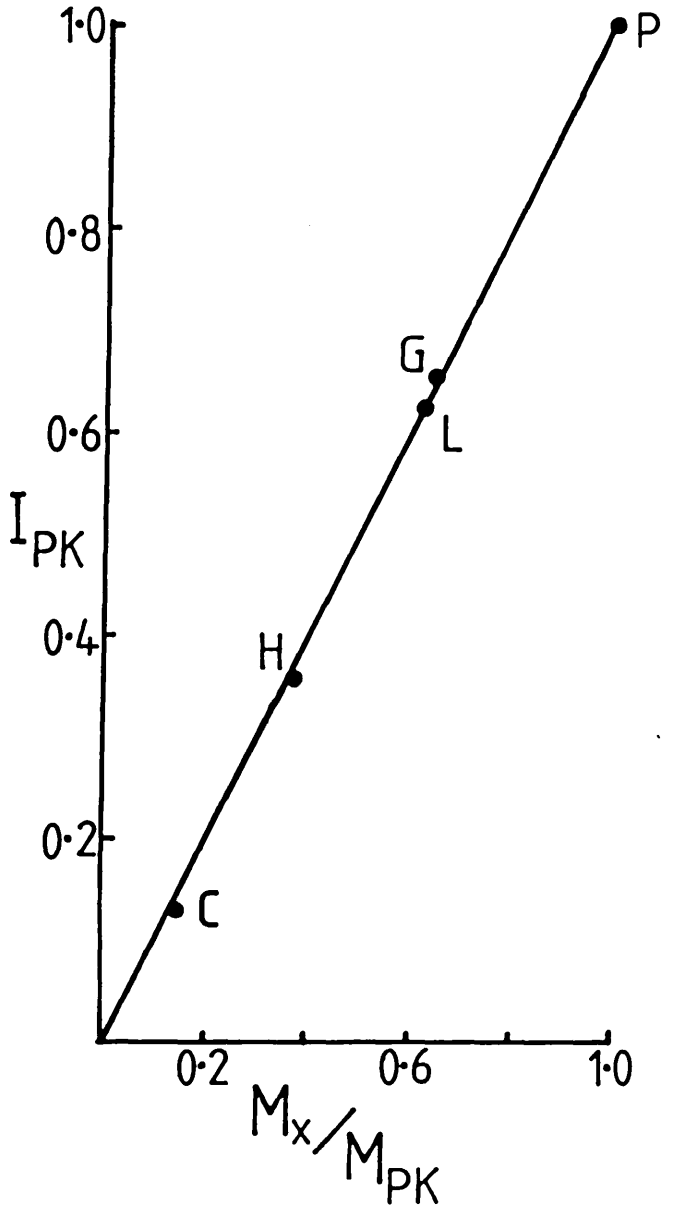

Fig 7.9 Calibration plot of lyophilised enzymes

Enzyme inactivation ratios (I_{PK}) were plotted against molecular weight ratios (M_x/M_{PK}). See Table 7.3. r=0.99

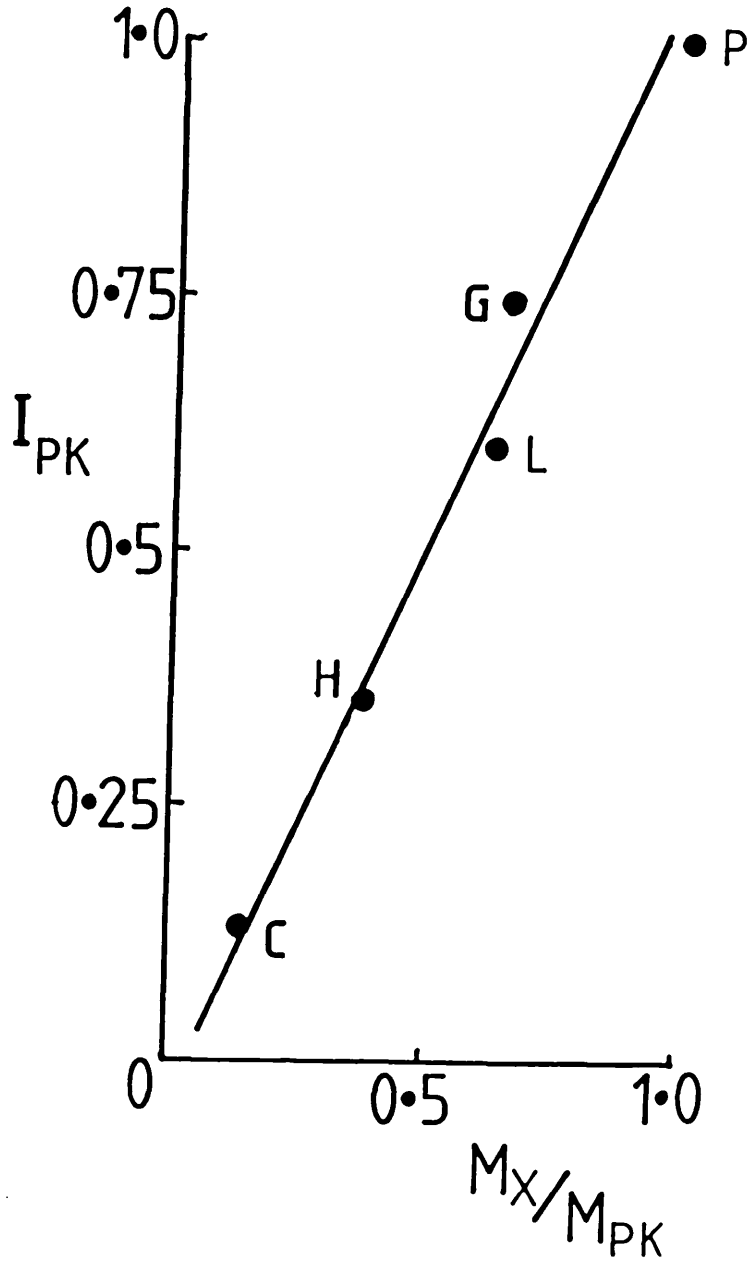

Fig 7.10 Calibration plot of frozen enzymes

Enzyme inactivation ratios were plotted against MW ratios. See Table 7.3. r=0.98.

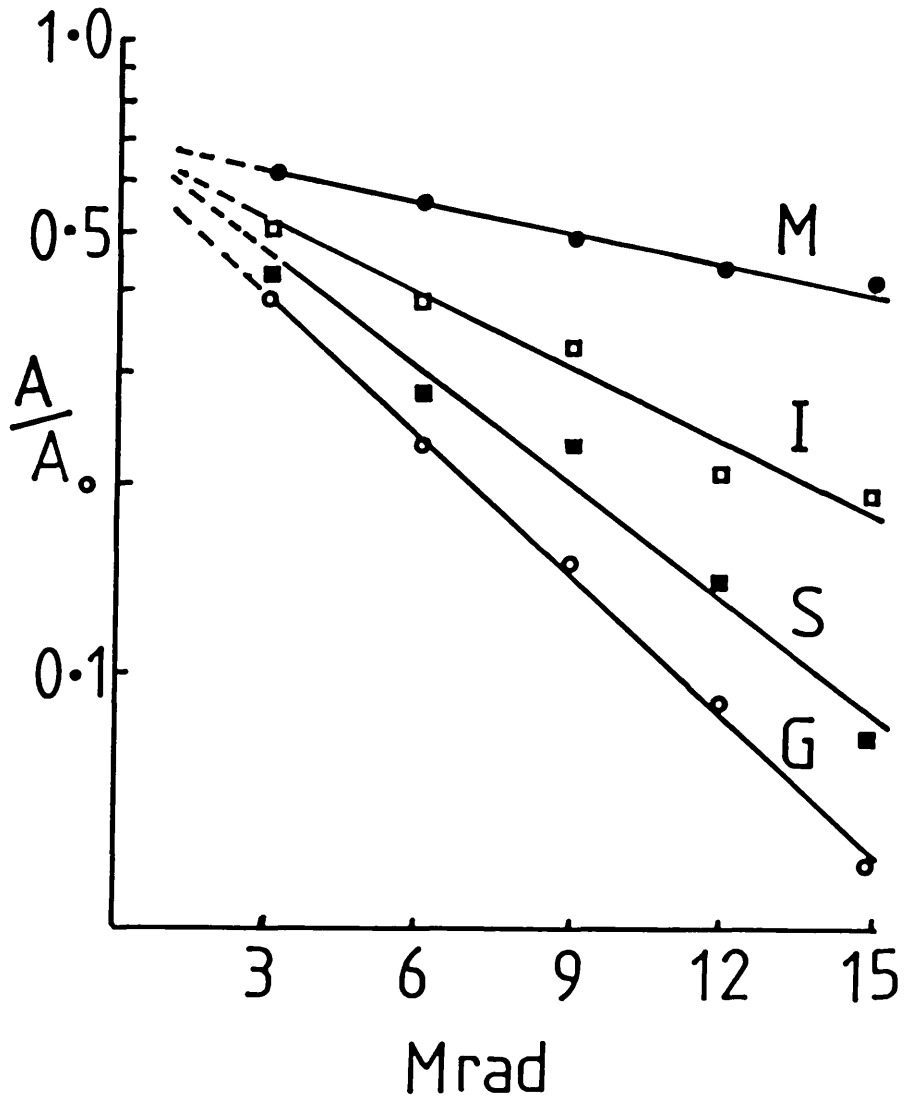

Fig 7.11 Radiation inactivation of lyophilised mitochondrial enzymes

Lyophilised rat liver mitochondrial enzymes were irradiated, then assayed for remaining activity (7.2.6).

M-malate dehydrogenase (DH), I-isocitrate DH, S-succinate DH, G-glutamate DH.

Table 7.4 Radiation inactivation of mitochondrial enzymes

Enzyme	Inactivation slope $x10^2$ (± S.D.)	Relative MW (K) (± S.D.)
	Lyophilised	
malate dehydrogenase	1.51 ± 0.32	60 ± 13
isocitrate dehydrogenase	-3.99 ± 0.52	158 ± 12
succinate dehydrogenase	-6.00 ± 0.31	238 ± 20
glutamate dehydrogenase	-7.30 ± 0.31	289 ± 12
	Frozen	
malate dehydrogenase	-1.58 ± 0.29	63 ± 12
isocitrate dehydrogenase	-3.68 ± 0.34	146 ± 13
succinate dehydrogenase	-2.73 ± 0.43	108 ± 17
glutamate dehydrogenase	-7.27 ± 0.41	288 ± 16

Values are from irradiations at -78°C and are expressed as the mean (± S.D.) for 3 determinations. Relative MW was obtained by extrapolation from enzyme calibration curves (Figs 7.9 + 7.10).

membranes, the enzyme calibration plot was derived from external enzyme standards, coirradiated within the same experiment.

With these complications arising from the use of lyophilised membranes, experiments with both frozen and lyophilised samples were carried out. Using samples obtained from the same mitochondrial membrane preparation and irradiated simultaneously, a direct comparison of the effect of irradiation in both states was possible. These experiments showed, that in frozen samples, the mitochondrial enzymes produced very similar inactivation slopes to those with lyophilised membranes, but did not extrapolate to give a low intercept (Fig. 7.12). This result indicated therefore, that the problem of a lower intercept must specifically be due to lyophilisation, as all other conditions in the experiment were identical. For these reasons, subsequent experiments using membranes were either only irradiated frozen, or both frozen and lyophilised.

Another major difference found using frozen membranes was for the SDH target size (108K), which now corresponded to the molecular weight of a monomer. This suggested that lyophilisation could specifically cause changes in the target size of integral membrane proteins. However, for the three other non-integral membrane enzymes, the target sizes in both frozen and lyophilised membranes were very similar, with MDH (63K and 60K, respectively) and ICDH (146K and 153K, respectively) corresponding closely to their respective literature molecular weight values of 70K and 150K. The values for MDH were also close to the 71K target size of MDH in the frozen and lyophilised state, found by Kempner and Haigler (1982), although they used the commercially purified enzyme. The GDH target size, although very similar, does seem consistently smaller (290K) than the

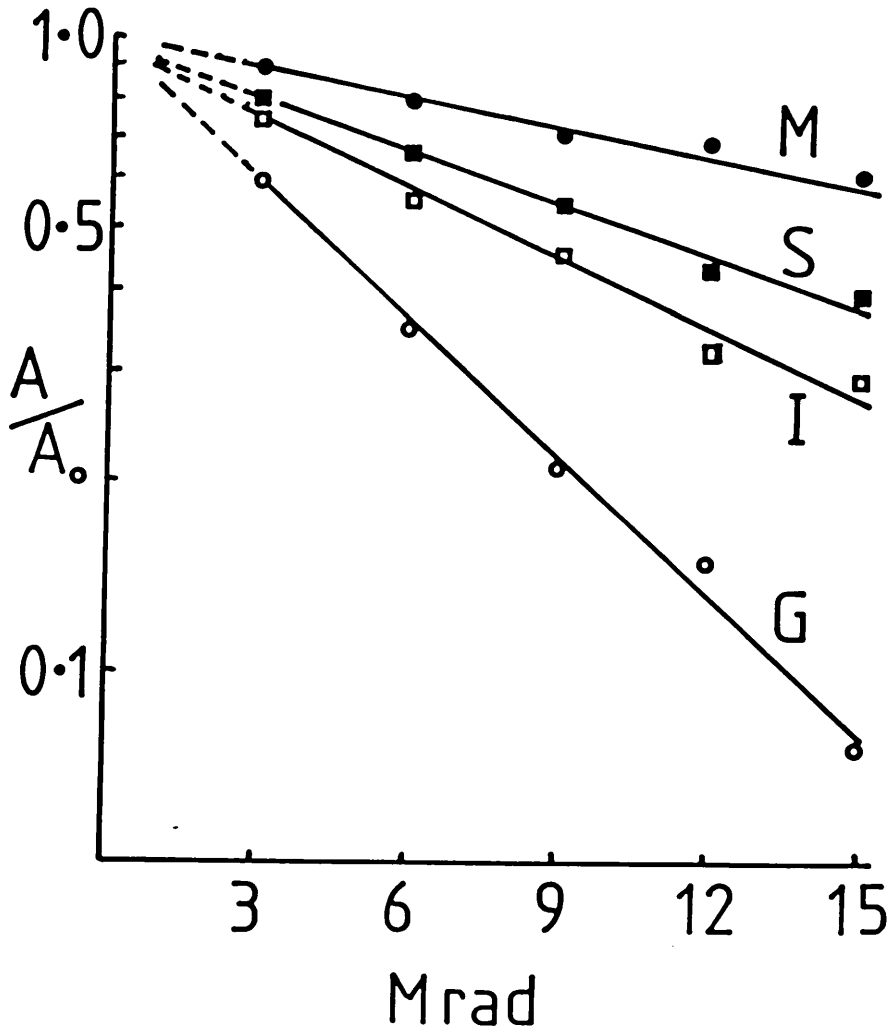

Fig 7.12 Radiation inactivation of frozen mitochondrial enzymes

Frozen rat liver mitochondrial membranes were irradiated, then assayed for remaining activity (7.2.6).

M-malate DH, I-isocitrate DH, S-succinate DH,

G-glutamate DH.

accepted molecular weight of 336K (Hucho and Janda, 1974). This is in accord with the study of Kempner and Miller (1983), who also found a target size smaller than the molecular weight (257K), for purified GDH from bovine liver, irradiated in both the frozen and lyophilised state.

7.3.6 Irradiation of IgG

For these experiments, a radiolabelled monoclonal IgG (^{125}I-3C4), specific for the SV40 virus T protein, was used. In an initial study, the optimal conditions for the assay of the antigenic and protein A binding sites, were determined with an undergraduate project student (Masiulanis, 1982).

For the target size determination of the antigenic binding site (F_{ab} region), the binding of ^{125}I-3C4 to antigen was measured by precipitation of the ^{125}I-3C4-T protein complex, using a second antibody and S. aureus membranes. This protocol was necessary because at the pH of 7 required for complex formation, 3C4, an IgG_1, does not bind tightly to protein A. Also, some of the 3C4 with an intact F_{ab} region may have an inactivated F_c region and therefore would not have been precipitated by the S. aureus membranes. Hence, the antibody-antigen complex could only be precipitated quantitatively, using the second monoclonal antibody, 419 (specific for a different site on the T protein), an IgG_2, which does bind to protein A at pH 7.

Determination of the protein A binding site (F_c region) target size, used a much simpler assay, measuring direct binding of ^{125}I-3C4 to immobilised protein A at pH 8. The results for F_{ab} and F_c region target sizes were both similar, but also surprising (Fig. 7.13 and 7.14). Instead of a target size

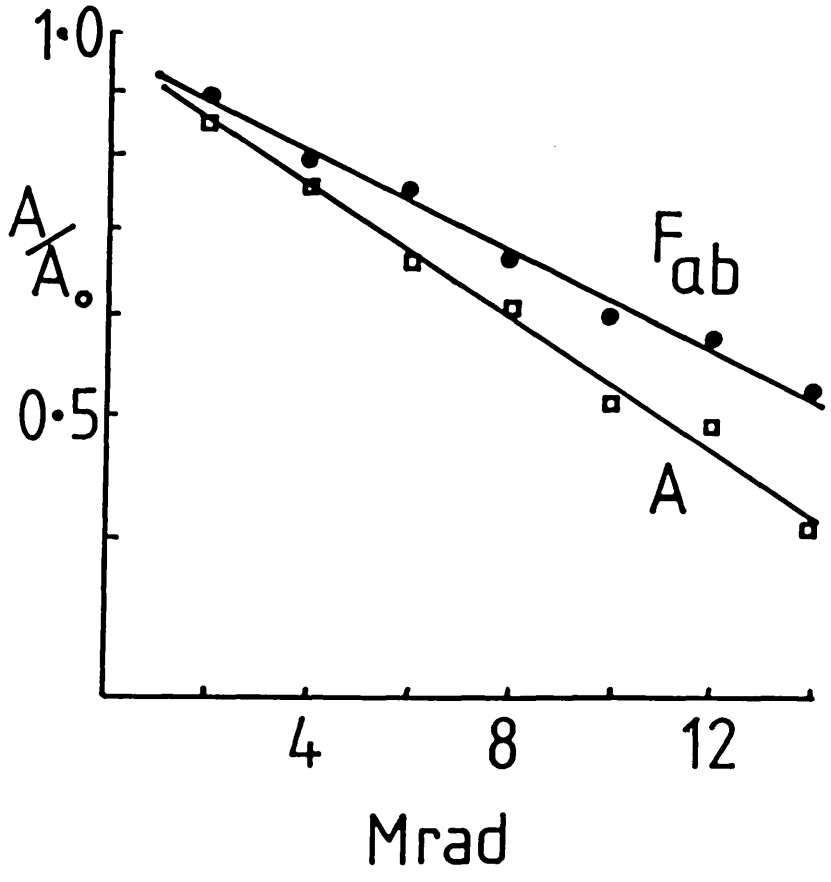

Fig 7.13 Radiation inactivation of IgG (F_{ab})

IgG was irradiated, and assayed for remaining antigenic binding activity (7.2.8).

A-horse liver ADH, F_{ab}, r=0.99: ADH, r=0.99.

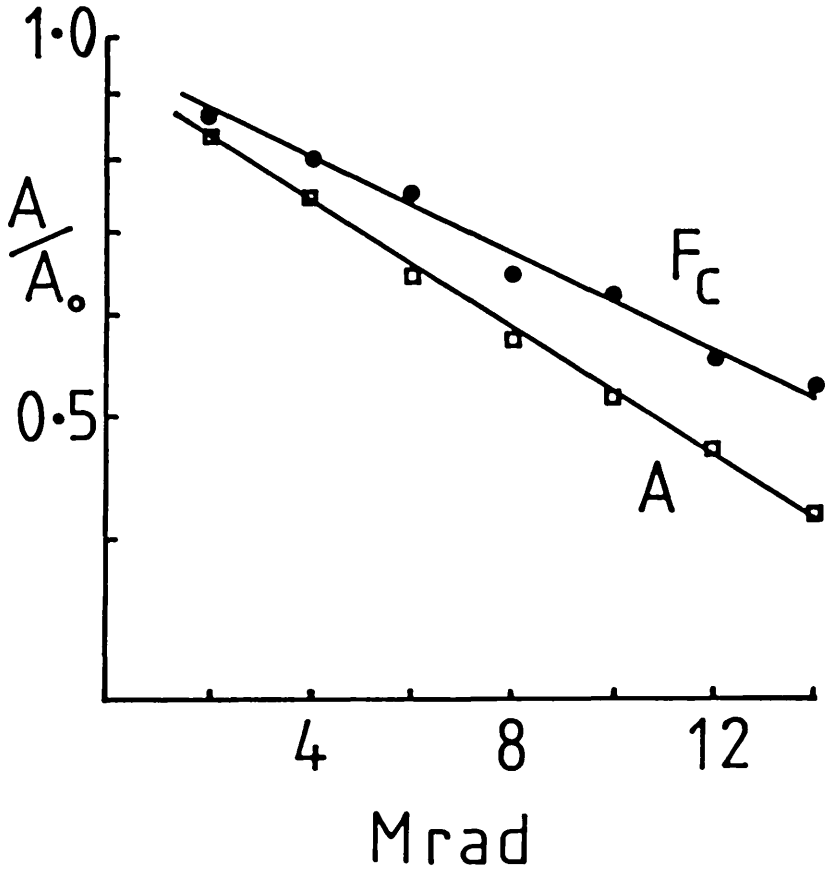

Fig 7.14 Radiation inactivation of IgG (F_c)

IgG was irradiated, and assayed for remaining Protein A binding activity (7.2.8).

A-hlADH. F_c, r=0.99: ADH, r=0.99

corresponding to the entire IgG molecule (160K), the values obtained were much smaller, 61K and 59K for F_{ab} and F_c regions, respectively. This target size, of approximately one third of the molecule, corresponds to the size of a single binding domain or "arm" of the molecule (Porter, 1959).

7.3.7 Irradiation of acetylcholinesterase

The heavy asymmetric form of acetylcholinesterase (AChE) from chick muscle was studied to test the possibility of radiation energy transfer through a large macromolecular enzyme complex (review Massoulié and Bon, 1982). In initial experiments, frozen crude muscle membranes prepared from one day old chicks were used. At this early developmental stage, the muscle AChE comprises 80% of a heavy, asymmetric form, and 20% of smaller, soluble tetrameric and dimeric forms (Fig. 7.15). If energy transfer did occur throughout the entire complex, then the inactivation profile of a crude muscle membrane preparation would be non-linear, due to the simultaneous inactivation of the different size forms of the same enzyme. However, the result obtained for the inactivation of AChE activity surprisingly, was linear (Fig. 7.16), with the target size of 116K corresponding to the molecular weight of a monomer, recently found in this laboratory to be ~105K (K.W. Tsim, personal communication). To verify this result, the membrane preparation was repeated, but instead of irradiating crude membranes, they were extracted using high salt and detergent to remove the heavy form from its basal membrane. The heavy form was then separated from the soluble forms on a 5-20% sucrose gradient and the peak fractions corresponding to the heavy form were collected. Aliquots were frozen and subjected to irradiation. The result was again found

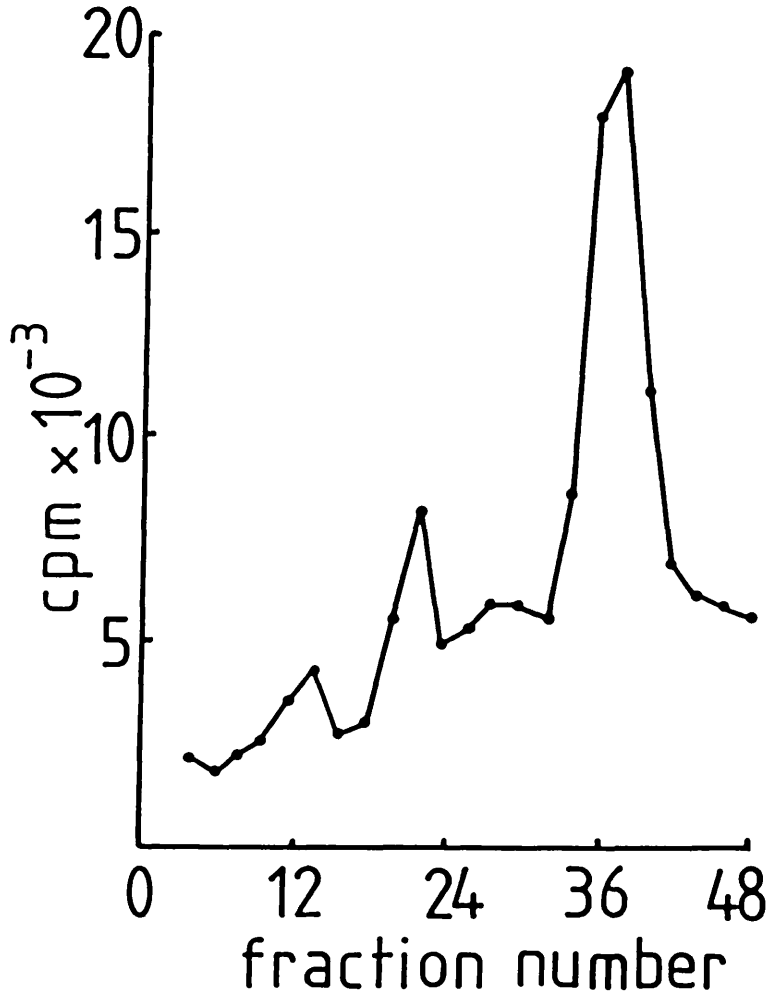

Fig 7.15 Sedimentation of chick muscle AChE

Triton X-100/NaCl solubilised AChE forms from one day old chick pectoral muscle (7.2.9) was applied to sucrose gradients (2.2.7). Gradients were fractionated and assayed for AChE activity (7.2.10).

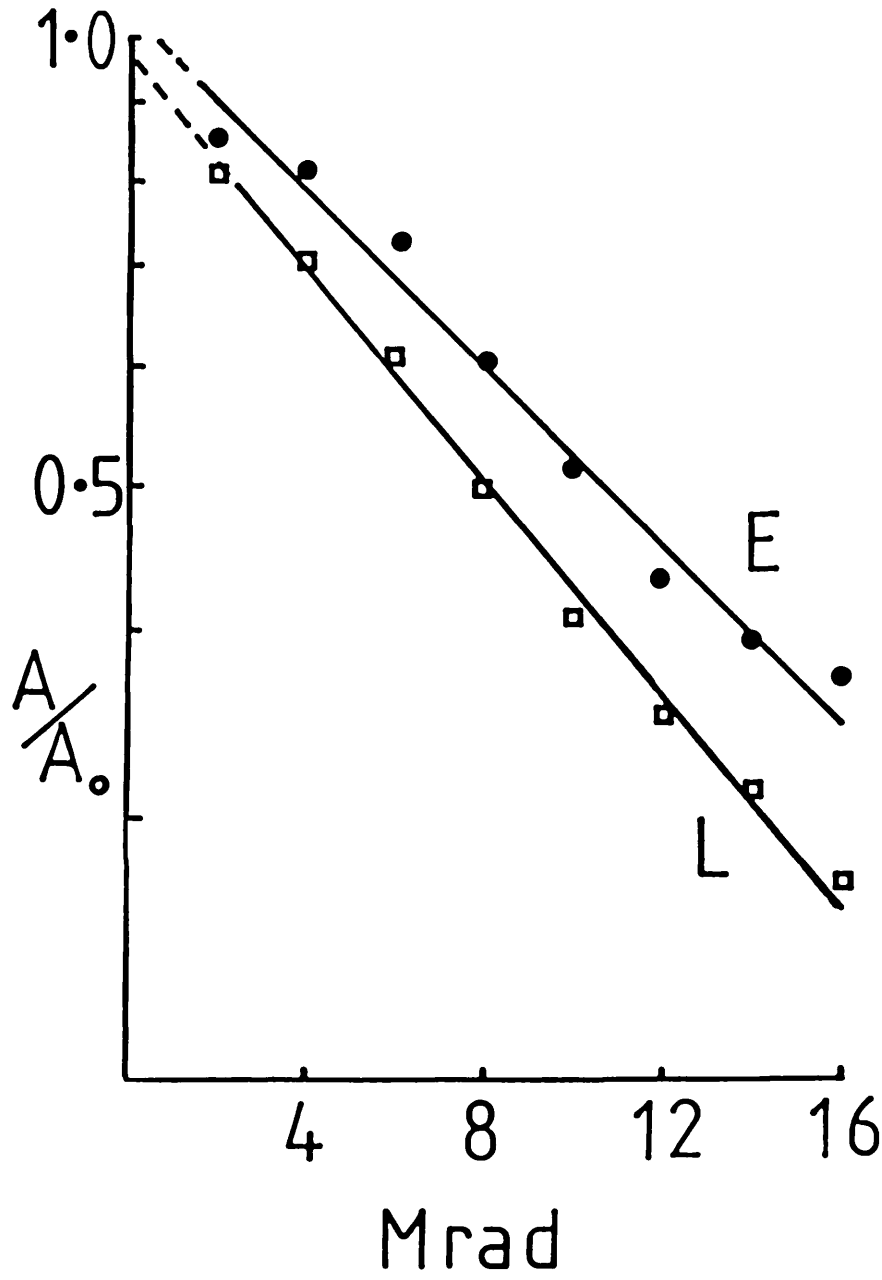

Fig 7.16 Radiation inactivation of chick muscle AChE

Chick pectoral muscle membranes were irradiated frozen, and assayed for remaining AChE activity (7.2.10).

L-LDH. AChE, r=0.98; LDH, r=0.99.

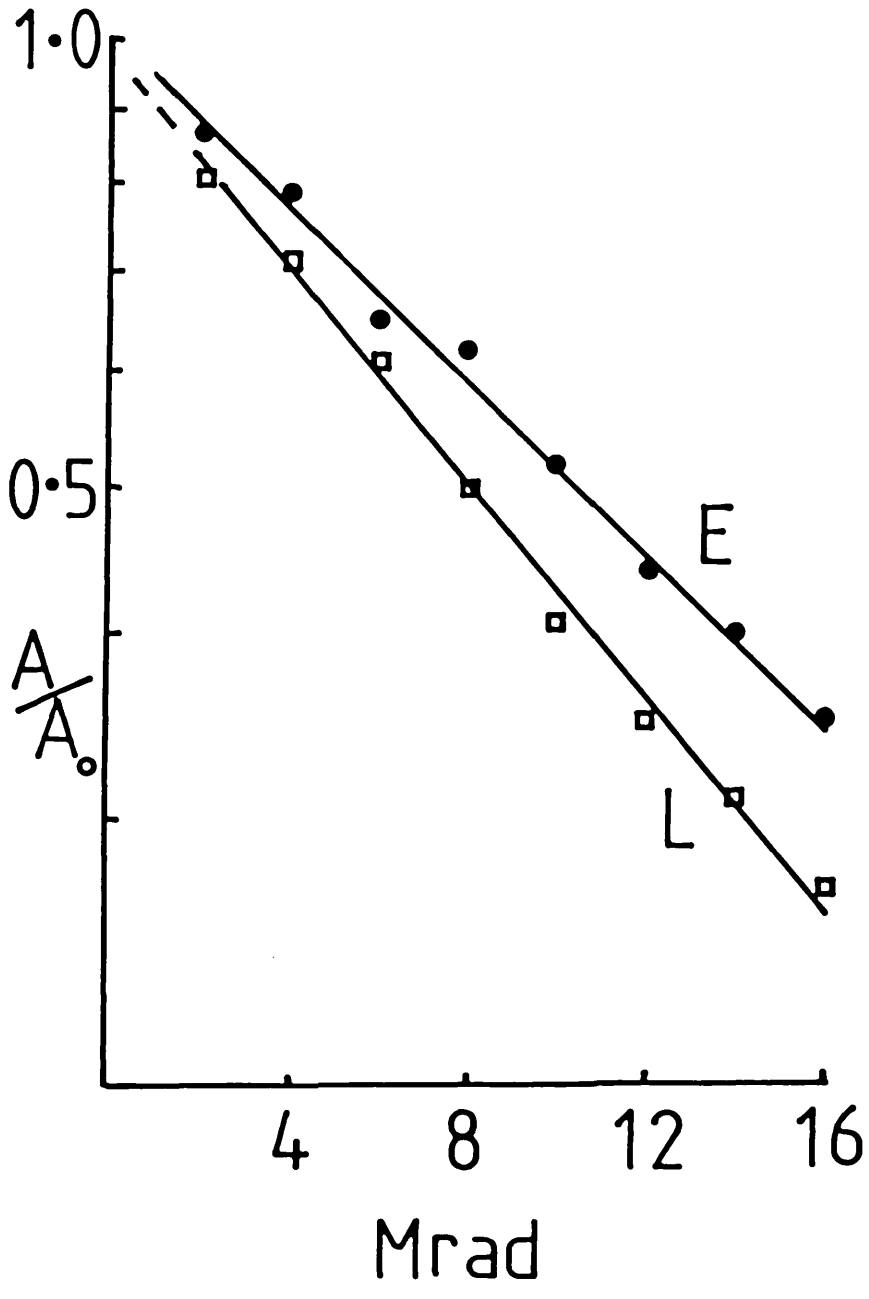

Fig 7.17 Radiation inactivation of 20S AChE

20S AChE prepared by sedimentation on sucrose gradients (Fig 7.15) was irradiated frozen, and assayed for remaining AChE activity (7.2.10).

L-LDH. AChE, r=0.98; LDH, r=0.99.

to display a similar inactivation profile, with the target size corresponding to the monomer molecular weight (Fig. 7.17). Hence, a direct test of radiation energy transfer occurring through this very large macromolecule proved negative.

CHAPTER 8 RADIATION INACTIVATION STUDIES ON MEMBRANE PROTEINS

8.1 MATERIALS

Materials and methods not fully described were as in 7.1 and 7.2.

All enzymes and protease inhibitors were from Sigma, GF/C filters from Whatman and ^{3}H- and ^{125}I-radioligands from Amersham International. Scintillant materials were from National Diagnostics. All other chemicals were of analytical grade.

Chicks were purchased from local farms and bovine cortex from a local abattoir. Sprague-Dawley rats were from the animal unit in this department.

All Ca^{2+}-ATPase experiments materials were generously provided by Dr. N.M. Green, National Institute for Medical Research, London.

8.2 METHODS

All irradiations described in this chapter were carried out at -78°C (in dry ice).

8.2.1 Preparation of rabbit muscle SR membranes for irradiation

Purified SR membranes were prepared according to the method of Meissner et al, (1973).

Rabbit skeletal muscle was homogenised (10ml/g) in 5mM histidine-HCl pH 7.2, 0.1M KCl. All subsequent operations were at 4°C. Pellets from the initial 1000g, 20 minutes and a second 8000g, 20 minutes spin were discarded, and the supernatant recentrifuged for 60 minutes at 100,000g. The pellet was

resuspended in 2 volumes of homogenisation buffer and layered onto 11-50% (w/v) sucrose gradients. After centrifugation at 10,000g for 60 minutes the middle band of membranes in the gradient was taken and recentrifuged for 60 minutes at 100,000g. The membrane pellet obtained was finally resuspended in 0.3M sucrose to ~30mg protein/ml, and stored at -80°C. This preparation was carried out with assistance from Mr. B. Trinnaman at the National Institute for Medical Research, London.

Preparations for irradiation experiments were carried out in 3 ways, as follows:

a) SR membranes were diluted to 2mg protein/ml with 50mM Tris-HCl pH 7, 0.3M sucrose, degassed and soluble enzymes added. Aliquots (0.2ml) were frozen in irradiation sample tubes with dry ice, then sealed under N_2.

b) SR membranes, diluted to 2mg/ml with H_2O, were degassed and soluble enzymes added. Samples (0.2ml) were freeze-dried overnight then sealed *in vacuo*.

c) SR membranes were solubilized by diluting to 2mg/ml in buffer F (Na phosphate 10mM pH 7, KCl 0.5M, $CaCl_2$ 0.1mM, $C_{12}E_9$ 4mg/ml, glycerol 20% v/v), degassed and soluble enzymes added. Samples (0.2ml) were frozen and sealed under N_2. Due to slight loss of activity with time, solubilised SR was assayed on the same day of irradiation.

8.2.2 *Assay of SR Ca^{2+}-ATPase activity*

Measurement of Ca^{2+}-ATPase activity was by the PK/LDH coupled enzyme method of Warren *et al*, (1974). ATP conversion to ADP by Ca^{2+}-ATPase, is reversed by the presence of PK and phosphoenol pyruvate (PEP), a reaction that produces pyruvate which is in turn reduced to lactate by LDH and NADH. With an excess of LDH and PK present, the Ca^{2+}-ATPase rate of ATP

degradation is essentially equivalent to the rate of NADH oxidation, measured at 340nm.

The Ca^{2+} ionophore, A23187 (Scarpa and Inesi, 1972) was added to SR membrane assays (1µg/ml) to destroy the Ca^{2+} ionic gradient, since during the assay, Ca^{2+} ions pumped into the vesicles would eventually result in inhibition of the Ca^{2+}-ATPase.

Ca^{2+}-independent ATPase activity, determined by addition to the assay medium of EGTA to 5mM, was generally 5-10% of the total activity.

Irradiated SR samples were reconstituted to 0.5ml with 50mM Tris-HCl pH 7, and aliquots taken (10-20µg protein) for assay of Ca^{2+}-ATPase activity in medium of the following composition:

Tris-HCl pH 7.5	60mM
$CaCl_2$	0.1mM
$MgCl_2$	6mM
KCl	0.13mM
PEP	0.8mM
ATP	3mM
NADH	0.2mM
Pyruvate kinase	10U/assay
Lactate dehydrogenase	50U/assay
A23187	1µg/assay

Measure OD change at 340 nm.

8.2.3 Preparation of rat brain membranes for irradiation

Rat brain membranes were prepared as described in Lai et al, (1984). All steps were carried out at 4°C. For each experiment,

forebrains from 10 Sprague-Dawley rats were Polytron (PT10) homogenised in 100ml of buffer E (TES-HCl 50mM pH 7.4, sucrose 0.32M, EDTA 1mM, benzamidine 1mM, DTT 1mM, PMSF 0.1mM, bacitracin 100µg/ml, soybean trypsin inhibitor 20µg/ml). The homogenate was centrifuged at 1000g, 10 minutes and the pellet rehomogenised in 100ml of buffer E and centrifuged (1000g, 10'). The two supernatants were combined, and the crude synaptosomal fraction pelleted at 49,000g, 30 minutes. The vesicles were then lysed by resuspending in 100ml of buffer E minus the sucrose, and pelleted as above. The membranes were resuspended to ~20mg protein/ml in an equal volume of H_2O, degassed and soluble enzymes added. Aliquots (0.4ml) were made into irradiation sample tubes, frozen in dry ice and sealed under N_2. For samples to be lyophilized, membranes were resuspended in 1mM DTT.

For some experiments, membranes were pretreated by incubation in buffer E containing 10 mM $MgCl_2$ at 30°C for 60 minutes before pelleting and resuspending in water.

8.2.4 Assay of opioid receptor binding activity

Various ^{3}H-radioligands were used to monitor the 3 major opioid receptor subtypes (Barnard and Demoliou-Mason, 1983).

[D-Ala^2, D-Leu^5]enkephalin (DADL, 36.5 Ci/mmol) measured the δ-sites, Tyr-D-Ala-Gly-(N-methyl)Phe-Gly-ol (DAGO 60 Ci/mmol) and dihydromorphine (DHM, 60 Ci/mmol) measured µ-sites and etorphine (30 Ci/mmol) or diprenorphine (38 Ci/mmol) + cold DADL and DAGO measured k-sites.

Irradiated rat brain membrane samples were reconstituted to 2ml with 10mM TES-HCl pH 7.4, 0.14M NaCl, 2mM $MgSO_4$. Aliquots of membranes were incubated (~0.2mg protein/ml) for 60 minutes at 30°C with 1nM ^{3}H-ligand, then filtered through premoistened

Whatman GF/C filters and rapidly washed with ice-cold buffer (3x5ml of 50mM TES-HCl pH 7.4). Filters were dried under an infra-red lamp and membranes solubilized overnight in soluene/toluene scintillant (14g PPO, 1.2g dimethyl POPOP, 200ml soluene made up to 2l with toluene), then counted in an Intertechnique scintillation spectrophotometer.

Non-specific binding was measured in the presence of 2µM cold ligand or etorphine.

Membrane preparation and assays were performed with the assistance of Dr. L. Newman, of this department.

8.2.5 Preparation of bovine cortex membranes for irradiation

Bovine cortex was homogenised (10ml/g) in 50mM Tris-HCl pH 7.4, 0.32M sucrose, 2.5mM $CaCl_2$ with a glass-teflon homogeniser (10 passes). All steps were performed at 4°C. The pellet from a 10 minute, 800g spin was discarded and the supernatant centrifuged for 30 minutes at 20,000g. The pelleted membrane vesicles were lysed in homogenisation buffer minus sucrose, then recentrifuged at 20,000g, 30 minutes. Membranes were resuspended in the same buffer, frozen at -20°C overnight, then thawed and centrifuged as above. This freeze-thawing cycle was repeated twice, in order to remove endogenous GABA from the membranes. After resuspension in water (~5mg protein/ml) the membranes were degassed, soluble enzymes added and 0.4ml aliquots made into irradiation sample tubes. Tubes were frozen in dry ice and samples sealed *in vacuo* (lyophilised) or under N_2 (frozen).

8.2.6 Assay of GABA/Bz receptor binding activity

Specific ^{3}H-ligands, muscimol (9 Ci/mmol) and flunitrazepam (84 Ci/mmol), were used to determine activity of the

GABA and Bz binding sites respectively of the GABA/Bz receptor complex (Sigel et al, 1983). Irradiated bovine cortex membrane samples were reconstituted to 1.6ml with 50mM Tris-HCl pH 7.4 and aliquots incubated (~0.5mg protein/ml) with ^{3}H-ligand (20nM muscimol or 5nM flunitrazepam) at 4°C for 1 hour. Membranes were then applied to presoaked Whatman GF/C filters and rapidly washed (3x5ml) with ice-cold 50mM Tris-HCl (pH 7.4) buffer. Filters were dried under an infra-red lamp and counted as in 8.2.4.

Non-specific binding was determined using 10μM flunitrazepam or 50μM muscimol.

8.2.7 Preparation of chick optic lobe membranes for irradiation

Optic lobe membranes from 1 day old chicks were prepared as described in 2.2.4. The pellet was resuspended in 3 volumes of H_2O, degassed and soluble enzymes added. Samples (0.4ml) were frozen and sealed under N_2 (frozen) or in vacuo (lyophilised).

8.2.8 Assay of chick optic lobe pnAChR binding activity

The supernatant from Triton X-100 (1%) solubilised irradiated membranes was assayed for ^{125}I-α BuTX (10nM) binding activity, after centrifugation, as described in 2.2.5.

8.2.9 Protein determination

Membrane protein concentrations were measured by the Lowry method (Lowry et al, 1951) as modified by Markwell et al, (1978) and described in 2.9.

8.3 RESULTS

8.3.1 Irradiation of rabbit muscle SR membranes

The Ca^{2+}/Mg^{2+}-ATPase in skeletal muscle SR vesicular membranes is the protein responsible for reducing the external Ca^{2+} concentration to μM levels, after muscle concentration, (review MacLennan and Holland, 1975). It was selected for target size studies, because, as well as being an integral membrane protein with an ion translocation channel, it has a molecular weight known to be ∿115K (Thorley-Lawson and Green, 1973; Rizzolo et al, (1976). The effect of freezing, lyophilisation and solubilisation on ATPase activity was examined. No activity loss was observed for any of these treatments (Table 8.1). The first irradiation experiment compared the target size of the ATPase in the lyophilised and frozen states. The result obtained showed that, similar to SDH in mitochondrial membranes, the target size for the ATPase increased in the lyophilised state, to approximately double that in frozen membranes (Table 8.2). From experiments with frozen membranes, it was apparent that the ∿250K target size obtained, corresponded approximately to an ATPase dimer (Fig. 8.2). Similarly, a target size of 210-250K was found by Hymel et al (1984), also for the rabbit skeletal muscle ATPase, using several assay methods including ATPase activity measurement.

The finding of Le Maire et al (1976), that detergent solubilized ATPase contained predominantly active monomers, suggested that irradiation of solubilized SR membranes might produce a target size corresponding to a monomer. However, these authors also found that there was a steady loss of activity of solubilized ATPase at room temperature. Therefore, activity loss

Table 8.1 Effect of freezing, lyophilisation and solubilization on activity of membrane proteins

Receptor binding activities were measured by radioligand binding and ATPase activity by the PK/LDH method.

Values are expressed as a % (± S.D.) of the activity in freshly prepared membranes.

	Frozen	Lyophilised	Solubilized
Ca^{2+}/Mg^{2+}-ATPase	98 ± 4	99 ± 2	100 ± 3
Opioid receptor			
μ site	96 ± 3	98 ± 3*	
δ site	98 ± 4	95 ± 6*	
GABA receptor	99 ± 4	96 ± 4	
Bz receptor	98 ± 3	95 ± 5	
ACh receptor	98 ± 5		

* Pretreated with 1mM DTT before lyophilisation.

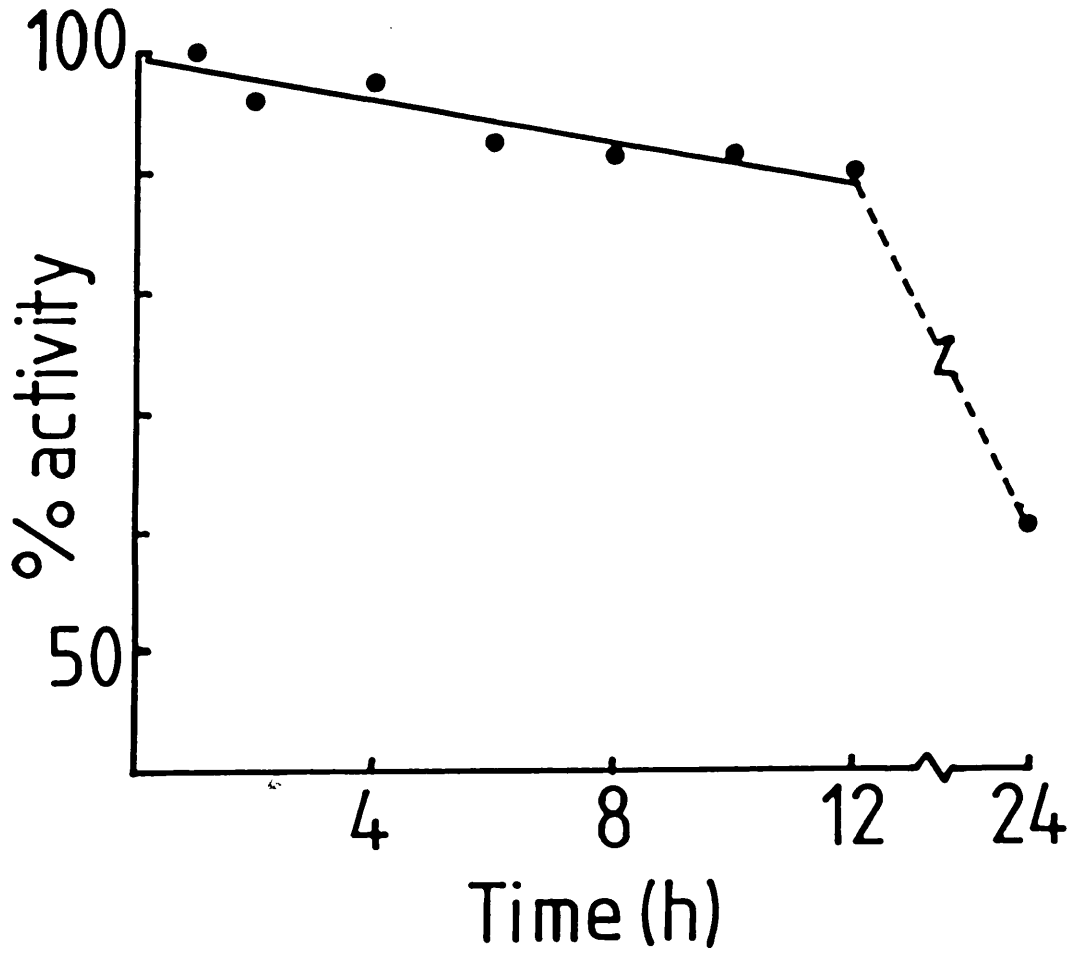

Fig 8.1 Decrease of Ca^{2+}-ATPase activity in frozen solubilised samples with time

Aliquots of SR membranes solubilised in $C_{12}E_9$ (8.2.1) were frozen and assayed for Ca^{2+}-ATPase activity at various times

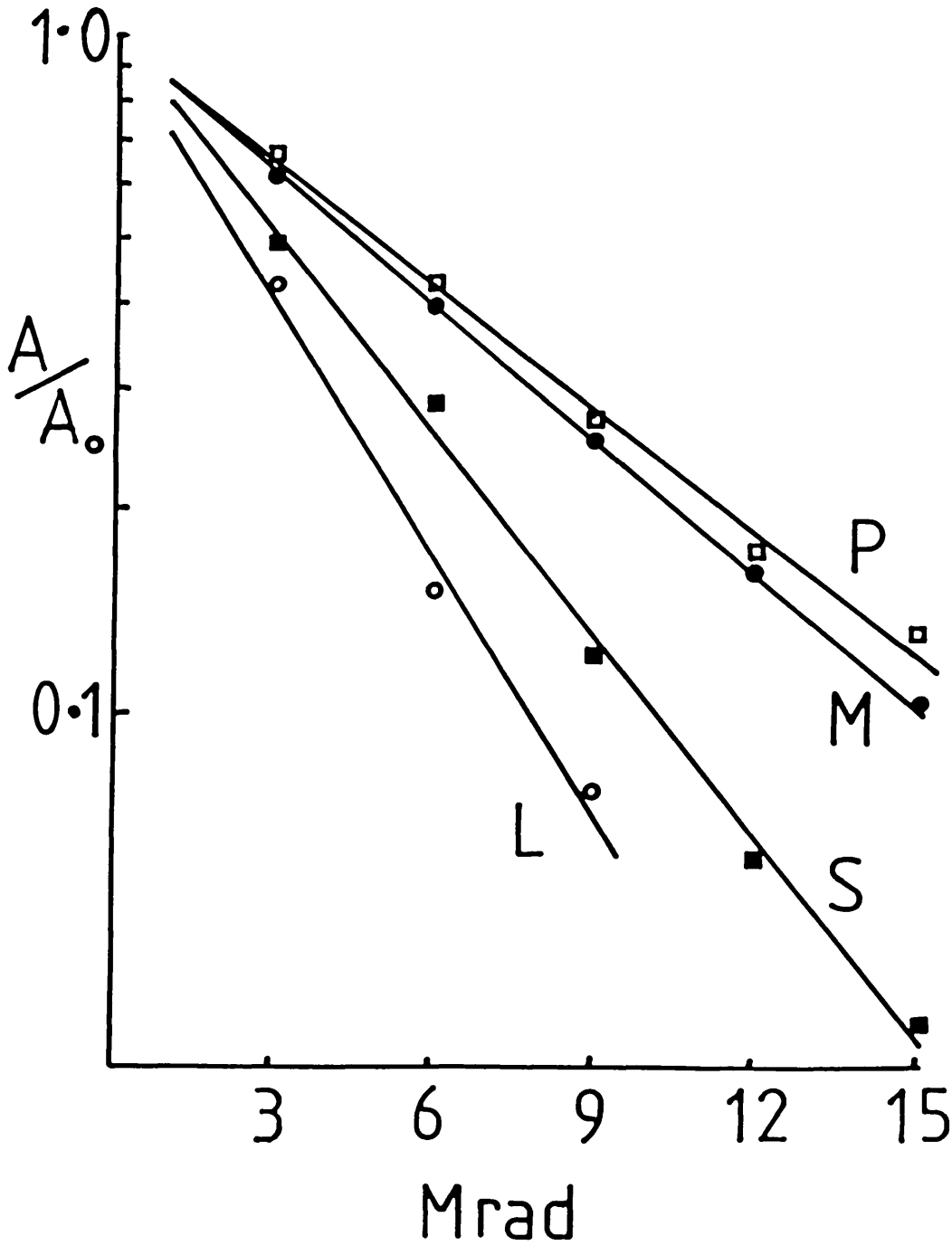

Fig 8.2 Radiation inactivation of Ca^{2+}-ATPase

SR membranes were irradiated after lyophilisation (L), solubilisation in $C_{12}E_9$ (S), or as untreated membranes (M). P-PK. PK, r=0.99; M, r=0.99; S, r=0.98; L, r=0.99.

of frozen solubilized ATPase with time was determined (Fig. 8.1). The rate of activity loss was significantly less than that reported for the ATPase in solution. Within a 12 hour period, there was a linear loss of activity of ~10%, after which the rate rapidly increased. Irradiation experiments using solubilized SR membranes were subsequently performed, so that the solubilization, irradiation and assay steps were all performed within 10 hours. The activity determined in each assay was adjusted upwards by between 5-9% according to the exact time of assay. Surprisingly, the inactivation plot revealed a target size greater than the molecular weight of both a monomer and dimer, with the slope corresponding to a size of ~320K. Suggestions that the result could be caused by aggregation of several monomers during the sample freezing process (in dry ice), led to experiments in which liquid nitrogen was used to freeze the samples. However, even with this "snap" freezing method, identical results were obtained.

8.3.2 Irradiation of rat brain membranes

The receptors in rat brain membranes for opiates and enkephalins are known to be multiple in nature. At least three subtypes, μ, δ and k have been characterised pharmacologically and by differential ligand binding (review Barnard and Demoliou-Mason 1983). However, neither the oligomeric or subunit composition of any of these receptors have been clearly established.

Using the μ-specific peptide and opiate ligands, DAGO and DHM respectively, the target size of the μ binding site in frozen rat brain membranes was determined from the loss of ligand binding after irradiation. For both ligands, identical

inactivation rates were obtained, giving a target size of ~105K. Using DADL, a δ-specific ligand, the δ binding site target size was measured similarly, producing a very similar target size of ~116K. As the inactivation slopes for both μ and δ sites were almost identical, the inactivation curves were combined, giving a mean target size of ~110K (Fig. 8.3).

For determination of the k-binding site target size, the non-specific opiate agonist and antagonist ligands, etorphine and diprenorphine respectively, were used. With addition of a 25 fold excess of cold DAGO and DADL in the assays to suppress binding to μ and δ sites respectively, the irradiation data for the k-binding site produced an unusual inactivation plot. The activity decay instead of showing a single component, corresponded to a biphasic curve. This indicated that a heterogenous population of 2 or more target sizes existed for the k-binding site (Fig. 8.4). The initial 40% loss of binding activity, had a slope slightly greater than that for μ and δ, however the remaining points of the inactivation curve corresponded to a much smaller target size of ~30K.

The experiments with 10mM $MgCl_2$ pretreatment, were designed to test a possible regulation of disulphide bridged subunits by cations (Barnard and Demoliou-Mason, 1983). Evidence for this would be shown by a change in target size after such pretreatment. However, no such evidence was found, as identical results to non-treated membranes were obtained.

The target sizes of the μ and δ binding sites were also determined in lyophilised membranes, pretreated with 1mM DTT. Pretreatment was necessary, as preliminary experiments in this laboratory (Peers, 1984) showed that a very steep inactivation slope was obtained for membranes lyophilised without DTT

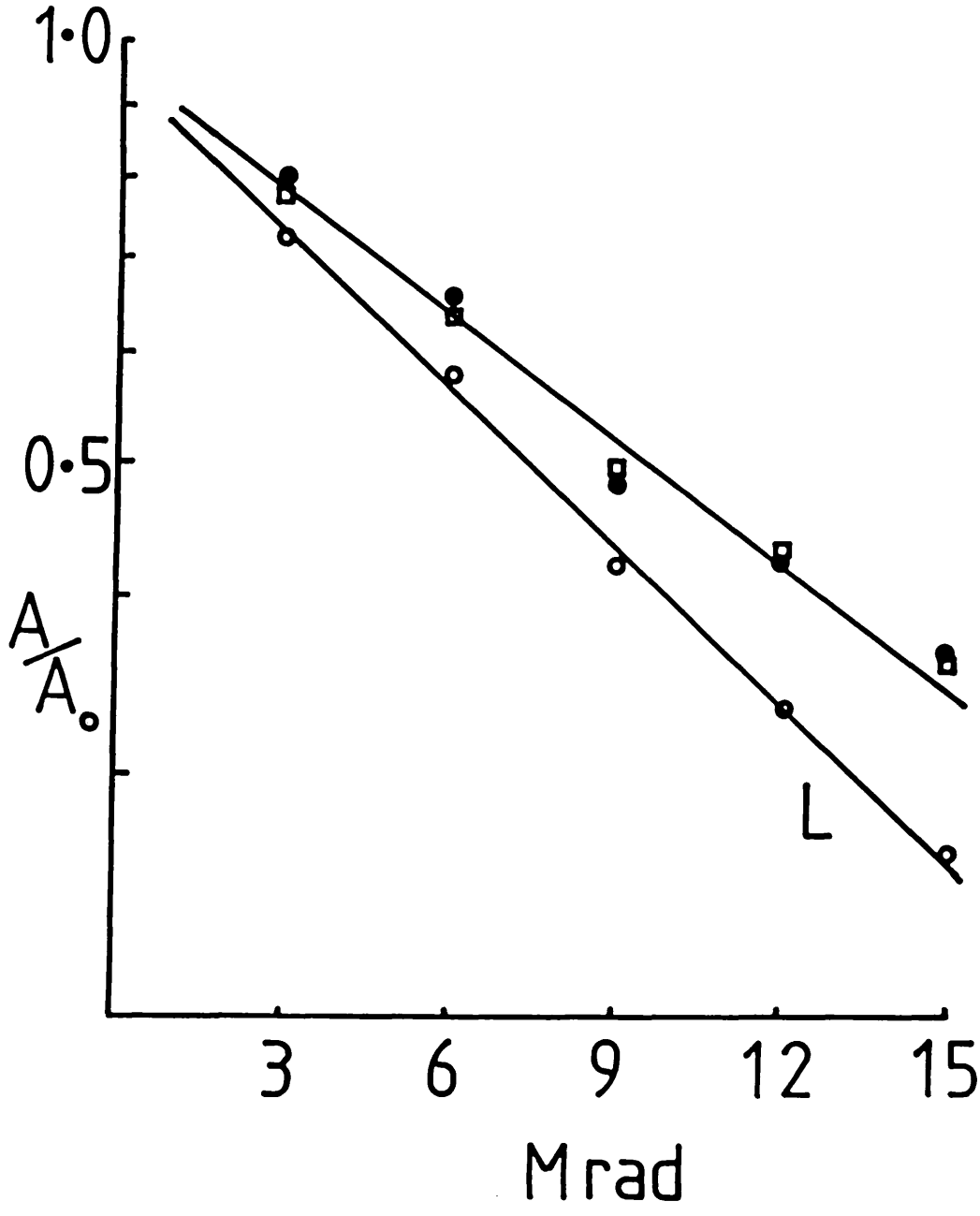

Fig 8.3 Radiation inactivation of μ- and δ-opioid sites

Rat brain membranes were irradiated frozen, and assayed for remaining μ- and δ-opioid binding activity (8.2.4).

L-LDH. Solid circles represent μ-binding sites and open squares the δ-binding sites.

μ-sites, r=0.98; S-site, r=0.98; L, r=0.99.

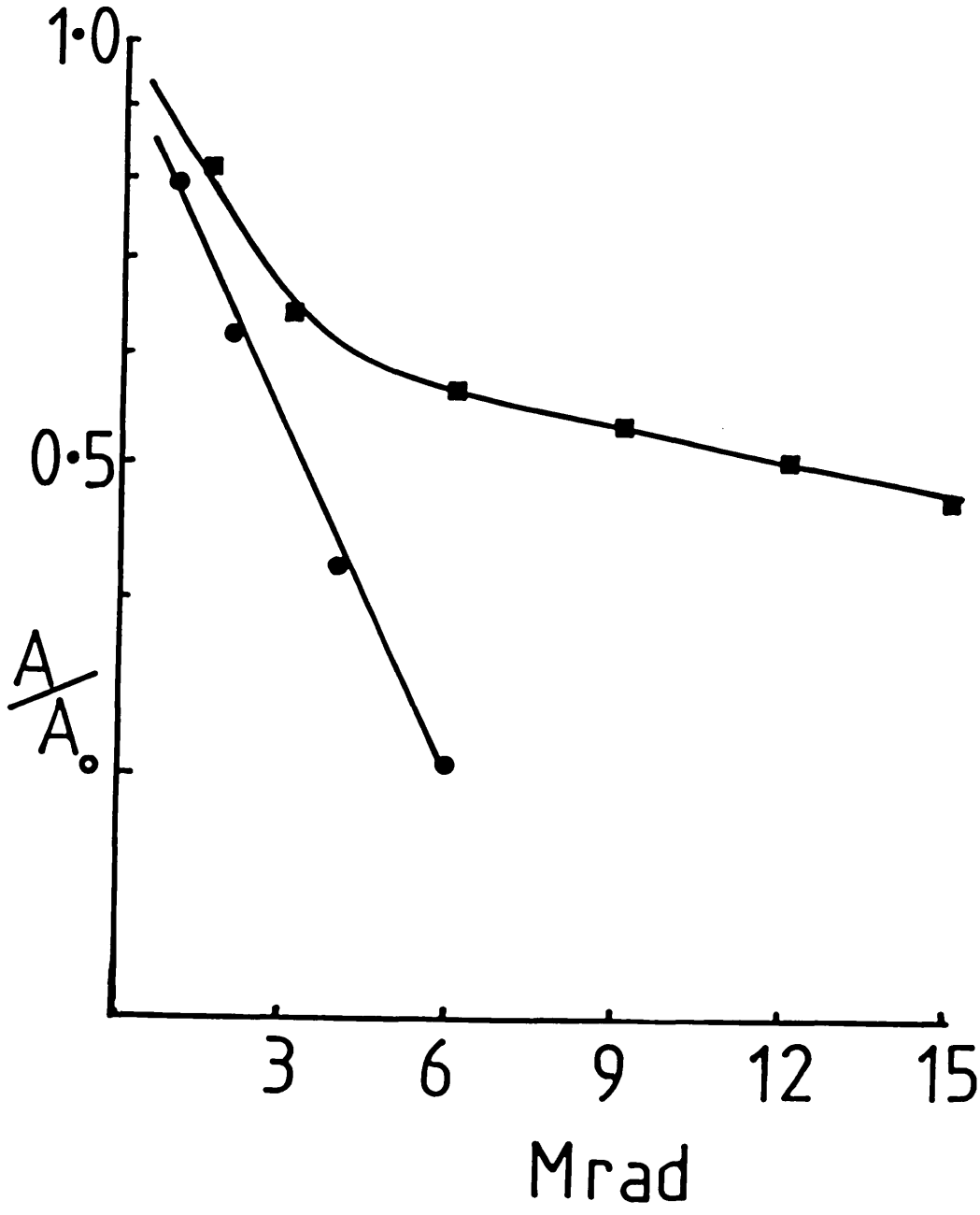

Fig 8.4 Radiation inactivation of k-opioid sites

Rat brain membranes were irradiated, the assayed for remaining opioid binding activity (8.2.4).

Solid circles represent δ/κ opioid binding activity in lyophilised membranes (r=0.99), and solid squares the k-binding activity in frozen membranes.

pretreatment. The pretreatment and lyophilisation process did not significantly reduce binding activity (Table 8.1), as was similarly found by MacLawhon et al (1983). However, irradiation of these membranes resulted in inactivation slopes for the μ and δ binding sites, almost three times that in frozen membranes (Fig. 8.4). This effect was comparable to that found with the Ca^{2+}-ATPase in lyophilised SR membranes.

The level of non-specific binding to membranes, determined in the presence of excess cold ligand, was between 12-18% of total binding in all experiments. Generally, lyophilised membranes had a slightly higher level of non-specific binding than frozen membranes.

8.3.3 Irradiation of bovine cortex membranes

Several recent conflicting reports on radiation inactivation of the GABA and Bz binding sites gave target sizes ranging from 50-220K (Paul et al, 1981; Chang and Barnard, 1982; Doble and Iversen, 1982). Therefore, a reinvestigation of the system was initiated in an attempt to clarify these incompatible results. Using radiolabelled muscimol and flunitrazepam to assay the specific binding of GABA and Bz binding sites, respectively, bovine cortex membranes, prepared by several freeze-thawing cycles to remove endogenous GABA, were shown to retain >94% of their initial binding activity after lyophilisation (Table 8.1). This confirmed the result, also found by Chang and Barnard (1982) and Doble and Iversen (1982), of essentially complete retention of activity after lyophilization. Simultaneous irradiation of frozen and lyophilized membrane samples was then performed, to determine if differences in target size existed between these two states (Fig. 8.5 and 8.6). In both lyophilised and frozen

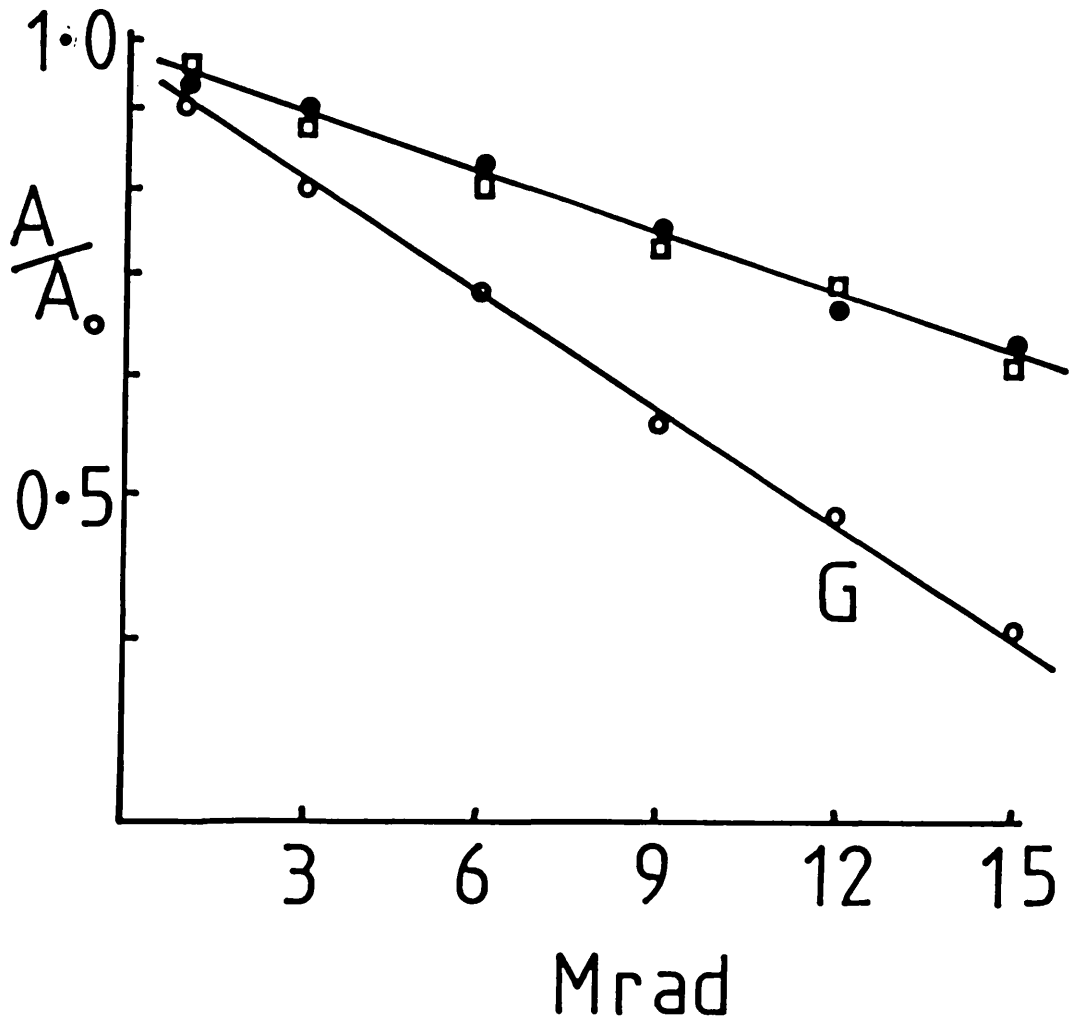

Fig 8.5 Radiation inactivation of frozen GABA and Bz sites

Bovine cortex membranes were irradiated , and assayed for remaining GABA and Bz binding activity (8.2.6).

G-glucose-6-phosphate DH. Solid circles represent GABA binding sites and open squares the Bz binding sites.

GABA site, r=0.98; Bz site, r=0.98; G6P-DH, r=0.99.

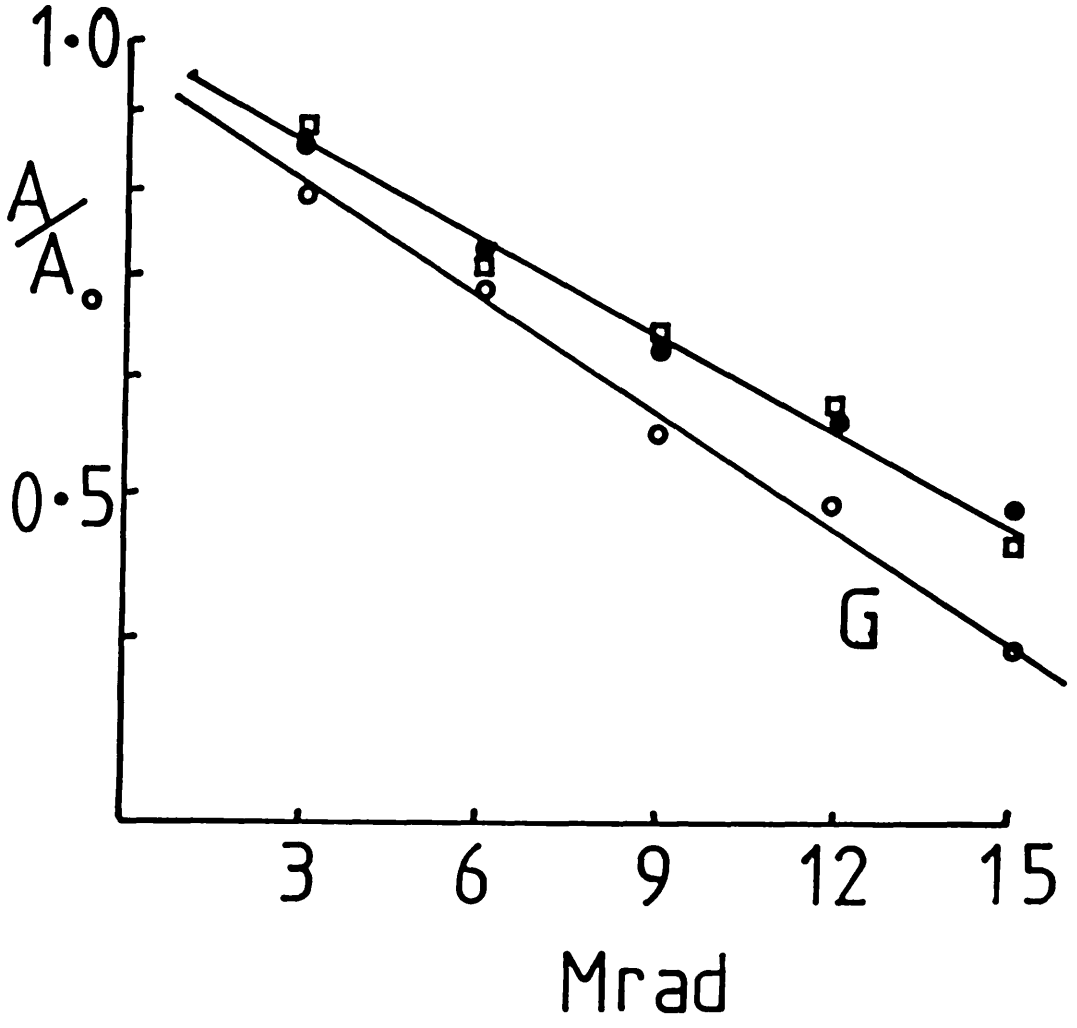

Fig 8.6 Radiation inactivation of lyophilised GABA and Bz sites

Bovine cortex membranes were irradiated, and assayed for remaining GABA and Bz binding activity (8.2.6).

G-G6P-DH. Solid circles represent GABA binding sites and open squares the Bz binding sites.

GABA site, r=0.98; Bz site, r=0.98; G6P-DH, r=0.98.

membranes, the target size for both GABA and Bz binding sites were identical (Table 8.2). This was in agreement with a previous report from this laboratory which also found identical inactivation profiles for these two sites, in lyophilised bovine cortex membranes (Chang and Barnard, 1982). However, the target sizes observed in frozen membranes, ~55K, were significantly smaller than the 220K found by Chang and Barnard (1982). The values were instead similar to the target sizes of 57K and 53K obtained for both GABA and Bz sites in frozen rat brain membranes by Paul et al (1981) and Nielsen and Braestrup (1982), respectively. Comparison between the inactivation profiles of frozen and lyophilised membranes revealed that the target size of 90K found for lyophilised membranes, corresponded to a ~70% increase in target size. This lyophilised value, which was similar to the 100K target size found by Doble and Iversen (1982) using lyophilised rat brain membranes, appeared to explain the discrepant results between various laboratories. The reports using frozen membranes always found a small (~50K) target size whilst lyophilised membranes always produced a larger size.

The non-specific binding levels in assays was between 6-10% for flunitrazepam and 15-20% for muscimol. As with rat brain membranes, lyophilised samples had slightly higher non-specific binding.

8.3.4 Irradiation of chick optic lobe membranes

Following the use of α BuTX for target size determination of the chick muscle nAChR (Lo et al, 1982), a study of the putative neuronal nAChR was considered. This would afford a comparison between the in situ sizes of both types of related molecules. Also, since the physical properties of the putative neuronal

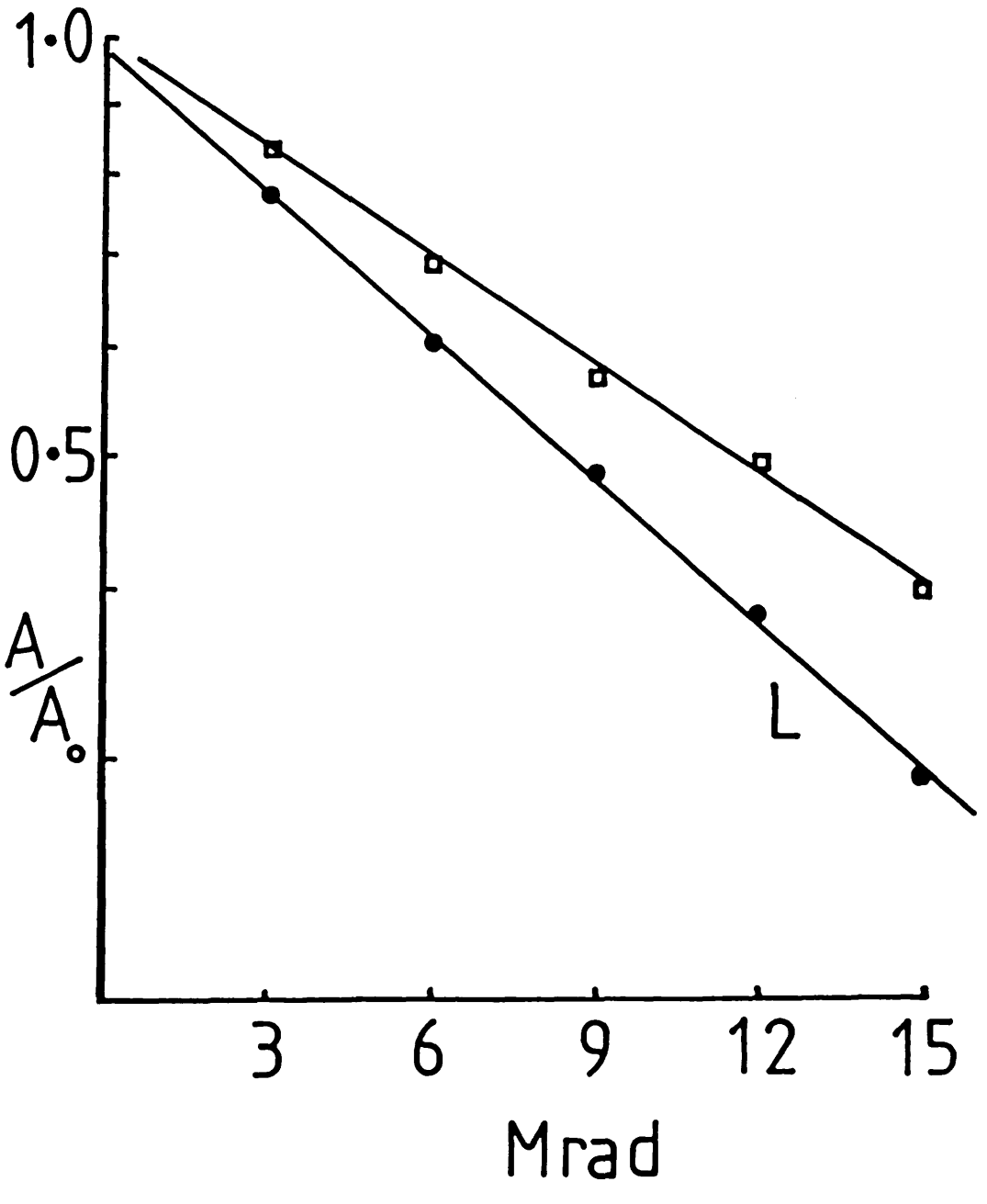

Fig 8.7 Radiation inactivation of α BuTX binding sites

Chick optic lobe membranes were irradiated frozen, and assayed for remaining α BuTX binding activity (8.2.8).

L-LDH. Open squares represent the α BuTX binding ste, r=0.98; LDH, r=0.99.

Table 8.2 Radiation inactivation of membrane proteins

Frozen	Inactivation Slope $x10^2$ (± S.D.)	Relative MW (± S.D.)
Ca^{2+}/Mg^{2+}-ATPase		
membranes	-6.60 ± 0.12	254 ± 30
solubilized	-9.92 ± 0.09	386 ± 34
Opioid receptor		
μ site	-2.65 ± 0.38	105 ± 15
δ site	-2.85 ± 0.24	116 ± 7
GABA receptor	-1.32 ± 0.15	54 ± 6
Bz receptor	-1.34 ± 0.16	55 ± 5
ACh receptor	-2.60 ± 0.26	104 ± 17
Lyophilised		
Ca^{2+}/Mg^{2+}-ATPase	-12.74	497
GABA receptor	- 2.25 ± 0.25	92 ± 13
Bz receptor	- 2.19 ± 0.19	89 ± 9

All values were determined at the irradiation temperature of -78°C.

nAChR in solution have been determined (Section I), and found to be slightly larger than the muscle receptor, their relative target sizes could be compared with their solution sizes. Assays for α BuTX binding were performed using solubilized membrane extracts from irradiated samples. This was because membranes extracted in 1% Triton, gave more reproducible assays, with non-specific binding levels of 18-25%, whilst assays using membranes had 25-33% non-specific binding.

Analysis of the inactivation slope for loss of αBuTX binding in frozen optic lobe membranes, produced a target size of ~100K. This was significantly smaller than the size found for the neuronal pnAChR in solution (Section I). However, it was very similar to the only report of a neuronal nAChR target size, of 108K by Lummis et al (1984), which was determined using insect neuronal membranes. They also measured loss of α BuTX binding as a function of radiation dose.

CHAPTER 9 DISCUSSION AND CONCLUSIONS

9.1 Practical considerations in radiation inactivation studies

The biological inactivation of macromolecules can be effected by any type of ionising radiation. This is evident from studies which have used various radiation sources such as α-particles, deuterons, protons and X-rays (Serlin and Fluke, 1956; Pollard, 1959; Darnell and Klotz, 1975). For target size determinations however, use of heavy fast particles is inferior to use of electrons or γ-rays. This arises from the necessity for the radiation to produce random ionisations, as well as to fully penetrate the sample thickness. Due to the high LET value of heavy fast particles (6.1), the above criteria are difficult to achieve without using particle accelerators, which would in turn produce highly unstable isotopes. The most practical choice therefore, was to use high energy electrons produced by a linear electron accelerator. Most target size studies conducted in other laboratories have also employed electron linacs, although one group has reported using γ-radiation emitted by a ^{60}Co source (Beauregard and Potier, 1982). There are disadvantages involved in using radioisotope sources. These are the low dose rates, which result in irradiations requiring several days to complete, and only being able to use lyophilised preparations.

In this, as in most other studies, many samples were coirradiated to reduce the time required, and hence the cost incurred by using hospital linacs (~£30/hr). Therefore, ensuring equal radiation dose to all coirradiated samples was achieved by the production of a uniform diverged beam. Generally, other authors have also employed diverged beams, although one report in which an unscattered beam was used, required that laborious

dosimetry be performed at every sample position in the beam (Ferry et al, 1983). The importance of this aspect of radiation inactivation studies is often not considered sufficiently and results in low correlation coefficients being observed for the inactivation slope.

At the commencement of this study, a controversy still existed over the temperature dependence of radiation sensitivity. The target sizes of several proteins were found to be markedly reduced at low temperature (Schlegel et al,1979; Kempner and Schlegel, 1979), whilst others were reported to be unaffected (Ostrovskii et al, 1969; Saccomani et al, 1981; Cuppoletti et al, 1981). The investigation made in this study, using an irradiation system capable of maintaining a constant irradiation temperature, agreed conclusively with the former findings, and a linear relationship between the logarithm of inactivation rate and time was observed. Although only 3 different temperatures were used here, essentially the same finding was subsequently reported by Kempner and Haigler (1982), in a study of malate dehydrogenase at +23°C and -135°C. The possibility that some enzymes were, and some were not sensitive to irradiation temperature was also disproved, as the same enzyme (MDH) had been used by Ostrovskii et al (1969). In addition, Kempner and Haigler (1982) also found evidence to suggest that previous results which showed a lack of temperature effect, was due to the use of temperature-sensitive dosimeters. Using the temperature-insensitive thermoluminescent dosimetry method, they found that the actual radiation dose received by the sample was completely unchanged by the ambient temperature, although the enzyme inactivation rate differed. There is at present no conclusive explanation for such a temperature effect of ionizing radiation

on biological and other material, and the target theory itself does not include any temperature factors. However, it could be envisaged that the decrease in chemical bond lengths at low temperature, is sufficient to impart extra stability to the molecule so that, when hit by a high energy electron, the probability of reaching the threshold limit that eventually results in biological inactivation, is reduced. This hypothesis is supported by the fact that indirect dosimetry systems that are based on a chemical colouration or discolouration, are also temperature sensitive, whereas thermoluminescent dosimetry which is a measurement of physically absorbed radiation energy, is not temperature dependent (Jung, 1984).

9.2 Radiation inactivation of enzymes, IgG and AChE

As already mentioned (6.3), one severe limitation of target size determination using the D_{37} empirical formula method, is the problem of accurately measuring the dose received by the sample. The method employed in this study to overcome possible errors due to varying degrees of radiation quenching, was to use concurrently irradiated enzyme standards of known MW (Lo *et al*, 1982). All enzymes thus experience the same irradiation conditions and the ratio of their inactivation rates will be proportional to their relative MWs.

Plotting the observed inactivation ratios of several enzymes versus their relative MWs resulted in a linear calibration curve, thus confirming its applicability as an alternative method of target size calculation. This approach has also recently been adopted by other authors using similar enzymes (Lilly *et al*, 1983; Venter *et al*, 1983; Kuno *et al*, 1985). The target size of the enzymes β-gal and aldolase however were anomalous, and

corresponded to sizes less than the oligomer. This phenomenon has also been reported for other enzymes (Kempner and Schlegel, 1979). In this study, aldolase, a tetramer of MW ~160K (Sia and Horecker, 1968), had a target size corresponding to ~half its MW, indicating that a dimeric inactivation had occurred. It may be possible that the aldolase molecule is arranged into two pairs of interacting subunits, such that a direct hit on one subunit of a pair results in inactivation of that pair, but does not impair the enzymatic function of the other pair. The case of β-gal is even more intriguing. This enzyme of MW 464K (Fowler and Zabin, 1977), appeared to inactivate with a target size of a monomer in the frozen state, and a dimer when lyophilised, even though it is a tetramer in solution with four 116K subunits. Similar findings have also been reported recently by Schwartz et al (1985), who found that β-gal's target size was 190K when lyophilised and 111K when frozen. In this case, the process of lyophilisation could possibly have caused conformational changes in the oligomer, such that two of the four subunits are brought closer together than when in a hydrated state. Also in the study by Kuno et al (1985), enzymes other than β-gal were used to produce a linear calibration curve. For calibration purposes, it is therefore better to select those enzymes which clearly display an oligomeric, or otherwise regular inactivation.

The phenomenon of oligomeric inactivation can be explained by the presence of energy transfer between the subunits of an oligomer. However, transfer of energy sufficient to inactivate an oligomer can be effected in two ways:

(i) ionization within one subunit, via a series of chemical reactions, causes bond breakage(s) in the adjacent subunit(s) resulting in inactivation of the oligomer, or,

(ii) ionization and loss of activity in one subunit results in oligomeric inactivation, due to a cooperative enzymatic (or other) activity mechanism requiring the intact structure of all subunits.

Evidence for both possibilities has been shown. Saccomani et al (1981), in a study of the gastric H^+/K^+-ATPase, found that loss of the 100K subunit on irradiation of the purified ATPase, measured by the loss of its Coomassie staining intensity on an SDS gel, corresponded to a target size of 270K, or trimer. This can only be explained by the transfer of ionization energy across all the subunits of a trimeric assembly, causing bond breakage in all three. Kempner and Miller (1983) approached the same problem using the hexameric enzyme glutamate dehydrogenase covalently labelled with fluorescein isothiocyanate (FITC). However, their analysis showed that although loss of enzymatic activity corresponded to a target size equivalent to that of the oligomer, the decrease in fluorescence of the FITC-labelled enzyme, and loss of staining intensity of the 56K subunit band on an SDS gel, corresponded closely to that of the subunit. They concluded that primary ionisations damaged only single polypeptides without any massive transfer of energy to other subunits, and enzymatic activity therefore, required all six subunits to be structurally intact.

The question of energy transfer has also been raised by other recent observations. One example, is the study of the pig kidney Na^+/K^+-ATPase (Richards et al, 1981). The target size of the Rb^+-occluding function was found to be 39K, whilst that of the p-nitrophenylphosphatase activity was 164K, which in turn is much smaller than the reported target size of the Na^+/K^+-ATPase activity, ~300K (Kepner and Macey, 1968; Ellory

et al, 1979; Peters et al, 1981). Based on biochemical evidence showing the ATPase to comprise two 120K α-chains and two 40-60K β-chains (Craig and Kyte, 1980), it was suggested that the ATPase activity target size corresponds to an $\alpha_2\beta_2$ structure, whereas the Rb^+-occluding function resides in the 40-60K subunit.

A similar effect to that with β-gal, was seen for the integral membrane enzyme, SDH. The larger target size obtained in lyophilised membranes suggests that it might occur as a dimer in the membrane, although its monomeric target size in frozen membranes implies that it can function as a monomer. This result for SDH, as for β-gal, also indicates that in these molecules, energy transfer through the oligomer occurs more readily in lyophilised than frozen samples. The precise reason for this behaviour is at present unknown.

The cause of the unexpectedly low intercept after irradiation of lyophilised mitochondrial membranes is unclear. Existence of a trace source of free radicals produced by low doses of radiation, which then cause biological inactivation, has been suggested (Barnard, 1984). This explanation is plausible and is supported by the mono-exponential activity decay observed even when the intercept effect occurs, and preliminary observations (F.A. Lai) which showed that this effect could be corrected by pretreatment with a radical scavenger/antioxidant such as DTT. In addition, mitochondrial membranes are known to produce unstable lipid peroxides when exposed to ionising radiations (Suno and Nagaoka, 1984; Obishi et al, 1984), and some fatty acids have been found very susceptible to peroxidation (Edwards et al, 1984). Therefore, it appears that the loss of a constant fraction of activity at all doses, could be attributed

to small amounts of these destructive components produced in irradiated lyophilised membranes.

The results from irradiation of IgG were peculiar, in that the target sizes obtained for both F_c and F_{ab} binding sites implied inactivation of a distinct region which corresponded closely in size to that of an "arm" or domain of the molecule. It is known that the IgG structure resembles a Y-shaped molecule (Fig 9.1) whose arms can swing out to an angle of 180°C, through a protease sensitive region acting as a hinge (Edelman, 1967). This unusual flexibility has been shown by electron microscopy of an IgG in various combinations with its hapten (Valentine and Green, 1967). Viewed by negative staining, a series of geometric forms was observed, which represented the different structures expected of a Y-shaped hinged molecule, with antigenic binding sites at the top of each of the two arms of the Y. Subsequent amino acid analysis of the hinge region has shown a large number of proline residues are present, which prevent the polypeptide chain assuming an α-helical conformation (Edelman et al, 1969). It could be argued therefore, that the domain inactivation of IgG is explained by the requirement of only a small region for binding activity and an ionization event in another region is not transmitted throughout the rest of the molecule. This would be possible due to the unique structural organisation of IgG into its 3 domains, as opposed to the traditional globular conformation of enzymes. In support of this suggestion, experiments have shown that cleavage of IgG by papain to produce 3 separated domains does not affect antigen binding activity of the Fab fragments (Porter, 1959). Further irradiation experiments using papain digested IgG could be useful in confirming this phenomenon of domain inactivation.

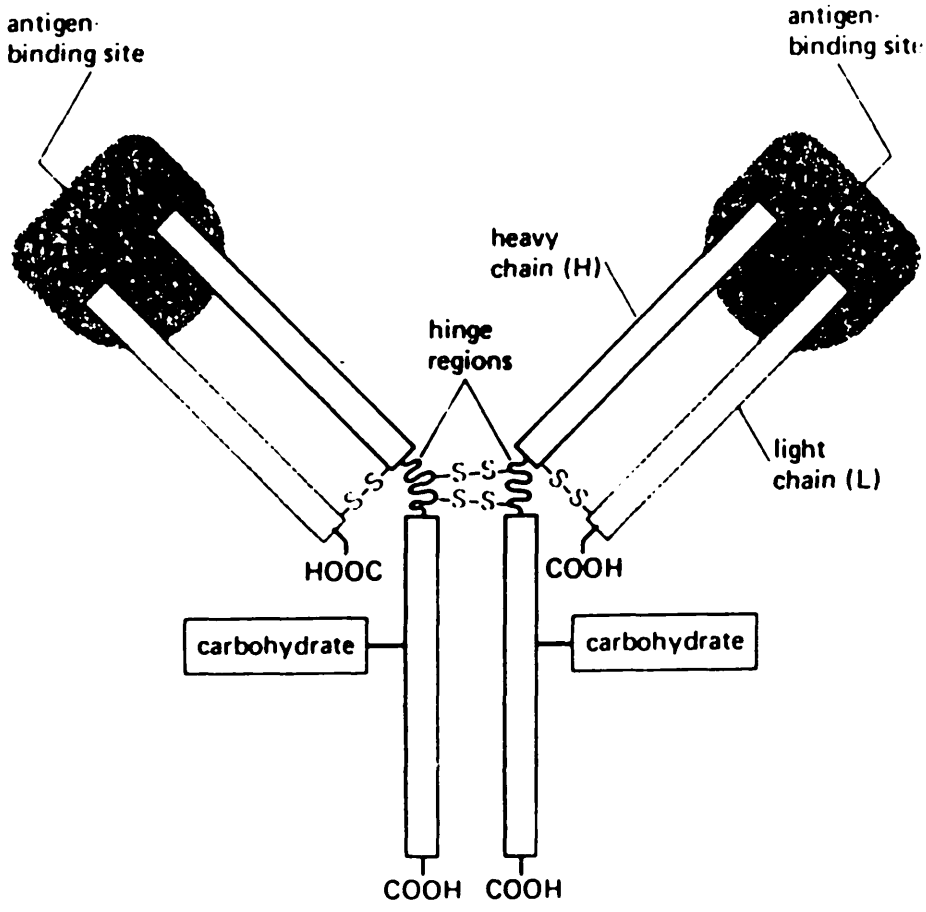

Fig 9.1 Diagram showing structure of IgG

The arrangement of polypeptide chains in the basic immunoglobulin structure (from Davis et al, 1975).

In chick skeletal muscle, four major forms of AChE are known to occur, and can be separated on the basis of their different sizes by centrifugation in sucrose gradients (Lyles et al, 1979). The focus of much interest recently has been the heaviest, 20S form, whose presence appears to be dependent on muscle innervation (Hall, 1973; Koenig and Vigny, 1978). This heavy form, by analogy to the heavy 16S form of AChE found in Torpedo and Electrophorus electric organs, is thought to comprise a dodecameric structure (Fig 9.2), with subunits linked covalently to a collagen tail through which the whole oligomer is anchored to the basal lamina (Bon et al, 1979). The total MW of the heavy form is probably >1000K and includes the ~100K collagen tail (Massoulie and Bon, 1982). This macromolecular complex would therefore be a good candidate to test for the possible occurrence of extensive radiation energy transfer. If energy transfer did take place through this large molecule on exposure to ionising radiation, then target analysis of a mixture of the heavy, medium and light AChE forms, would theoretically result in a non-linear inactivation curve (Verkman et al, 1984). The concave-upward inactivation curve expected from the independent destruction of an activity present on oligomers of different MW, has been exemplified by the study on adenylate cyclase by Schlegel et al (1979). The observation for AChE of a linear inactivation curve with a target size of 116K corresponds to the size of a monomer, since recently a 105K subunit has been isolated after SDS-PAGE of purified chick muscle 20S AChE (K.W. Tsim, personal communication). Hence, it appears that in this macromolecular complex, radiation energy transfer did not occur. A similar observation has also been made by Kempner et al (1980), in which target size analysis of the different activities on a polyenzyme

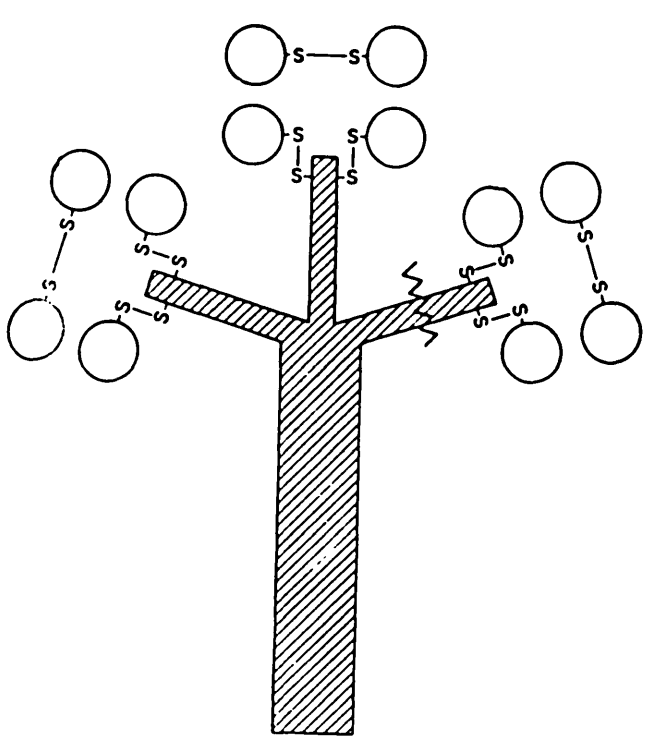

Fig 9.2 Diagram showing structure of AChE

Schematic arrangement of the heavy form of AChE from eel electroplax (from Rosenberry and Richardson, 1977).

cluster, produced sizes corresponding to individual enzymes. That a clearly mono-exponential decay was obtained also supports the view that subunits of all the various AChE forms are identical in size, and are probably connected along the same biosynthetic pathway (Massoulie and Bon, 1982). Although the chick muscle AChE target size obtained here is larger than the 75K target size determined for Electrophorus AChE (Levinson and Ellory, 1974), the difference could be due to the presence of smaller subunits in the latter species. The fact that the chick AChE heavy form is 20S as compared to 16S in Electrophorus and Torpedo, further supports this possibility. An alternative explanation might be that presence of detergent had contributed to the target size of the 20S AChE subunits, since it was isolated by Triton extraction and sucrose gradient sedimentation. However, this possibility is unlikely, as an identical size was found in crude muscle membrane preparations and recent studies have shown that target sizes of several soluble proteins in the presence and absence of detergent were unchanged (Beauregard and Potier, 1984).

9.3 Radiation inactivation of integral membrane proteins

(i) Ca^{2+}-ATPase

The Ca^{2+}-ATPase is responsible for the active transport of Ca^{2+} through the sarcoplasmic reticulum. Ca^{2+} translocation is known to be dependent on conformational changes in the protein but details of the precise mechanism remains unresolved (Tanford, 1983). The MW of purified skeletal muscle Ca^{2+}-ATPase was found by SDS-PAGE to be ~115K (Thorley-Lawson and Green, 1973; Rizzolo et al, 1976), similar to the results from recent cDNA analysis of a related Ca^{2+}-ATPase, which displayed a MW of 110K (McLennan et al, 1985). Structural studies have suggested that

Ca^{2+}-ATPase molecules formed dimeric (Fig 9.3), or higher oligomeric complexes in the membrane, and that these could represent the minimal transport units (Wang et al, 1979; Napolitano et al, 1983; Taylor et al, 1984). However, in favour of the opposing view that a functional monomer exists, other reports have shown that the solubilised monomeric Ca^{2+}-ATPase retains many important properties such as ATP hydrolysis (Moller et al, 1982), release of Ca^{2+} from two high affinity sites (Martin et al, 1984), ability to catalyse resynthesis of ATP from ADP after a "jump" in Ca^{2+} concentration (Martin and Tanford, 1984; Kosk-Kosicka et al, 1983) and the conformational changes involved in energy transduction (Andersen et al, 1985). In an attempt to obtain further evidence for either possibility, the technique of target size analysis was applied to this protein in situ. The ~250K target size obtained from the loss of Ca^{2+}-dependent ATPase activity, clearly supports the conclusions made from freeze fracture electron microscopy (Napolitano et al, 1983) that a dimer existed in the membrane, and is also in close agreement with a similar target size study subsequently reported by Hymel et al, (1984). In the latter study, as well as the loss of Ca^{2+}-ATPase activity, the decrease in Ca^{2+} pumping activity and staining intensity of the Ca^{2+}-ATPase 115K band were also measured, and all three approaches accorded well with an overall target size of 210-250K. The evidence from both structural and target size studies therefore support the presence of a dimeric Ca^{2+}-ATPase in the membrane. In addition, based on kinetic evidence from preparations of oligomeric and monomeric Ca^{2+}-ATPase, Yamamoto et al (1984) have suggested that the presence of some form of oligomeric interaction was likely, in order to explain the

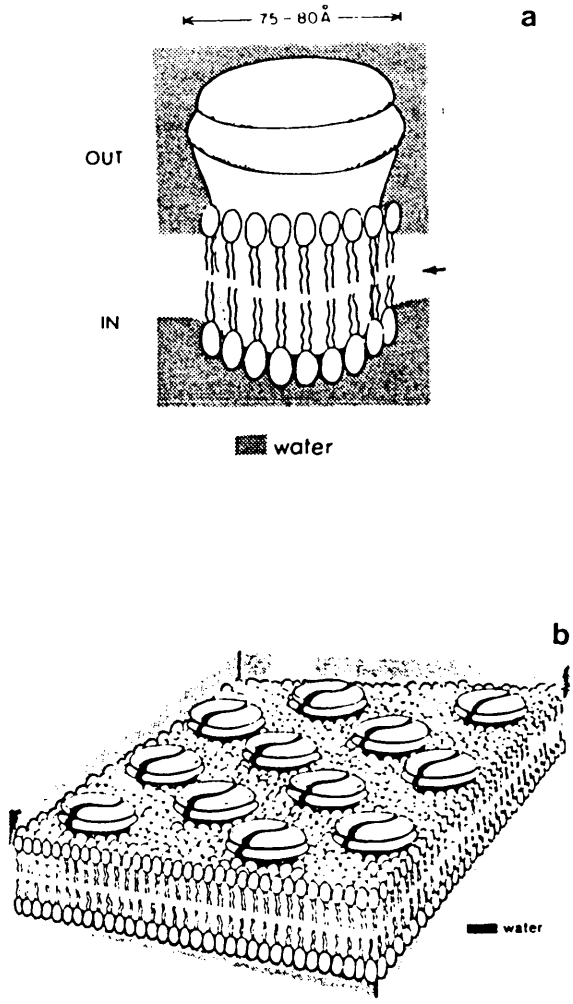

Fig 9.3 Diagram showing structure of Ca^{2+}-ATPase in SR membranes

a Cross-sectional representation of the Ca^{2+}-ATPase.

b Schematic representation of the Ca^{2+}-ATPase complex in the SR membrane (from Napolitano et al, 1983).

coupling of the ATPase reaction with Ca^{2+} translocation.

The finding of a target size greater than 250K in solubilised Ca^{2+}-ATPase preparations was surprising, since monomeric Ca^{2+}-ATPase has been shown to be present under such conditions (Le Maire et al, 1976). A possible explanation of this observation is that on freezing the solubilised samples, Ca^{2+}-ATPase dimers were reformed. The larger than dimer target size could also then be explained by the binding of detergent, which, although not of consequence for soluble proteins, has been shown to result in an average increase of 24% in the target size of integral membrane proteins (Beauregard and Potier, 1984). Using the figure quoted above, this would imply that the 320K obtained corresponded to a target size of 240K, a value very close to that found using frozen membranes. The large target size obtained for the Ca^{2+}-ATPase in lyophilised membranes was also unexpected, as it corresponds approximately to inactivation of a tetramer. Due to the proximity of Ca^{2+}-ATPase molecules in the membrane, lyophilisation may possibly have caused molecules to aggregate so closely, that inactivation of several monomers was effected by a single electron impact.

From the evidence obtained here by target size studies and by analogy to other ion translocating membrane proteins such as the nAChR, it can be suggested that the contact area between two or more subunits of an oligomeric protein would be a more likely place for an ion translocation channel. However, the example of bacteriorhodopsin should be noted also, since this protein appears to be fully functional in the monomeric state (Corradino, 1983) even though it exists in the membrane as a trimer (Leerbeck and Sondergaard, 1980). Similarly, a situation like that of Torpedo nAChRs may occur, where the existence of dimers has been shown not to be of functional importance (Anholt et al, 1980).

(ii) Opioid receptor

Although at least three subtypes of opioid binding site have been identified in mammalian brain, attempts to purify and characterise the corresponding receptors have generally been unsuccessful (Barnard and Demoliou-Mason, 1983). One major difficulty in such studies has been the preparation of detergent solubilised receptors which are both active and stable (Bidlack et al, 1981). Early studies by Simon et al (1975) using gel filtration chromatography, found an etorphine bound protein of 370K in solubilised rat brain, and a report by Zukin and Kream (1979) showed that a protein, also of 370K, was cross-linked to ^{3}H-enkephalin. However, in both these solubilised membrane preparations the opioid receptors were not active. Application of the radiation inactivation method was therefore a logical approach to take, as it does not require membrane proteins to be solubilised (Barnard, 1984). Also, if two or more subtypes were situated on the same oligomer, then one possible feature of such an association in situ, would be a common target size. While investigation of this possibility was in progress, two reports appeared on the application to this receptor class of the radiation inactivation method. Using cultured neuroblastoma-glioma cells (line NG108-15) in the lyophilised state, McLawhon et al (1983) obtained a target size of 200K for the δ receptor, whereas Ott et al (1983) found a target size of 90K for the μ, δ and k-receptors in frozen rat brain slices, and for the δ receptor in frozen NG108-15 cells. It was therefore of additional interest to try to resolve these differences.

The target size of 110K for both μ and δ receptors obtained in this study using frozen rat brain membranes (Lai et al, 1984), was essentially in agreement with the value obtained by Ott et al

(1983). However, the results using lyophilised membranes were similar to those of McLawhon et al (1983). In this case, although μ and δ receptors again displayed identical inactivation profiles, the target size was significantly larger. As both lyophilised and frozen membranes were irradiated under identical conditions in this study, the target size differences reported appeared to be real, and not due to experimental errors. One possible explanation for the difference observed would be an aggregation of receptors occurring in lyophilised membranes, such that a hit in one destroys several binding sites in the aggregate. This behaviour is therefore analogous to that observed with Ca^{2+}-ATPase in lyophilised SR membranes. The observation of a common dose dependence for both μ and δ sites in both states, does however, concur with their coexistence on the same receptor, although it could also be due to two homologous proteins each carrying one of these classes of binding site. In contrast to the μ and δ sites, the behaviour of the k-binding sites on irradiation was very different. The biphasic curve obtained, suggests that k-binding sites are present on two structures of different size. This is similar to previously observed biphasic curves for the glucagon receptor and adenyl-cyclase (Schlegel et al, 1979). A possible explanation of this effect may be that a population of k-binding sites was dissociated from an oligomeric complex, since the homogenisation buffer used contain DTT. This would also then explain why Ott et al (1983), did not see a biphasic curve since they used intact frozen tissue in their irradiations. A recent target size study of the various subtypes of 5-HT binding sites in rat brain, has also yielded similar results to those observed here (Gozlan et al, 1985). These authors found that both 5-HT_2 and 5-HT_3

binding sites displayed monoexponential inactivation curves whilst the 5-HT_{1A} and 5-HT_{1B} sites produced identical curvilinear patterns, and which they suggested was due to their presence on complex polymeric structures. In contrast, study of the D_1 and D_2 receptors for dopamine has shown that these two sites are present on structures of different target size (Nielsen et al, 1984). Similarly, the V_1 and V_2 isoreceptors for vasopressin have also been shown to have distinct target sizes (Crause et al, 1984).

Klee et al (1982) have reported a δ receptor subunit of 58K, after affinity labelling of NG108-15 cells followed by SDS-gel analysis of the labelled subunits. More recently, Newman and Barnard (1985) have reported affinity labelling of a μ receptor subunit also with a MW of 58K. These latter two observations add further evidence for the possible location of both μ and δ sites on the same size subunit and suggests that the target size of 110K obtained here, is due to a dimer of identical 58K subunits. Whether the μ and δ sites are on the same subunit or on different subunits has yet to be determined.

(iii) GABA/Bz receptor

The binding sites for GABA and benzodiazepines in brain are believed to be present on the same receptor complex (reviews Olsen, 1982; Costa and Guidotti, 1979). This view arose from the demonstration of enhancement of benzodiazepine binding by GABA (Martin and Candy, 1978), and has been supported by experimental evidence that, in solution, both receptors have similar physical properties (Gavish and Snyder, 1981; Stephenson et al, 1982). The manner in which these binding sites are related is not yet understood, although several models have been proposed (Thomas

and Tallman, 1984; Skolnick and Paul, 1982).

MW determination of the GABA/Bz receptor complex has been approached using various techniques such as gel filtration chromatography, sucrose density gradient centrifugation and calculation of Stokes radius. These have resulted in estimated MW values of 200-350K (Yousufi et al, 1979; Chang and Barnard, 1982; Stephenson et al, 1982). Similarly, many reports have appeared on the application of target size analysis to brain benzodiazepine binding sites. The wide variety of results observed, fall into the following three distinct groups: 51-57K (Paul et al, 1981; Doble and Iversen, 1982; Nielsen et al, 1983; Nielsen and Braestrup, 1983), 90-100K (Doble and Iversen, 1982) and 220K (Chang and Barnard, 1982). In the latter study by Chang and Barnard (1982), the GABA binding site target size was also determined and an identical size of 220K was observed, adding further evidence for the coexistence of both GABA and benzodiazepine sites on the same receptor complex.

As a result of the contrasting and obviously incompatible target size data obtained for the benzodiazepine binding site, a reinvestigation of both GABA and benzodiazepine binding sites in the frozen and lyophilised state, was made. The results obtained in this study seem to clarify the previous confusing situation. Using frozen membranes, the target size for both GABA and benzodiazepine binding sites were identical, and was clearly consistent with the lowest of the three values given above, whilst use of lyophilised membranes was consistent with the 90-100K value. It appeared therefore, that the target size value of 90-100K obtained by Doble and Iversen (1982), was specifically due to lyophilisation, since they used lyophilised membranes and the same figure was reproduced here only when lyophilised

membranes were used. The reason for this increase in target size when lyophilised membranes are used is not readily apparent, as the membrane preparation and experimental conditions were identical. The most likely reason seems to be that a specific lyophilisation-induced aggregation of subunits occurred and thus resulted in an increased target size. The similar observations with Ca^{2+}-ATPase and the opioid receptor subtypes when lyophilised membranes were used, support this explanation and also suggests that this aggregation effect could be common to all membrane proteins.

The small target size of GABA and benzodiazepine binding sites in frozen membranes, correlates closely with sizes of the putative subunit(s) possessing the benzodiazepine site, since studies in which ^{3}H-flunitrazepam photolabelled proteins were subjected to SDS-PAGE, revealed bands with apparent MWs of 48-62K (Mohler et al, 1980; Gavish and Snyder, 1981; Thomas and Tallman, 1981). Additionally, in a reported purification of the GABA/Bz receptor complex (Sigel et al, 1983), two major bands of 57K and 53K were observed, both of which specifically labelled with flunitrazepam, thus further supporting the view that the target size obtained corresponded to inactivation of single subunits. Although this study infers the possibility that both GABA and benzodiazepine binding sites are on an identical subunit, as was also suggested by Chang and Barnard (1982), further evidence for this situation is required. One approach might be to synthesize a photoaffinity label for the GABA binding site and showing the subunit(s) to be identical to those seen labelled by flunitrazepam. The observation of a 220K target size in lyophilised membranes (Chang and Barnard, 1982), is probably due to the use of β-gal as an enzyme standard, since this study has

shown it to inactivate as a dimer when lyophilised.

The cage convulsant TBPS has been reported (Squires et al, 1982) to bind with high affinity to the chloride channel believed to be integral to the GABA/Bz receptor complex (Olsen and Leeb-Lundberg, 1981). A recent study of the TBPS binding site was found to give a target size of 140K (Schwartz et al, 1985). From this observation, it was suggested that the GABA/Bz receptor comprised a ~50K subunit, which contained both GABA and benzodiazepine binding sites, and a 140K subunit containing the TBPS binding site. However, this suggestion does not correlate with the observation of only 57K and 53K subunits in purified receptor preparations (Sigel et al, 1983), and seems more likely to be due to the TBPS binding site being in close proximity to three subunits of an oligomeric complex containing four to five ~50-60K subunits. This latter situation would then be analogous to the interaction of local anaesthetics with the ion channel of the nAChR, which has been suggested to involve binding to several of the five nAChR subunits (Kaldany and Karlin, 1983). Here again, synthesis of a TBPS derivative for photolabelling may be useful in determining whether this binding site is on one or more of the ~50-60K subunits already isolated.

(iv) pnAChR

In conjunction with the studies on the solubilised pnAChR (Section I), target size analysis was applied to the loss of ^{125}I-α BuTX binding to irradiated chick optic lobe membranes. The 100K target size obtained, was much smaller than the MW of 354K calculated for the Triton solubilised pnAChR by sucrose gradient sedimentation and gel filtration chromatography. This is similar to the only other target size for neuronal nAChRs,

reported recently by Lummis et al, (1984). In that study, which used invertebrate CNS membranes (cockroach), a target size of 108K was observed for the α BuTX binding site, and was shown to be distinct from the 78K target size for the mAChR, as measured by N-methylscopolamine binding. As for the solubilised chick optic lobe pnAChR, solubilised invertebrate CNS nAChRs have been found to exhibit similarly large MWs (>400K, Rudloff et al, 1980; Schmidt-Glenewinkel et al, 1981). Thus it appears that these target sizes observed, could only correspond to inactivation of one or two subunits of a nAChR oligomer. The target size obtained here is very close to the ∿98K subunit size found in purified chick optic lobe pnAChR preparations, and implies, if these two sites are equivalent, that this apparent ∿98K subunit is actually a dimer of the 57K subunit, since only the latter subunit has been shown to specifically bind α BuTX (Norman et al, 1982). Alternatively, if the ∿98K protein is not a 57K dimer, as was concluded earlier (Section I), the target size could represent inactivation of the 57K subunit and another proximal subunit which could be either a 47K or 72K subunit or possibly another 57K subunit. The two studies of neuronal pnAChR target size performed so far are therefore not in accord with the nAChR target size found by Lo et al, (1982). In that study, Lo et al (1982) found a target size of ∿290K for various muscle nAChRs, in close agreement with their oligomeric size. However, the early report of a nAChR target size by Barnard et al (1978) of ∿90K, is similar to that found here. This implies that, as suggested earlier for the target size study of the GABA/Bz receptor complex, use of β-gal by Lo et al (1982) led to an over estimate of nAChR target size. Also their use of lyophilised membranes may have contributed to an aggregation effect similar to that

observed in this study for other membrane proteins. This possibility however, requires confirmation by further target size studies using lyophilised chick optic lobe membranes.

9.4 Concluding remarks

The many attractions of the technique of target size analysis have been recently realised, as evidenced by the almost exponential increase in the number of publications made reporting its application. The advantages of this approach include, the method's independence of the presence of other proteins i.e. no purification steps are required, the applicability to receptors and other proteins present in membranes even when in low concentration (provided a sensitive assay is available), and the observation of identical inactivation profiles which would be expected from the presence of more than one type of binding site on a single polypeptide. However, from the results obtained in this study, one should not assume that a general rule exists in the interpretation of target size analysis data. This is most perspicuous from the following observations.

1. The use of soluble enzymes often assumed to give oligomeric inactivation, is not a universal phenomenon as shown by the target sizes of the enzymes β-gal and aldolase.

2. For some proteins with unconventional structures such as immunoglobulins, radiation inactivation reveals a target size corresponding to inactivation of a single domain of the molecule.

3. Radiation inactivation of large macromolecular complexes such as the heavy 20S form of AChE, reveals only a subunit target size.

4. Membrane proteins appear to display different target sizes

when membranes are lyophilised as compared to using frozen membranes.

5. Membrane protein target sizes have been shown to correspond to inactivation of oligomers, monomers and subunits.

It is therefore obvious, that target size analysis by radiation inactivation should not be used in isolation, but as part of a general approach, using a variety of techniques, to study the size of biological molecules.

REFERENCES

REFERENCES

Abood,L.G., Latham,W., and Grassi,S. (1983) Proc. Natl. Acad. Sci. USA 80, 3536.

Adams,P.R. (1981) J. Memb. Biol. 58, 161.

Andersen,J.P., Jorgensen,P.L., and Moller,J.V. (1985) Proc. Natl. Acad. Sci. USA 82, 4573.

Andersen,J.P., Moller,J.V. and Jorgensen,P.L. (1982) J. Biol. Chem. 257, 8300.

Andrews,H.L. (1974) in Radiation Biophysics, New Jersey, Prentice Hall Inc.

Andrews,P. (1964) Biochem J. 91, 222.

Anholt,R., Lindstrom,J. and Montal,M. (1980) Eur. J. Biochem. 109, 481.

Arimatsu,Y., Seto,A. and Amano,T. (1978) Brain Res. 147, 165.

Ascher,P., Large,W.A. and Rang,H.P. (1979) J. Physiol. 295, 139.

Augenstein,L.G. Brustad, T. and Mason,R. (1964) Adv. Radiat. Biol. 1, 228.

Bardsley,M.E. and Roberts,P.J. (1985) Biochem. Biophys. Res. Commun. 126, 227.

Barhanin,J., Schmid,A., Lombet,A., Wheeler,K.P., Lazdunski,M. and Ellory,J.C. (1983) J. Biol. Chem. 258, 700.

Barnard,E.A. (1984) in Investigation of membrane-located receptors, Plenum Publishing Corp.

Barnard,E.A., Beeson,D., Bilbe,G., Constanti,A., Conti-Tronconi,B.M., Dolly,J.O., Dunn,S.M.D., Mehraban,F., Richards,B.M., and Smart,T.G. (1983) Cold Spring Harb. Symp. Quant. Biol. 48, 109.

Barnard,E.A., and Demoliou-Mason,C. (1983) Brit. Med. Bull. 39, 37.

Barnard,E.A. and Dolly,J.O. (1982) Trends in Neurosci. 5, 325.

Barnard,E.A. and Dolly,J.O. (1984) Biochem. Pharm. 33, 841.

Barnard,E.A., Dolly,J.O., Lang,B., Lo,M. and Shorr,R.G. (1979) Adv. Cytopharm. 3, 409.

Barnard,E.A., Dolly,J.O., Lo,M. and Mantle,T. (1978) Biochem. Soc. Trans. 6, 649.

Barnard,E.A., Miledi,R. and Sumikawa,K. (1982) Proc. Roy. Soc. Lond. B215, 241.

Barnard,E.A., Wieckowski,J. and Chiu,T.H. (1971) Nature 234, 207.

Barrantes,F.J. (1978) J. Mol. Biol. 124, 259.

Barrantes,F.J. (1983) Int. Rev. Neurobiol. 24, 259.

Bartfeld,D. and Fuchs,S. (1979) Biochem. Biophys. Res. Commun. 89, 512.

Beauregard,G. and Potier,M. (1982) Anal. Biochem. 122, 379.

Beauregard,G. and Potier,M. (1984) Anal. Biochem. 140, 403.

Beers,R.F. and Sizer,I.W. (1952) J. Biol. Chem. 195, 599.

Beisenherz,G., Boltze,H.J., Bucher,T., Czok,R., Garbade,K.H., Meyer-Arendt,E. and Pfleiderer,G. (1953) Z. Naturforsch. 8b, 555.

Berg,D.K., Kelly,R.B., Sargent,P.B., Williamson,P. and Hall,Z.W. (1972) Proc. Natl. Acad.Sci. USA 69, 147.

Berrie,C.P., Birdsall,N.J.M., Haga,K., Haga,T. and Hulme,E.C. (1984) Br. J. Pharmac. 82, 839.

Berry,R.J. and Marshall,C.H. (1969) Phys. Med Biol. 14, 585.

Betz,H. (1981) Eur. J. Biochem. 117, 131.

Betz,H. (1983) J.Neurosci. 3, 1333.

Betz,H. and Pfeiffer,F. (1984) J. Neurosci. 4, 2095.

Betz,H. Graham,D. and Rehm,H (1982) J. Biol. Chem. 257, 11390.

Betz,H., Schmitt,B., Becker,C.M., Grenningloh,G., Rienitz,A. and

Knaus,P. (1985) Biochem. Soc. Bull. 7, (4) 7.

Bichsel,H. (1966) in Radiation Dosimetry, Acad. Press Inc., NY.

Bidlack,J.M., Abood,L.G., Osei-Gyimah,P. and Archer,S. (1981) Proc. Natl. Acad. Sci. USA 78, 636.

Blanchard,S.G., Quast,U., Reed,K., Lee,T., Schimerlik,M.I., Vandlen,R., Claudio,T., Strader,C.D., Moore,H.P.M. and Raftery,M.A. (1979) Biochemistry 18, 1875.

Bland,B.M., Kostpopoulos,G.K. and Phillis,J.W. (1974) Can. J. Physiol. Pharmacol. 52, 966.

Block,G.A. and Billiar,R.B. (1979) Brain Res. 175, 381.

Bon,S., Vigny,M. and Massoulie,J. (1979) Proc. Natl. Acad. Sci. USA 76, 2546.

Bosmann,H.B. (1972) J. Biol. Chem. 247, 130.

Boulter,J., Evans,K., Goldman,D., Martin,G., Treco,D., Heinemann,S. and Patrick,J. (1986) 319, 368.

Boulter,J., (1985) J. Neurosci. 5, 2545.

Boyd,N.D. and Cohen,J.B. (1980) Biochemistry 19, 5344.

Bowman,B.J., Berenski,C.J. and Jung,C.Y. (1985) J. Biol. Chem. 260, 8726.

Bradley,P.B. and Dray,A. (1976) Br. J. Pharmacol. 57, 599.

Brecha,N., Francis,A. and Schechter,N. (1979) Brain Res. 167, 273.

Brockes,J.P. and Hall,Z.W. (1975) Biochemistry 14, 2092.

Brown,D.A. and Fumagalli,L. (1977) Brain Res. 129, 165.

Buttery,P.J. and Rowsell,E.V. (1971) Anal. Biochem. 39, 297.

Carbonetto,S.T., Fambrough,D.M. and Muller,K.J. (1978) 75, 1016.

Chamberlain,B.K., Berenski,C.J., Jung,C.Y. and Fleischer,S. J. Biol. Chem. 258, 11997.

Chang,C.C. and Lee,C.Y. (1963) Arch. Int. Pharmacodyn. Ther. 144, 241.

Chang,C.C. Yant,C.C. Hamaguchi,K. Nakai,K. and Hayashi,K. (1971) Biochim. Biophys. Acta 236, 164.

Chang,H.W. and Bock,E. (1977) Biochemistry 16, 4513.

Chang,L.R. (1981) PhD thesis, Univ. of London.

Chang,L.R. and Barnard,E.A. (1982) J. Neurochem. 39, 1507.

Chang,L.R., Barnard,E.A., Lo,M.M.S. and Dolly,J.O. (1981) FEBS Letts. 126, 309.

Changeux,J.P. (1981) Harvey Lect. 75, 85.

Changeux,J.P., Bon,F., Cartaud,J., Devillers-Thiery,A., Giraudat,J., Heidmann,T., Holton,B., Nghiem,H.O., Popot,J.L., Van Rapenbusch,R. and Tzartos,S. (1984) Cold Spring Harb. Symp. Quant. Biol. 48, 35.

Changeux,J.P., Kasai,M. and Lee,C.Y. (1970) Proc. Natl. Acad. Sci. USA 67, 1241.

Chiappinelli,V.A. (1983) Brain Res. 277, 9.

Chiappinelli,V.A. (1984) Trends in Pharmacol. Sci. (Oct.) 425.

Chiappinelli,V.A. and Dryer,S. (1984) Neurosci. Letts. 50, 239.

Chiappinelli,V.A. and Lee,J.C. (1985) J. Biol. Chem. 260, 6182.

Chiappinelli,V.A., Cohen,J.B. and Zigmond,R.E. (1981) Brain Res. 211, 107.

Chirgwin,J.M., Przybyla,A.E., MacDonald,R.J. and Rutter,W.J. (1979) Biochemistry 18, 5294.

Clarke,S. (1975) J. Biol. Chem. 250, 5459.

Clarke,P.B.S., Schwartz,R.D., Paul,S.M., Pert,C.M. and Pert,A. (1985) Nature 243, 41.

Claudio,T., Ballivet,M., Patrick,J. and Heinemann,S. (1983) Proc. Natl. Acad. Sci. USA 80, 1111.

Collip,P.J., Carsten,A., Chen,S.Y., Thomas,J. and Maddiah,V.T. (1974) Biochem. Med. 10, 312.

Colquohoun,D. and Rang,H.P. (1976) Mol. Pharm. 12, 519.

Conti-Tronconi,B.M., Dunn,S.M.J., Barnard,E.A., Dolly,J.O., Lai,F.A., Ray,N. and Raftery,M.A. (1985) Proc. Natl. Acad. Sci. USA 82, 5208.

Conti-Tronconi,B.M., Gotti,C.M., Hunkapiller,M.W., and Raftery,M.A. (1982b) Science 218, 1227.

Conti-Tronconi,B.M., Hunkapiller,M.W., Lindstrom,J.M. and Raftery,M.A. (1982a) Proc. Natl. Acad. Sci. USA 79, 6489.

Conti-Tronconi,B.M., Hunkapiller,M.W., Lindstrom,J.M. and Raftery,M.A. (1984) J. Receptor Res. 4, 801.

Conti-Tronconi,B.M., Hunkapiller,M.W. and Raftery,M.A. (1984a) Proc.Natl. Acad.Sci. USA 81, 2631.

Conti-Tronconi,B.M. and Raftery,M.A. (1982) Ann. Rev. Biochem. 51, 491.

Corradino,R.A. (1983) Nature 243, 41.

Costa,E. and Guidotti,A. (1979) Ann. Rev. Pharmacol. Toxicol. 19, 531.

Craig,W.S. and Kyte,J. (1980) J. Biol.Chem. 255, 6262.

Crause,P., Boer,R. and Fahrenholz,F. (1984) FEBS Letts. 175, 383.

Craven,G.R., Steers,E., and Anfinsen,C.B. (1965) J. Biol. Chem. 240, 2468.

Crowther,J.A. (1924) Proc. Roy. Soc. Lond. B96, 207.

Cuppoletti,J., Jung,C.Y. and Green,F.A. (1981) J. Biol. Chem. 256, 1305.

Curtis,D.R. and Crawford,J.M. (1969) Ann. Rev. Pharmacol. 9, 209.

Curtis,D.R. and Ryall,R.W. (1966) Expl. Brain Res. 2, 66.

Dale,H.H., Feldberg,W. and Vogt,M. (1936) J. Physiol. 86, 353.

Damle,V and Karlin,A. (1978) Biochemistry 17, 2039.

Darnell,D.W. and Klotz,I.M. (1975) Biochim. Biophys. Acta 166, 651.

Dartinger,H and Jung,H. (1970) in Molecular Radiation Biology NY Springer-Verlag.

Davis,D.R., Padlan,E.A and Segal,D.M. (1975) Ann. Rev. Biochem. 44, 639.

Davis,K.A. and Hatefi,Y. (1971) Biochemistry 10, 2509.

Day,M.J. and Stein G. (1951) Nature 168, 644.

DeBlas,A. and Mahler,H.R. (1978) J. Neurochem. 30, 563.

Dennis,M.J., Harris,A.J. and Kuffler,S.W. (1971) Proc. Roy. Soc. Lond. B177, 509.

Devillers-Thiery,A., Giraudat,J., Bentaboulet,M. and Changeux,J.P. (1983) Proc. Natl. Acad. Sci. USA 80, 2067.

Dionne,V.E., Steinbach,J.H. and Stevens,C.F. (1978) J. Physiol. 281, 421.

Doble,A. and Iversen,L.L. (1982) Nature 295, 522.

Dolly,J.O. and Barnard,E.A. (1977) Biochemistry 16, 5053.

Dolly,J.O. Nockles,E.A.V., Lo,M.M.S. and Barnard,E.A. (1981) Biochem. J. 193, 919.

Dreyer,F., Peper,K. and Sterz,R. (1978) J.Physiol.281, 421.

Drum,D.E., Harrison,J.H., Li,T.L., Bethune,J.L. and Vallee,B.L. (1967) Proc. Natl. Acad. Sci. USA 57, 1434.

Dudai,Y. and Segal,M. (1978) Brain Res. 154, 167.

Dufton,M.J. and Hider,R.C. (1983) Crit. Rev. Biochem. 14, 113.

Duggan,A.W., Hall,J.G. and Lee,C.Y. (1976) Brain Res. 107, 166.

Dunn,S.M.J., Conti-Tronconi,B.M. and Raftery,M.A. (1983) Biochemistry 22, 2512.

Dutreix,J.M. and Dutreix,A. (1968) Symp. on high energy radiation therapy dosimetry N.Y. Acad.Sci, NY.

Dwyer,T.M., Adams,D. and Hille,B. (1980) J. Gen. Physiol. 75, 459.

Eccles,J.C. (1964) in The physiology of synapses Springer-Verlag, Berlin.

Edelman,G.M. (1967) Nobel Symp. 3, 89.

Edelman,G.M., Cunningham,B.A., Gall,W.E., Gottlieb,P.D., Ruttishauser,U. and Waxdal,M.J. (1969) Proc. Natl. Acad. Sci. USA 63, 78.

Edwards,J.C., Chapman,D., Cramp,W.A. and Yatvin,M.V. (1984) Progr. Biopyhs. Molec. Biol. 43, 71.

Einarson,B., Gullick,W., Conti-tronconi,B.M. and Lindstrom,J. (1982) Biochemistry 21, 5295.

Eisenstadt,M.L. and Schwartz,J.H. (1975) J. Gen. Physiol. 65, 293.

Ellory,J.C. (1979) TIBS (May) N99.

Ellory,J.C., Green,J.R., Jarvis,S.M. and Young,J.D. (1979) J. Physiol. 295, 10.

Eterovic,V.A. and Bennett,E.L. (1974) Biochim. Biophys. Acta 362, 346.

Fambrough,D.M. (1979) Physiol. Rev. 59, 165.

Ferry,D.R., Goll,A. and Glossmann,H. (1983) N.S. Arch. Pharmacol. 323, 292.

Fewtrell,C., Kempner,E., Poy,G. and Metzger,H. (1981) Biochemistry 20, 6589.

Field,J. (1960) Handbook of physiology, Am. Physiol. Soc., Williams and Wilkins, Baltimore,MD.

Finer-Moore,J. and Stroud,R.M. (1984) Proc. Natl. Acad. Sci. USA 81, 155.

Fish,W.W. (1975) Meths. Memb. Biol. 4, 189.

Fluke,D.J. (1966) Radiat.Res. 28, 677.

Fluke,D.J. (1972) Radiat.Res. 51, 56.

Folk,J.E. and Schirmer,E.W. (1963) J. Biol. Chem. 238, 3884.

Fowler,A.V. and Zabin,I. (1977) Proc. Natl. Acad. Sci. USA 74, 1507.

Fowler,J.F. and Attix,F.M. (1966) in Radiation Dosimetry Volume II, Acad. Press Inc., NY.

Fraser,C.M. and Venter,J.C. (1982) Biochem. Biophys. Res. Commun. 109, 21.

Freeman,J.A. (1977) Nature 269, 218.

Freeman,J.A. and Lutin,W.A. (1975) Trans. Am. Soc. Neurochem. 6, 143.

Freeman,J.A. and Nicholson,C. (1975) J. Neurophysiol. 38, 369.

Freeman,J.A., Schmidt,J.T. and Oswald,R.E. (1980) Neurosci. 5, 929.

Fricke,H. (1934) Cold Spring Harb. Symp. Quant. Biol. 2, 241.

Froehner,S.C. and Rafto,S. (1979) Biochemistry 18, 301.

Fumagalli,L. and DeRenzis,G. (1984) Neurochem. Int. 6, 355.

Fumagalli,L., DeRenzis,G. and Miani,N. (1976) J. Neurochem. 27, 47.

Furshpan,E.J. and Potter,D.D. (1959) J. Physiol. 145, 289.

Gavish,M. and Snyder,S.H. (1981) Proc. Natl. Acad. Sci. USA 78, 1939.

Gershoni,J.M., Hawrot,E. and Lentz,T.L. (1983) Proc. Natl. Acad. Sci. USA 80, 4973.

Goll,A., Ferry,D.R. and Glossmann,H. (1983) FEBS Letts. 157, 63.

Gotti,C., Conti-Tronconi,B.M. and Raftery,MA. (1982) Biochemistry 21, 3148.

Gotti,C., Spagnoli,D., Omini,C. and Clementi,F. (1985) Neurosci. Letts. 57, 227.

Gozlan,H., Emerit,M.B., Hall,M.D., Nielsen,M. and Hamon,M. (1985) Biochem. Pharm.

Graham,D., Pfeiffer,F., Simler,R. and Betz,H. (1985) Biochemistry 24, 990.

Grant,G.A. and Chiappinelli,V.A. (1985) Biochemistry 24, 1532.

Gray,E.G. and Whittaker,V.P. (1962) Cell 16, 661.

Greene,L.A. (1976) Brain Res. 111, 135.

Gruol,D.J., Kempner,E.S. and Bourgeois,S. (1984) J. Biol. Chem. 259, 4833.

Gurdon,J.B., Lane,C.D., Woodland,H.R. and Marbaix,G. (1971) Nature 233, 177.

Guy,R. (1984) Biophys. J. 45, 249.

Haigler,H.T., End,D. and Kempner,E.S. (1985) J. Biol. Chem. 260, 2178.

Hall,Z.W. (1973) J. Neurobiol. 4, 343.

Hanley,M.R., Bennett,E.L. and Lukas,R.J. (1978) Neurosci. Abstr. 4, 514.

Harmon,J.T. and Jamieson,G.A. (1985) Biochemistry 24, 58.

Harmon,J.T., Kahn,C.R., Kempner,E.S. and Schlegel,W. (1980) J. Biol. Chem. 255, 3412.

Harlow,E., Crawford,L.V., Pim,D.C. and Williamson,N.M. (1981) J. Virol. 39, 861.

Harry,J. (1962) Br. J. Pharm. Chemother. 19, 42.

Hatefi,Y. and Stiggal,D.L. (1978) Meths. Enz. 53, 21.

Heidmann,T. and Changeux,J.P. (1978) Ann. Rev. Biochem. 47, 317.

Heidmann,T., Oswald,R.E. and Changeux,J.P. (1983) Biochemistry 22, 3112.

Henley,E.J. (1954) Nucleonics 12, 62.

Herrick,R.M., Hunkapiller,M.W., Hood,L.E. and Dreyer,W.J. (1981) J. Biol. Chem. 256, 7990.

Hess,G.P., Pasquale,E.B., Walker,J.N. and McNamee,M. (1982) Proc. Natl. Acad.Sci. USA 79, 963.

Heuser,J.E., Reese,T.S. and Landis,D.M.D. (1974) J. Neurocytol. 3, 109.

Heuser,J.E. and Salpeter,S.R. (1979) J. Cell Biol. 82, 150.

Hodgkin,A.L. (1951) Biol. Rev. 26, 339.

Honore,T., Nielsen,M. and Braestrup,C. (1984) Life Sci. 35, 2257.

Houslay,M.D., Ellory,J.C., Smith,G.A., Hesketh,T.R., Stein,J.M., Warren,G.B. and Metcalfe,J.C. (1977) Biochim. Biophs. Acta 467, 208.

Huang,L.M., Catterall,W.A. and Ehrenstein,G. (1978) J. Gen. Physiol. 71, 397.

Hucho,F., Bandini,G. and Suarez-Isla,B.A. (1978) Eur. J. Biochem. 83, 335.

Hucho,F. and Janda,M. (1974) Biochem. Biophys. Res. Commun. 57, 1080.

Hughes,S.M., Harper,G. and Brand,M.D. (1984) Biochem Biophys. Res. Commun. 122, 56.

Hunkapiller,M.W. and Hood,L.E. (1983) Meths. Enz. 91, 486.

Hunt,S. and Schmidt,J. (1978) Brain Res. 157, 213.

Hunt,S. and Schmidt,J. (1979) Neurosci. 4, 585.

Hussey,R.G. and Thompson,W.R. (1923) J. Gen. Physiol. 5, 647.

Hymel,L., Maurer,A., Berenski,C., Jung,C.Y. and Fleischer,S. (1984) J. Biol. Chem. 259, 4890.

Illingworth,J.A. and Tipton K.F. (1970) 118, 253.

Jacob,M.H. and Berg,D.K. (1983) J. Neurosci. 3, 260.

Jacob,M.H., Berg,D.K. and Lindstrom,J. (1984) Proc. Natl. Acad.Sci. USA 81, 3223.

Jaenicke,R. and Knof,S. (1968) Eur. J. Biochem. 4, 157.

Jaenicke,R., Schmid,D. and Knof,S. (1968) Biochemistry 7, 919.

Jarvis,S.M., Young,J.D. and Ellory,J.C. (1980) Biochem. J. 190, 373.

Johnson,C.D. and Russell,R.L. (1975) Anal. Biochem. 64, 229.

Jung,C.Y. (1984) in Mol. and Chem. charactn. of memb. receptors,

Alan Liss Inc., NY.

Jung,C.Y., Hsu,T.L., Hah,J.S., Cha,C. and Haas,M.N. (1980) J. Biol. Chem. 255, 361.

Kagawa,Y.(1969) J. Biochem. (Tokyo) 65, 925.

Kaldany,R.R. and Karlin,A. (1983) J. Biol. Chem. 258, 6232.

Kao,P.N., Dwork,A.J., Kaldany,R.R.J., Silver,M.L., Wideman,J., Stein,S. and Karlin,A.(1984) J. Biol. Chem. 259, 11662.

Karlin,A. (1969) J. Gen. Physiol. 54, 245s.

Karlin,A. (1980) in The cell surface and neuronal function, Elsevier,NY.

Karlin,A., Holtzman,E. Yodh,N. Lodel,P. Wall,J. and Hainfield,J. (1983) J. Biol. Chem. 258, 6678.

Karlin,A., McNamee,M.G., Weill,C.L. and Valderrama, . (1976) Meths. Mol. Biol. 9, 1.

Karlsson,E., Arnberg,H. and Eaker,D. (1971) Eur. J. Biochem. 21, 1.

Karlsson,E., Heilbronn,E. and Widlund,L. (1972) FEBS Letts. 28, 107.

Karzmark,C.J. and Pering,N.C. (1973) Phys. Med. Biol. 18, 321.

Karzmark,C.J., White,J. and Fowler,J.F. (1964) Phys. Med. Biol. 9, 273.

Katz,B. and Thesleff,S. (1957) J. Physiol. 138, 63.

Katz,B. and Miledi,R. (1965) Proc. Roy. Soc. Lond. B161, 483.

Kehoe,J. (1972) J. Physiol. 225, 85.

Kemp,G., Furner,R.L. and Morley,B.J. (1980) Soc. Neurosci. Abstr. 6, 210.

Kempner,E.S. and Haigler,H.T. (1982) J. Biol. Chem. 257, 13297.

Kempner,E.S. and Miller,J.H (1983) Science 222, 586.

Kempner,E.S., Miller,J.H., Schlegel,W. and Hearon,J.Z. (1980) J. Biol. Chem. 255, 6826.

Kempner,E.S. and Schlegel,W. (1979) Anal. Biochem. 92, 2.

Kepner,G.R. and Macey,R.I. (1968) Biochim. Biophys. Acta 163, 188.

Kistler,J., Stroud,R.M., Klymkowsky,M.W., Lancalette,R.A. and Fairclough,R.H. (1982) Biophys. J. 37, 371.

Klee,W.A., Simonds,WF. Sweat,F.W., Burke,J.R. Jacobson,A.E. and Rice,K.C. (1982) FEBS Letts. 150, 125.

Klymkowsky,M.W. and Stroud,R.M. (1979) J. Mol. Biol. 128, 319.

Klymkowsky,M.W., Heuser,J.E. and Stroud,R.M. (1980) J. Cell Biol. 85, 823.

Koenig,J. and Vigny,M. (1978) Nature 271, 75.

Koike,H. Kandel,E.R. and Schwartz,J.H. (1974) J. Neurophysiol. 37, 815.

Kosk-Kosicka,D., Kurzmack,M. and Inesi,G. (1983) Biochemistry 22, 2559.

Kouvelas,E.D., Dichter,M.A. and Greene,L.A. (1978) Brain Res. 154, 183.

Kouvelas,E.D. and Greene,L.A. (1976) Brain Res. 113, 111.

Krenz,W., Tashiro,T., Wachtler,K., Whittaker,V. and Witzemann,V. (1980) Neurosci. 5, 617.

Krnjevic,K. (1974) Physiol. Rev. 54, 418.

Kuffler,S.W. and Yoshikami (1975a) J.Physiol. 244, 703.

Kuffler,S.W. and Yoshikami,(1975b) J. Physiol 251, 465.

Kuno,T., Kobo,N. and Tanaka,C. (1985) Biochem. Biophys. Res. Commun. 129, 639.

Laemmli,U.K. (1970) Nature 227, 680.

Lai,F.A., Newman,E.L., Peers,E.M. and Barnard,E.A. (1984) Eur. J. Pharm. 103, 349.

Laurent,T.C. and Killander,J. (1964) J. Chromatogr. 14, 317.

Lea,D. (1946) in Actions of radiations on living cells,

Cambridge Univ. Press, London.

Lea,D.,Smith,K.M., Holmes,B., Markham,R. (1944) Parasitol. 36, 110.

Lee,C.Y., Chang,S.L., Kau,S.T. and Luh,S.H. (1972) J. Chromatogr 72, 71.

Lee,C.Y. (1970) Clin. Toxicol. 3, 457.

Leerbeck,E. and Sondergaard,H. (1980) Br. J. Nutr. 44, 7.

Leibowitz,M.D. and Dionne,V.E. (1984) Biophys. J. 45, 153.

LeMaire,M., Jorgensen,K.E., Roigaard-Petersen,H. and Moller,J.V. (1976) Biochemistry 15, 5805.

Lentz,T.L. and Chester,J. (1977) J. Cell Biol. 75, 258.

Leprince,P (1983) Biochemistry 22, 5551.

Levinson,S.R. and Ellory,J.C. (1973) Nature New Biol. 245, 122.

" " " (1974) Biochem. J. 137, 123.

Lilly,L., Fraser,C.M., Jung,C.Y., Seeman,P. and Venter,J.C. (1983) Mol. Pharm. 24, 10.

Lindstrom,J., Anholt,R., Einarson,B., Engel,A., Osame,M. and Montal,M. (1980a) J. Biol. Chem. 255, 8340.

Lindstrom,J., Einarson,B. and Merlie,J. (1978) Proc. Natl. Acad. Sci. USA 75, 769.

Lindstrom,J., Gullick,W.J., Conti-Tronconi,B.M. and Ellisman (1980b) Biochemistry 19, 4791.

Lo M.M.S. (1981) PhD thesis, Univ. of London.

Lo,M.M.S., Barnard,E.A. and Dolly,J.O. (1982) Biochemistry 21, 2210.

Lowry,D.M., Rosenbrough,N.J., Farr,A.L. and Randall,R.J. (1951) J. Biol. Chem. 193, 265.

Lowy,J., McGregor,J., Rosenstone,J. and Schmidt,J. (1976) Biochemistry 15, 1522.

Lukas,R.J. (1984) Biochemistry 23, 1152.

Lukas,R.J. and Bennett,E.L. (1980a) J. Biol. Chem 225, 5573.

" " (1980b) Mol. Pharm. 17, 149.

Lukas,R.J., Morimoto,M. and Bennett,E.L. (1979) Biochemistry 18, 2384.

Lukasiewicz,R.J. and Bennett,E.L. (1978) Biochim. Biophys. Acta 544, 294.

Lukasiewicz,R.J., Hanley,M.R. and Bennett,E.L. (1978) Biochemistry 17, 2308.

Lummis,S.C.R., Sattelle,D.B. and Ellory,J.C. (1984) Neurosci. Letts. 44, 7.

Lyles,J.M., Silman,I. and Barnard,E.A. (1979) J. Neurochem. 33, 727.

MacLennan,D.H. and Holland,P.C. (1975) Ann.Rev. Biophys. Bioeng. 4, 377.

MacLennan,D.H., Brandl,C.J., Korczak,B. and Green,N.M. (1985) Nature 316, 696.

Maelicke., Fulpius,B.W., KLETT,R.P. and Reisch,E. (1977) J. Biol. Chem. 257, 4811.

March,S.C., Parikh,I. and Cuatrcasas,P. (1974) Anal. Biochem. 60, 149.

Markwell,M.A.K., Haas,S.M, Bieber,L.L. and Tolbert,N.E. (1978) Anal.Biochem. 87, 206.

Marshall,L.M. (1981) Proc. Natl. Acad.Sci. USA 78, 1948.

Martin,B.M., Chubber,B.A. and Maelicke,A. (1983) J. Biol. Chem. 258, 8174.

Martin,B.R., Stein,J.M., Kennedy,E.C., Doberska,C.A. and Metcalfe,J.C. (1979) Biochem. J. 184, 253.

Martin,D.W. and Tanford,C. (1984) FEBS Letts. 177, 146.

Martin,D.W., Tanford,C. and Reynolds,J.A. (1984) Proc. Natl. Acad. Sci. USA 81, 6623.

Martin,I.L. and Candy,J.M. (1978) Neuropharm. 17, 993.

Martin,R.G. and Ames,B.N. (1961) J. Biol. Chem. 236, 1372.

Masiulanis,D. (1982) Project report, Biochemistry Dept., Imperial College. London.

Massoulie,J. and Bon,S. (1982) Ann. Rev. Neurosci. 5, 57.

McLaughlin,J.S. (1966) in Radiation dosimetry Vol. III, Acad. Press Inc., NY.

McLawhon,R.W., Cermak,D., Ellory,J.C. and Dawson,G. (1983) J. Neurochem. 41, 1286.

McQuarrie,C., Salvaterra,P.M., DeBlas,A., Routes,J. and Mahler,H.R. (1976) J. Biol. Chem. 251, 6335.

Mehraban,F. (1983) PhD thesis, Univ. of London.

Mehraban,F., Kemshead,J.T. and Dolly,J.O. (1984) Eur. J. Biochem. 138, 53.

Meissner,G., Conner,G.E. and Fleischer,S. (1973) Biochim. Biophys. Acta 298, 246.

Mendez,B., Valenzuela,P., Martal,J.A. and Baxter,J.D (1980) Science 209, 695.

Merlie,J.P., and Sebbane,R, (1981) J. Biol. Chem. 256, 3605.

Meunier,J.C., Olsen,R.W. and Changeux,J.P. (1972) FEBS Letts. 24, 63.

Meunier,J.C., Olsen,R.W., Menez,A., Fromageot,P. and Changeux,J.P. (1972b) Biochemistry 11, 1200.

Meunier,J.C., Sugiyama,H., Cartaud,J., Sealock,R. and Changeux,J.P. (1973) Brain Res. 62, 307.

Michaelson,., Vandlen,R., Bode,J., Moody,T., Schmidt,J. and Raftery,M.A. (1974) Arch. Biochem. Biophys. 165, 796.

Miledi,R. and Szczepaniak,A.C. (1975) Proc. Roy. Soc. Lond. B190, 267.

Miledi,R., Parker,I. and Sumikawa,K. (1982) EMBO J. 1, 1307.

Mills,A. and Wonacott,S. (1984) Neurochem. Int. 6, 249.

Mishina,M., Kurosaki,T., Tobimatsu,Y., Morimoto,Y., Noda,M., Yamamoto,T., Terao,M., Lindstrom,J., Takahashi,T., Kono,M. and Numa,S. (1984) Nature 307, 604.

Mohler,H., Battersby,M.K. and Richards,J.G. (1980) Proc. Natl. Acad. Sci. USA 77, 1666.

Moller (1982) Mol. Cell. Biochem. 42, 83.

Momoi,M.Y. and Lennon,V.A. (1982) J. Biol. Chem. 257, 12572.

Moore,W.M. and Brady,R.N. (1976) Biochim Biophys. Acta 444, 252

Morley,B.J. and Kemp,G.E. (1981) Brain Res. Rev. 3, 81.

Morley,B.J., Lorden,J.F., Brown,G.B., Kemp,G.E. and Bradley,R.J. (1977) Brain Res. 134, 161.

Murphey,W.H., Kitto,G.B., Everse,J. and Kaplan,N.O. (1967) Biochemistry 6, 603.

Napolitano,C.A., Cooke,P., Segalman,K. and Herbette,L. (1983) Biophys. J. 42, 119.

Nastuk,W.L. (1953) Fed.Proc. 12, 102.

Nathanson,N.M. and Hall,Z.W. (1979) Biochemistry 18, 3392.

Neubig,R.R. and Cohen,J.B. (1979) Biochemistry 18, 5465.

Neubig,R.R, Krodel,E.K., Boyd,N.D. and Cohen,J.B. (1979) Proc. Natl.Acad.Sci.USA 76, 690.

Newman,E.L. and Barnard,E.A. (1985) Biochemistry

Nielsen,M and Braestrup,C. (1983) Eur. J. Pharm. 96, 321.

Nielsen,M., Honore,T. and Braestrup,C. (1983) Biochem. Pharm. 32, 177.

Nielsen,M., Klimek,V. and Hyttel,J. (1984b) Life Sci. 35. 325.

Nielsen,T.B., Lad,P.M., Preston,M.S., Kempner,E., Schlegel,W. and Rodbell,M. (1981) Proc. Natl. Acad. Sci. USA 78, 722.

Nielsen,T.B., Totsuka,Y., Kempner,E.S. and Field,J.B. (1984a) Biochemistry 23, 6009.

Noda,M., Takahashi,H., Tanabe,T., Toyosato,M., Furutani,Y., Hirose,t., Asai,M., Inayama,S., Miyata,. and Numa,S. (1982) Nature 299, 793.

Noda,M., Takahashi,H., Tanabe,T., Toyosato,M., Kikyotami,S., Furutani,Y., Hirose,T., Takashima,H., Inayama,S., Miyata,T. and Numa,S. (1983b) Nature 302, 528.

Noda,M., Takahashi,H., Tanabe,H., Toyosato,M., Kikyotami,S., Hirose,T., Asai,M., Takashima,H., Inayama,S., Miyata,T.and Numa,S. (1983a) 301, 251.

Noda,M., Furutani,Y., Takahashi,H., Toyosato,M., Tanabe,T., Shmizu,S., Kikyotami,S., Kayano,T., Hirose,T., Inayama,S. and Numa,S. (1983c) Nature 305, 818.

Norman,A. and Ginoza,W. (1958) Radiat. Res. 9, 77.

Norman,R.I. (1981) PhD thesis, Univ. of London.

Norman,R.I., Mehraban,F., Barnard,E.A. and Dolly,J.O. (1982) Proc. Natl. Acad. Sci. USA 79, 1321.

Northrop,J.H. (1934) J. Gen. Physiol. 17, 359.

Numa,S., Noda,M., Takahashi,H., Tanabe,T., Toyosato,M., Furutani,Y. and Kikyotani,S. (1983) Cold Spring Harb. Symp. Quant. Biol. 48, 57.

Oakley,B.R., Kirsch,D.R. and Morris,N.R. (1980) Anal. Biochem. 105, 361.

Obishi,N., Ohkawa,H., Miike,A., Tatano,T. and Yagi.K. (1984) Biochem. Int. 10, 205.

Olive,C. and Levy,H.R. (1971) J. Biol. Chem. 246, 2043.

" " (1975) Meths. Enz. 41, 196.

Olsen,R. and Leeb-Lundberg,F. (1981) in GABA and benzodiazepine receptors, Raven Press,NY.

Olsen,R.W. (1982) Ann. Rev. Pharm. Toxicol. 22, 7166.

Orcutt,B.C. and Dayhoff,M.O. (1975) Matrix Topology Program

MATTOP, NBR Report No. 09810-751101, Natl. Biomed. Res. Found. Washington, DC.

Ostrovskii,D.N., Tsfasman,I.M. and Gel-man,N.S. (1969) Biokhimya 34, 993.

Oswald,R.E. and Changeux,J.P. (1981) Biochemistry 20, 7166.

Oswald,R.E. and Freeman,J.A. (1979) J. Biol. Chem. 254, 3419.

" " (1981a) Neurosci. 6, 1.

" " (1981b) Brain Res. 218, 406.

Oswald,R.E., Schmidt,J.T., Norden,J.J. and Freeman,J.A. (1980) Brain Res. 187, 113.

Ott,S., Costa,T., Hietel,B., Schlegel,W. and Wuster,M. (1983) N.S. Arch. Pharmacol. 324, 160.

Pardee,J.D., Bamburg,J.R. (1979) Biochemistry 11, 2245.

Patrick,J. and Stallcup,W.R. (1977a) J. Biol. Chem. 252, 8629.

Patrick,J. and Stallcup,W.B. (1977b) Proc. Natl. Acad. Sci. USA 74, 4689.

Patrick,J., Stallcup,W.B., Zavanelli,M. and Ravdin,P. (1980) J. Biol. Chem. 255, 526.

Paul,S.M., Kempner,E.S. and Skolnick,P. (1981) Eur. J. Pharm. 76, 465.

Pauly,M. and Rajewsky,B. (1956) in Progress in radiobiology, Oliver and Boyd, Edinburgh.

Peers,E.M. (1984) PhD thesis, Univ. of London.

Peters, W.H.M., DePont,J.J.H.H.M., Koppers,A. and Bonting,S.L. (1981) Biochim.Biophys. Acta 641, 55.

Phillis,J.W. (1974) in The physiology of synapses, Pergamon Press.

Pitts,O.M., Priest,D.G. and Fish,W.W. (1974) Biochemistry 13, 888.

Pollard,E.C. (1959) Rev.Mod.Phys. 31, 273.

Pollard,E., Powell,W.F. and Reaume,S.H. (1952) Proc.Natl. Acad. Sci. USA 38, 173.

Polz-Tejera,G., Schmidt,J. and Karten H.J. (1975) Nature 258, 349.

Popot,J.L. and Changeux,J.P. (1984) Physiol. Rev. 64, 1162.

Porter,C.W. and Barnard,E.A. (1975) J. Memb. Biol. 20, 31.

Porter,R.R. (1959) Biochem. J. 73, 119.

Raftery,M.A., Dunn,S.M.J., Conti-tronconi,B.M., Middlemas,D.S. and Crawford,R.D. (1984) Cold Spring Harb. Symp. Quant. Biol. 48, 21.

Raftery,M.A., Hunkapiller,M.W., Strader,C.D. and Hood,L.E. (1980) Science 208, 1454.

Rang,H.P. and Ritter,J.M. (1970) Mol.Pharm. 6, 357.

Ravdin,P.M. and Berg,D. (1979) Proc. Natl. Acad. Sci USA 76, 2072.

Rehm,H. and Betz,H. (1984) J. Biol. Chem. 259, 6865.

Reynolds,J.A. and Karlin A. (1978) Biochemistry 17, 2035.

Richards,D.E., Ellory,J.C. and Glynn,I.M. (1981) Biochim. Biophys. Acta 648, 284.

Rizzolo,L.J., LeMaire,M., Reynolds,J.A. and Tanford,C. (1976) Biochemistry 15, 3433.

Rodbell,M. (1980) Nature 284, 17.

Rodbell,M., Lin,M.C., Salomon,Y., Londos,C., Harwood,J.P., Martin,B.R., Rendell,M. and Berman,M. (1975) Adv. Cyclic Nucl. Res. 5, 3.

Romano,C. and Goldstein,A. (1980) Science 210, 647.

Rosenberry,T.L. and Richardson,J.M. (1977) Biochemistry 16, 3550

Rudloff,E., Jimenez,F. and Bartels,J. (1980) in Receptors for neurotransmitters, hormones and pheromones in insects, Elsevier, Amsterdam.

Saccomani,G., Sachs,G., Cuppoletti,J. and Jung,C.Y. (1981) J. Biol. Chem. 256, 7727.

Sakmann,B. (1978) Fed. Am. Soc. Exp. Biol. 37, 2654.

Salvaterra,P.M. and Foders, . (1979) J. Neurochem. 32, 1509.

Salvaterra,P.M. and Mahler,H.R. (1976) J. Biol. Chem. 251, 6327.

Salvaterra,P.M., Gurd,J.M., Mahler,H.R. (1977) J. Neurochem. 29, 345.

Salvaterra,P.M., Mahler,H.R. and Moore,W.J. (1975) J. Biol. Chem. 250, 6469.

Scarpa,A. and Inesi,G. (1972) FEBS Letts. 22, 275.

Schechter,N., Francis,A., Deutsch,P.G. and Gazzaniga,M.S. (1979) Brain Res. 116, 57.

Schechter,N., Francis,A., Pezzemanti,L. and Schmidt,J. (1978) Toxicon. 16, 245.

Schlegel,W. and Kempner,E.S. (1984) in Investigation of memb. located receptors, Plenum Press.

Schlegel,W., Kempner,E.S. and Rodbell,M. (1979) J. Biol. Chem. 254, 5168.

Schleifer,L.S. and Eldefrawi,M.E. (1974) Neuropharmacol. 13, 53.

Schmidt,J. (1977) Mol. Pharm. 13, 283.

Schmidt,J. and Raftery,M.A. (1972) Biochem. Bophys. Res. Commun. 49, 572.

Schmidt,J. and Raftery,M.A. (1973) Anal.Biochem. 52, 349.

Schmidt,J.T. and Freeman,J.A. (1979) Invest. Opth. Suppl. 280.

" " (1980) Brain Res. 189, 129.

Schmidt-Glenewinkel,T., Venkatesh,T.R. and Hall,L.M. (1981) Soc. Neurosci. Abstr. 7, 703.

Schmidt-Nielsen,B.K., Gepner,J.I., Teng,N.N.H. and Hall,L.M. (1978) J. Neurochem. 29, 1013.

Schwartz,M., Axelrod,D., Feldman,E.L. and Agranoff,B.M. (1980)

Brain Res. 194, 171.

Schwartz,R.D., Thomas,J.W., Kempner,E.S., Skolnick,P. and Paul,S.M. (1985) J. Neurochem. 45, 108.

Scubon-Mulieri,B. and Parsons,R.C. (1977) J. Gen. Physiol. 69, 431.

Segal,M., Dudai,Y. and Amsterdam,A. (1978) Brain Res. 148, 105.

Serlin,I. and Fluke,D.J. (1956) J.Biol.Chem. 223, 727.

Setlow,R. and Doyle,B. (1953) Arch. Biochem. Biophys. 46, 46.

Setlow,R.B. (1952) Arch. Biochem. Biophys. 36, 328.

Seto,A., Arimatsu,Y. Amano,T. (1977) Neurosci. Letts. 4, 115.

" " " (1981) J. Neurochem. 37, 210.

Shipolini,R.A., Bailey,G.S., Edwardson,J.A. and Banks,E.C. (1973) Eur. J. Biochem. 40, 337.

Shorr,R.G., Lyddiatt,A., Lo,M.M.S., Dolly,J.O. and Barnard,E.A. (1981) Eur. J. Biochem. 116, 143.

Sia,C.L. and Horecker,B.L. (1968) Arch. Biochem. Biophys. 123, 186.

Sigel,E., Stephenson,F.A., Mamalaki,C. and Barnard,E.A. (1983) J. Biol. Chem. 258, 6965.

Simon,E.J., Hiller,J.M. andEdelman,I. (1975) Science 190, 389.

Simon,P., Swillens,S. and Dumont,J.E. (1982) Biochem. J. 205, 477.

Sine,S.M. and Taylor,P. (1979) J. Biol. Chem. 254, 3315.

Smith,E.L. and Stockell,A. (1954) J. Biol. Chem.) 501.

Skolnick,P. and Paul,S.M. (1982) Int. Rev. Neurobiol. 23, 103.

Smith,M.A., Margiotta,J.F. and Berg,D.K. (1983) J. Neurosci. 3, 2395.

Sobel,A., Weber,M. and Changeux,J.P. (1977) Eur. J. Biochem. 80, 215.

Sotelo,C., Llinas,R. and Baker, . (1974) J. Neurophysiol. 37, 541.

Sottocasa,G.L., Kuylenstierna,B. Ernster,L. and Bergstrand,A. (1967) Meths. Enz. 10, 448.

Squires,R.F., Casida,J.E., Richardson,M. and Saederup,E. (1982) Mol. Pharm. 23, 236.

Stephenson,F.A., Watkins,A.E. and Olsen,R.W. (1982) Eur. J. Biochem. 123, 291.

St. John P.A., Froehner,S.C., Goodenough,D.A. and Cohen,J.B. (1982) J. Cell Biol. 92, 333.

Strader,C.D., Lazarides,E. and Raftery,M.A. (1980) Biochem. Biophys. Res. Commun. 92, 365.

Suarez,M.D., Revzin,A., Narlock,R., Kempner,E.S., Thompson,D.A. and Ferguson-Miller,S. (1984) J. Biol. Chem. 259, 13791.

Sumikawa,K., Houghton,M., Emtage,J.S., Richards,B.M. and Barnard,E.A. (1981) Nature 292, 862.

Sumikawa,K., Mehraban,F., Dolly,J.O. and Barnard,E.A. (1982a) Eur. J. Biochem. 126, 465.

Sumikawa,K., Houghton,M., Smith,J.C., Bell,L., Richards,B.M. and Barnard,E.A. (1982b) Nucl. Acid Res. 10, 5809.

Suno,M. and Nagaoka. A. (1984) Biochem. Biophys. Res. Commun. 125, 1046.

Swanson,L.W., Lindstrom,J., Tzartos,S., Schmued,L.C., O Leary,D.D.M. and Cowan,M. (1983) Proc. Natl. Acad.Sci.USA 80, 4532.

Swillens,S. and Dumont,J.E. (1980) Life Sci. 27, 862.

Syapin,P.J., Salvaterra,P.M. and ENgelhardt,J.K. (1982) Brain Res. 231, 365.

Takai,T., Noda,M., Furutani,Y., Takahashi,H., Notake,M., Shimizu,S., Kayano,T., Tanabe,T., Tanaka,K. Hirose,T., Inayama,S. and Numa,S. (1984) Eur.J. Biochem.143, 109.

Takeuchi,A. and Takeuchi,N. (1960) J. Physiol. 154, 52.

Tanabe,T., Noda,M., Furutani,Y., Takai,T., Takahashi,H., Tanaka,K., Hirose,T., Inayama,S. and Numa,S. (1984) Eur. J. Biochem. 144, 11.

Tanford,C. (1961) in Physical chem. of macromols. Wiley,NY.

Tanford,C. (1983) Ann. Rev. Biochem. 52, 379.

Tanford,C. and Reynolds,J.A. (1976) Biochim. Biophys. Acta 457, 133.

Tanford,C., Nozaki,Y., Reynolds,J.A. and Makino,S. (1974) Biochemistry 13, 2369.

Taylor,J.F. (1955) Meths. Enz. 1, 310.

Taylor,K., Dux,L. and Martonosi,A.(1984) J. Mol. Biol. 174, 193.

Thomas,J.W. and Tallman,J.F. (1981) J. Biol. Chem. 256, 9838.

" " (1984) in Brain receptor meths.,Acad. Press, NY.

Thomas,W.E, Brady,R.N. and Townsel,J.G. (1978) Arch. Biochem. Biophys. 187, 53.

Thorley-Lawson,D.A. and Green,N.M. (1973) Eur. J. Biochem. 40, 403.

Tindall,R.S.A., Kent,M., Baskin,F. and Rosenberg,R.N. (1978) J. Neurochem. 31, 859.

Toldi,J., Joo,F., Adam,G., Feher,O. andWolff,J.R. (1983) Brain Res. 262, 323.

Tolkovsky,A. and Levitzki,A. (1978) in Hormones and cell regulation 2, 89.

Tzartos,S.J. and Changeux,J.P. (1983) EMBO J. 2, 381.

Tzartos,S.J. and Lindstrom,J. (1980) Proc. Natl. Acad. Sci. USA 77, 755.

Tzartos,S.J., Rand,D.E., Einarson,B.L. and lindstrom,J. (1981) J. Biol. Chem. 256, 8635.

Valentine,R.C. and Green,N.M. (1967) J. Mol. Biol. 27, 615.

Vallee,B.L. and Hoch,F.L. (1955) Proc. Natl. Acad. Sci. USA 41, 327.

Vandlen,R.L., Wu,W.C.S., Eisenach,J.C. and Raftery,M.A. (1979) Biochemistry 18, 1845.

Velick,S.F. and Furfine,C.S. (1963) in The enzymes 7, 243.

Venter,J.C., Fraser,C.M., Schaber,J.S., Jung,C.Y. Bolger,G. and Triggle,D.J. (1983) J. Biol. Chem. 258, 9344.

Verkman,A.S., Skorecki,K. and Ausiello,D.A. (1984) Proc. Natl. Acad. Sci. USA 81, 150.

Vogel,Z. and Nirenberg,M. (1976) Proc. Natl. Acad. Sci.USA 73, 1806.

Vogel,Z., Sytkowski,A.J. and Nirenberg,M.W. (1972) Proc. Natl. Acad. Sci. USA 69, 3180.

Vollmer,R.T. and Fluke,D.J. (1967) Radiat. Res. 31, 867.

Wang,C.T., Saito,A. and Fleischer,S. (1979) J. Biol. Chem. 254, 9209.

Wang,G.K., Molinaro,S. and Schmidt,J. (1978) J. Biol. Chem. 253, 8507.

Wang,G.K. and Schmidt,J. (1976) Brain Res. 114, 524.

Warner,R.C. (1958) Arch. Biochem. Biophys. 78, 494.

Warren,G.B., Toon,P.A., Birdsall,N.J.M., Lee,A.L. and Metcalfe,J.C. (1974) Proc. Natl. Acad. Sci. USA 71, 622.

Weber,M. and Changeux,J.P. (1974) Mol. Pharm. 10, ±.

Weiland,G., Georgia,B., Wee,V. ,T., Chignell,C.F. and Taylor,P. (1976) Mol.Pharm. 12, 1091.

Williamson,J.R. and Corkey,B.E. (1969) Meths. Enz. 65, 434.

Wilson,P.T., Lentz,T.L. and Hawrot,E. (1986) Proc. Natl. Acad. Sci. USA in press.

Wise,D.S., Karlin,A. and Schoenborn,B.P. (1979) Biophys. J. 28, 473.

Wolosin,J.M., Lyddiatt,A., Dolly,J.O. and Barnard,E.A. (1980) Eur. J. Biochem. 109, 495.

Yamamoto,T., Yantorno,R.E. and Tonomura,Y. (1984) J. Biochem. (Tokyo) 95, 1783.

Yoshida,K. and Imura,H. (1979) Brain Res. 172, 453.

Yousufi,A.K.M., Thomas,J.W. and Tallman,J.F. (1979) Life Sci. 25, 463.

Zingsheim,H.P., Barrantes,F.J., Frank,J., Jaenicke,W. and Negebauer,D.C. (1982a) Nature 299, 81.

Zingsheim,H.P., Negebauer,D.C., Frank,J., Jaenicke,W. and Barrantes,F.J. (1982b) EMBO J. 1, 541.

Zukin,R.S. and Kream,R.M. (1979) Proc. Natl. Acad. Sci. USA 76, 1593.

ABBREVIATIONS

ACh	acetylcholine
AChE	acetylcholinesterase
ADH	alcohol dehydrogenase
α BuTX	α-bungarotoxin
ANS	autonomic nervous system
ATAS	amino-terminal amino acid sequence analysis
β-gal	β-galactosidase
BAC	bromoacetylcholine
carbachol	carbamyl choline
CAT	choline acetyltransferase
CBL	castor bean lectin
Con A	concanavalin A
CNBr	cyanogen bromide
CNS	central nervous system
DADL	(D-Ala^2,D-Leu^5)-enkephalin
DAGO	Tyr-D-Ala-Gly-(N-methyl)Phe-Gly-ol
DEAE	diethylaminoethyl
DHM	dihydromorphine
D_2O	deuterium oxide
DTT	dithiothreitol
DV 493	Dendroaspis viridis 493 toxin
GABA	gamma-aminobutyric acid
GDH	glutamate dehydrogenase
ICDH	isocitrate dehydrogenase
k-BuTX	kappa-bungarotoxin
LCH	lens culinaris haemagglutinin
LDH	lactate dehydrogenase
LET	linear energy transfer

linac	linear electron accelerator
mAbs	monoclonal antibodies
mAChR	muscarinic acetylcholine receptor
MBTA	4-(N-maleimido) benzyltrimethylammonium
MDH	malate dehydrogenase
mRNA	messenger RNA
MW	molecular weight
nAChR	nicotinic acetylcholine receptor
NG	neuroblastoma glioma
nmj	neuromuscular junction
PAGE	polyacrylamide gel electrophoresis
PC 12	pheochromocytoma cell line 12
pI	isoelectric point
PK	pyruvate kinase
PMSF	phenylmethyl sulphonyl fluoride
pnAChR	putative neuronal nAChR
poly A	poly adenylated
RNA	ribonucleic acid
SDH	succinate dehydrogenase
SDS	sodium dodecyl sulphate
STI	soybean trypsin inhibitor
SR	sarcoplasmic reticulum
$s_{20,w}$	sedimentation coefficient
TBPS	tertiary butyl bicyclo phosphorothionate
TLD	thermoluminescent dosimetry
TTX	tetrodotoxin
$\bar{v}$	partial specific volume
WGA	wheat germ agglutinin

AGONISTS

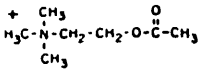

ACETYLCHOLINE

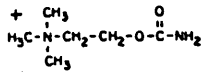

CARBAMOYLCHOLINE

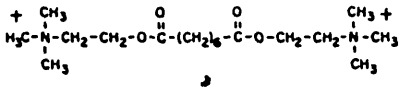

SUBERYLDICHOLINE

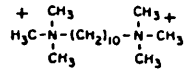

DECAMETHONIUM

AFFINITY LABELING AGENTS

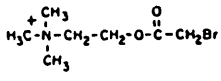

BROMOACETYLCHOLINE

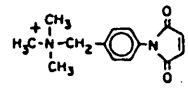

4-(N-MALEIMIDO) BENZYL-
TRIMETHYLAMMONIUM (MBTA)

COMPETITIVE ANTAGONISTS

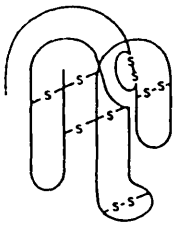

α - BUNGAROTOXIN

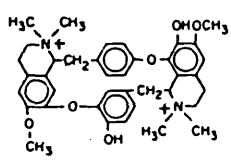

(+) - TUBOCURARINE

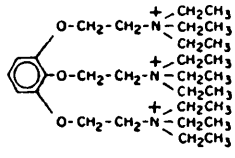

GALLAMINE

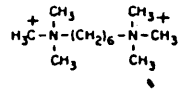

HEXAMETHONIUM

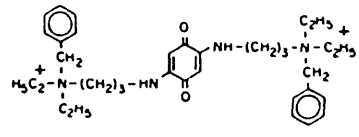

BENZOQUINONIUM

NON-COMPETITIVE ANTAGONISTS

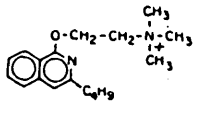

TRIMETHISOQUIN

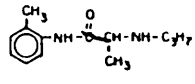

PRILOCAINE

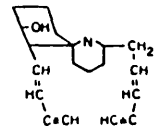

HISTRIONICOTOXIN

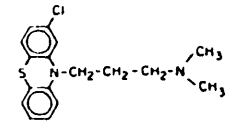

CHLORPROMAZINE

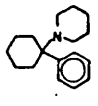

PHENCYCLIDINE

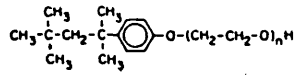

TRITON X-100 (n = 9-10)

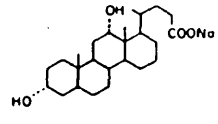

SODIUM CHOLATE